Autonomous Link-Adaptive Schemes for Heterogeneous Networks with Congestion Feedback

Syed Amaar Ahmad

Dissertation submitted to the Faculty of the
Virginia Polytechnic Institute and State University
in partial fulfillment of the requirements for the degree of

Doctor of Philosophy
in
Electrical Engineering

Luiz A. DaSilva, Co-chair
Claudio C. R. M. da Silva, Co-chair
Sheryl B. Ball
Allen B. MacKenzie
Yaling Yang

February 11, 2014
Blacksburg, Virginia

Keywords: Heterogeneous networks, End-to-end goals, Power control, Carrier aggregation, Topology adaptations, Dynamic Systems, Dual Connectivity

Autonomous Link-Adaptive Schemes for Heterogeneous Networks with Congestion Feedback

Syed Amaar Ahmad

(ABSTRACT)

LTE heterogeneous wireless networks promise significant increase in data rates and improved coverage through (i) the deployment of relays and cell *densification*, (ii) carrier aggregation to enhance bandwidth usage and (iii) by enabling nodes to have *dual connectivity*. These emerging cellular networks are complex and large systems which are difficult to optimize with centralized control and where mobiles need to balance spectral efficiency, power consumption and fairness constraints.

In this dissertation we focus on how decentralized and autonomous mobiles in multihop cellular systems can optimize their own local objectives by taking into account end-to-end or network-wide conditions. We propose several link-adaptive schemes where nodes can adjust their transmit power, aggregate carriers and select points of access to the network (relays and/or macrocell base stations) autonomously, based on both local and global conditions. Under our approach, this is achieved by disseminating the dynamic congestion level in the backhaul links of the points of access. As nodes adapt locally, the congestion levels in the backhaul links can change, which can in turn induce them to also change their adaptation objectives. We show that under our schemes, even with this dynamic congestion feedback, nodes can distributedly converge to a stable selection of transmit power levels and points of access. We also analytically derive the transmit power levels at the equilibrium points for certain cases. Moreover, through numerical results we show that the corresponding system throughput is significantly higher than when nodes adapt greedily following traditional link layer optimization objectives.

Given the growing data rate demand, increasing system complexity and the difficulty of implementing centralized cross-layer optimization frameworks, our work simplifies resource

allocation in heterogeneous cellular systems. Our work can be extended to any multihop wireless system where the backhaul link capacity is limited and feedback on the dynamic congestion levels at the access points is available.

In the name of Allah, the Gracious, Ever Merciful

In loving memory of Abiji and Nani

Acknowledgements

My PhD at Virginia Tech has been quite a learning experience. Despite numerous challenges and hurdles along the way, I have been able to complete the dissertation with the grace of God. I would like to acknowledge my wife Batool's love, support, encouragement and help during this time. It is to her that I would like to dedicate my effort. My parents, siblings, friends and other elders also contributed immensely with prayers and words of encouragement. Without them it simply would not have been possible for me to persevere and complete the work.

My advisors Luiz DaSilva and Claudio da Silva need to be thanked for support and patience with my ideas. Finally, I am indebted to Virginia Tech's Engineering Education Department which has provided me a teaching opportunity since 2011.

Contents

List of Figures

List of Tables

Chapter 1

Introduction

The emergence of Fourth-generation (4G) LTE wireless standards promises significant increase in data throughput and better coverage than what current networks can support [1–3]. The prominent features of LTE include (i) deployment of relays to provide a low-cost solution for better coverage [4] (ii) cell densification through heterogeneous networks (HetNets) [5], (iii) carrier aggregation (CA) to enhance bandwidth for higher data rates [6] and (iv) dual connectivity [7]. When coupled with distributed resource management, this motivates the need for link-adaptive algorithms and schemes which can enable high data rates and better energy consumption by taking into account network-wide conditions in multihop cellular systems.

Optimization of emerging wireless networks which are complex and large systems is hard to achieve with centralized control. In this dissertation we focus on how mobiles can act as a decentralized set of autonomous decision-makers that optimize their own local objectives by adapting their transmit power or Point of Access (PoA) or by aggregating carriers. In future wireless systems, mobiles will need to balance spectral efficiency, power consumption and fairness constraints by taking into account end-to-end goals [8]. We explore how a mobile or User Equipment (UE) may select its current adaptation goal based on the latest network-wide conditions and then leverage channel aggregation, transmit power, and topology adaptation capability accordingly.

Our approach is in contrast to typical resource allocation problems to maximize some network-wide cross-layer objective function with either centralized or distributed implementations [9–17]. Moreover, our approach incorporates end-to-end performance considerations for relay-based cellular systems, unlike [18–23], where local adaptations are based only on physical layer performance metrics.

1.1 Problem Statement

Our work studies link adaptations made in an autonomous and distributed manner by mobile radio nodes in a cellular multihop network by taking into account end-to-end goals to achieve network-wide objectives. We wish to explore the conditions under which it is beneficial to make local adaptations in such a manner. We study how individual nodes can adapt their parameters (such as transmit power, channels of operation and Points of Access), based on feedback from the network, so as to optimize their own objectives in a convergent fashion. Individual link adaptations impact one another due to the broadcast nature of the wireless medium and may possibly create non-convergent interaction. We focus on designing techniques and schemes which are efficient, adaptive and flexible for heterogeneous or multihop networks.

1.2 Research Issues

We apply both an analytical approach and a simulation-based study to examine the impact of link adaptations on network-wide or end-to-end performance when congestion information can be disseminated to the UEs. The analytical approach is needed to study the properties and attributes of the adaptations that we propose in the next sections and to compare against the case when radio nodes adapt without any network-wide considerations.

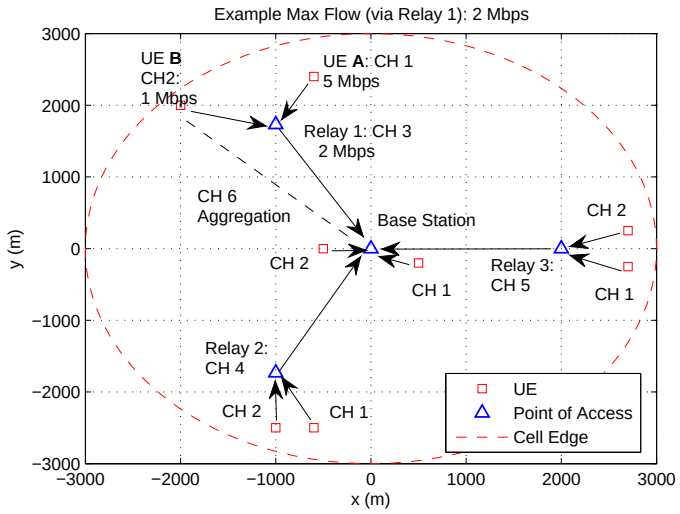

Figure 1.1: A sample network topology with channel assignments. Each mobile unit or User Equipment (UE) adapts to maximize its own objective based on its observation of the current network-wide conditions.

An Illustration

As an illustration of a multihop cellular network consider Fig. 1.1, with 3 relays which forward UE data to a base station. The backhaul capacity of Relay 1 is less than the aggregate incoming data rate (i.e. the relay-to-base station link is a rate-limiting or *bottleneck* link). If the UEs A and B, that are attached to Relay 1 have knowledge of the congestion at the relay (i.e. a *network-wide condition*), these nodes could reduce their transmit power (and data rate) to conserve battery life until the congestion is alleviated, or they could migrate to alternative Points of Access (i.e. perform topology adaptations). In contrast, if the backhaul capacity of the relay was larger than the aggregate incoming data rate, the adaptation choice of these nodes, with this knowledge, might be to maximize data rate and perform carrier aggregation. Moreover, if a node could attach to multiple Points of Access simultaneously (e.g. UE B forwarding to both the relay and the base station), then it could stream data to the base station via two routes. With dual connectivity, its power allocation or topology adaptation strategy to optimize end-to-end data rate would again depend on link-layer performance but also require knowledge of the congestion condition at the relay. These examples illustrate that the adaptation objective of a UE should depend on both *local* and *global* conditions. The former depends on its link-layer considerations whereas the latter

is based on knowing whether its links are bottleneck links or not.

Research Problems

We propose to address the following general questions in this dissertation:

1. Under what conditions is it beneficial to make local adaptation decisions based on network-wide conditions or end-to-end goals?

Local adaptations for point-to-point links have been well-studied, especially in the context of power control [24, 25], topology control [26, 27] and channel assignment problems [28]. We are interested in designing adaptation schemes for transmit power, channel and topology control in multihop cellular networks by taking into account end-to-end goals. Moreover, we also define how information about network-wide conditions (i.e. in term of which are the bottleneck links) can be distributed to the UEs so as to enable them to have better adaptation choices.

2. What is an appropriate link adaptation algorithm?

We are interested in devising the adaptation algorithm for a node given the dynamic network-wide conditions from its vantage point. For instance, a node could operate in a transmit power minimization mode when it is forwarding its data via a relay that is suffering congestion, as the preceding example illustrates. Conversely, in the case when the node has aggregated multiple channels on a direct link to the base station, it could apply the water-filling transmit power allocation to maximize its data rate [29].

3. How is the conflict between different adaptation choices resolved?

A multihop network can suffer congestion when mobiles are sending a higher aggregate data rate than what can be supported on a relay backhaul. In Fig. 1.1 UE nodes A and B are sending 5 Mbps and 1 Mbps to a relay with a backhaul capacity of 2 Mbps. The adaptation strategy for the relay node could be to increase its backhaul link capacity to alleviate the

congestion. In contrast, the adaptation approach for the UEs could be to reduce, maintain or even increase their transmit power levels as the backhaul capacity is being increased. For instance, either only node B (with the 5 Mbps data rate) could decrease its transmit power whereas node A (with a lower 1 Mbps) can still adapt for data rate maximization. Alternatively, both nodes A and B could switch to transmit power minimization. A third possibility could even be for one of the UEs to attach to the base station to bypass the congested relay. However, if the backhaul capacity was large enough (e.g. 20 Mbps), both the nodes could adapt in a greedy manner to maximize their data rates. Our work explores strategies that help resolve the conflict between adaptation choices available to the nodes.

4. Can the link adaptations converge to a stable transmit power selection and topology?

In addition to transmit power and carrier aggregation, when nodes can dynamically select their PoAs this can lead to topology stability issues. Greedy and unconstrained adaptations by nodes may lead to transient choice of a PoA and consequently result in erratic system throughput. We consider mechanisms that ensure that the adaptations converge to a stable network topology and transmit power levels.

5. What is the impact of global knowledge as opposed to local knowledge?

With local knowledge, nodes are limited to adapting in a greedy fashion to optimize link layer performance only. In contrast, with global knowledge about congestion conditions, a node may select between optimizing its end-to-end data rate performance or transmit power consumption. We explore the effect on system performance when nodes have global knowledge about the bottleneck links in the network.

1.3 Convergence and Feasibility

Cross-layer optimization schemes that maximize a network-wide utility function essentially require all nodes in a wireless network to conform to a common objective [16]. In contrast, when mobiles are autonomous, the resource allocations transform into a distributed problem where each agent (radio node) is prioritizing its own goals above those of the others. There-

fore, in such a system an important performance objective is that the adaptive interactions between the nodes converge to a stable and *feasible* solution.

Convergence is an important property of a multi-agent system which ensures that the system throughput or other performance metrics do not become erratic or fluctuate rapidly. If the local adaptations do not converge, then the network performance becomes unreliable or unpredictable. In the context of adaptive power and topology control, system feasibility refers to when all nodes can, in principle, achieve a degree of fairness or reliability in terms of a minimum SINR [19, 30]. Thus, a desirable outcome of any adaptive power or topology control scheme is that a maximum number of nodes can distributedly achieve the minimum target SINR even if each node is allocating resources to achieve its own local objective.

We simplify the resource allocation problem by letting each node set its own local objectives. This lets us get around the difficulty in implementing network-wide utility functions for large and complex networks. At the same time, the decentralized adaptation algorithms that solve each node's local objective also need to achieve convergence, feasibility as well provide system throughput improvement.

1.4 Contribution and Organization

This dissertation explores the impact of three adaptation parameters (i) transmit power, (ii) channel and (iii) topology assignments.

- In Chapter 2, we provide the literature review and background for the dissertation work.
- In Chapter 3, we explore adaptive schemes when nodes can only adapt their transmit power levels. We first propose a Marginal Power Efficiency-based Adaptation (MPEA) scheme for data maximization over time-varying wireless channels. Nodes autonomously adapt their transmit power keeping a differential measure of power efficiency, defined as the additional capacity obtained per unit of transmit power, at a desirable threshold. We combine the MPEA with the well-known Foschini-Miljanic

(FM) algorithm [18] into a power control scheme for a multihop cellular network where nodes can dynamically adapt to both local and global conditions. We consider two variants of this scheme in terms of which nodes switch between choosing either the MPEA or the FM algorithm. We also derive a closed-form expression for fixed points to which the power allocations converge under either variant of the scheme and illustrate a significant improvement in the system throughput.

- In Chapter 4, we extend our analysis to when nodes can also aggregate channels and change their Points of Access in the network in addition to performing transmit power control. We propose an adaptation mechanism whereby the UEs optimize a combination of achieved data rate and energy consumption by appropriate selection of their transmit power, channels, and Point of Access to the network. Our results show these adaptations provide better system throughput than adaptations that simply consider current channel quality indicators, combined with greedy channel aggregation.

- In chapter 5, we look when nodes have dual connectivity to multiple Points of Access and perform distributed power allocation. In currently deployed networks, a UE can either establish a direct link to the base station or a link to the relay (establishing a two-hop route to the base station), but not both. We consider the benefit in allowing mobiles to split their transmit power over simultaneous links to the base station and the relay, in effect transmitting two parallel flows. We model decisions by the UEs as to (i) which point of access to attach to (either a relay, base station or both) and (ii) how to allocate transmit power over these links so as to maximize total capacity. We show that this additional flexibility in the selection of multiple points of access leads to substantial aggregate capacity increase, as compared with when nodes operate in a fixed network topology. We again show that these decisions converge under certain conditions without any cooperation between the nodes and derive a closed-form expression for the transmit power at the equilibrium point.

- Finally, in Chapter 6, we provide a summary of the contributions and future direction of research.

Chapter 2

Background

We divide the literature review into four categories (i) distributed power control, (ii) topology adaptations in cellular networks, (iii) impact of carrier aggregation, and (iv) adaptations in multipoint relay-based cellular systems. We also identify the research problems in each of these categories that have not been studied previously and which this dissertation addresses.

In Fig. 2.1 we highlight the broad approaches to resource allocation problems in wireless networks and position the work in this dissertation in that context. At one end of the spectrum, the problem is addressed within the framework of network-wide utility optimization (e.g. maximizing some network-wide utility or achieving throughput-optimality [11]) that can then be realized by either centralized or distributed algorithms. On the other hand, given that emerging wireless systems are complex and large, letting radio nodes be autonomous in optimizing their own local objectives helps simplify resource allocations. In this context, this dissertation attempts to push the paradigm of the local and autonomous adaptations from the link layer [18, 20, 22, 23, 31–34] towards a more network-centric approach.

2.1 Distributed Power Control

Power control for point-to-point links in cellular networks has been widely studied as an important factor to control Signal-to-Interference-and-Noise Ratios (SINR), which in turn

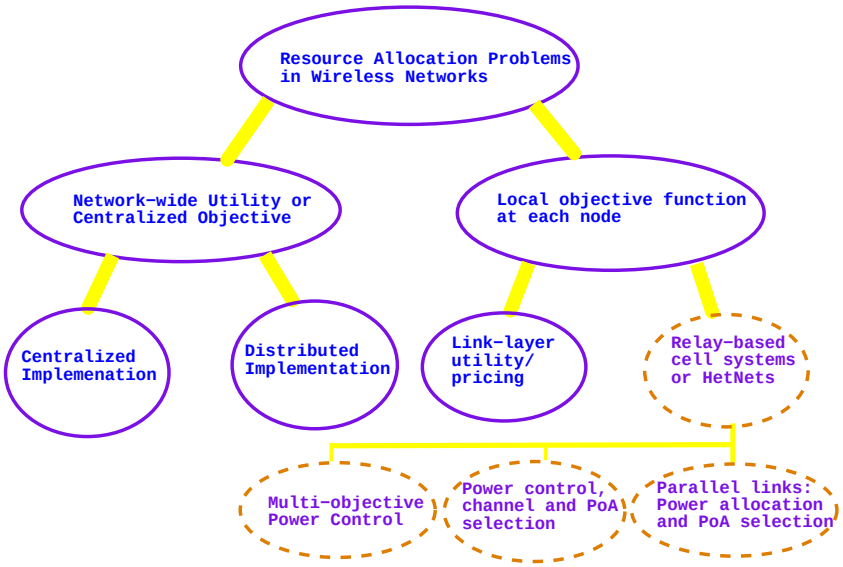

Figure 2.1: In the context of the literature, the focus of this dissertation (dashed) is on local resource allocation algorithms for autonomous mobiles in multihop cellular systems.

determines Quality-of-Service (QoS) metrics such as transmission rate, outage and delay. We first review some well-known transmit power control algorithms which we compare under the framework of our proposed schemes.

Foschini-Miljanic Algorithm

A seminal contribution for distributedly achieving fixed SINR targets was by Foschini and Miljanic [18]. The target SINRs are always achieved, as long as the system is feasible. Feasibility refers to when all links can achieve their target SINRs, in theory, given the underlying interference structure in the network [19, 30]. Under the Foschini-Miljanic (FM) algorithm, transmitters converge to their target SINRs with minimum aggregate transmit power. This algorithm has been followed by a surge of research on convergence properties of distributed power control and has been combined with other power control schemes [17, 19, 33, 34]. Under the FM algorithm, nodes set a high power when link quality drops and conversely decrease it as the channel improves. From an information-theoretic perspective, the FM algorithm can be viewed as a *channel inversion* approach [29].

Despite its wide applicability in current cellular systems, there are limitations to the FM

algorithm [17]. Setting large target SINRs may decrease the likelihood of system feasibility (i.e. nodes may not then achieve the high target SINRs but needlessly increase transmit power and interference), whereas, conversely, with low target SINRs, system resources may be under-exploited, in particular for elastic data applications [17].

Opportunistic Power Control

Opportunistic Power Control (OPC) is suitable for data services where maintaining a constant SINR is not necessary and variation in latency can be tolerated [22, 31]. Since the wireless channel is inherently time-varying, under OPC, a user increases his power to transmit more information when the channel gain is large and interference is low. Data rate can then be adjusted accordingly using adaptive modulation and coding techniques.

Moreover, OPC has also been incorporated with the FM algorithm [33, 34] such that a transmitter can switch between OPC and FM algorithms depending on the link quality. The OPC-FM combination algorithm [34] enables nodes to both satisfy the feasibility (SINR) requirement as well as let higher data rates be supported when channel conditions are favorable.

Utility-based Local Power Control

An alternative approach to power control that has been widely studied in literature is based on the notion of pricing or utility functions of link quality [32]. A characteristic of such schemes is that each radio node (user) adapts to maximize its own net-utility, which is defined as utility derived from its current performance minus the cost associated with the resource allocations. Such algorithms do not suffer from divergence, which is achieved by softening the SINR requirement using the notion of utility functions [23][20]. Different utility functions have been formulated especially in the context of non-cooperative games, such as throughput per unit power consumption, frame outage, Shannon capacity and sigmoid-like softened SINR requirement [32]. Similarly, [33, 34] have proposed several utility functions based on variants of their OPC-FM combination algorithm, to give a game-theoretic flavor

to their adaptation schemes. *Nash equilibirum* is an important system performance metric for such transmit power schemes, as it indicates a point where distributed adaptations by the nodes have converge to a solution [35]. At the equilibrium point no node can derive any further benefit by unilaterally deviating from its current resource allocations.

A basic feature of the transmit power games in [20, 23, 32–34] is that nodes can only optimize their performance for link-layer metrics. These papers provide useful insights into the convergence properties in wireless networks with point-to-point links. However, their scope is limited in addressing the issues that emerge when nodes transmit messages over multihop networks.

Waterfilling

Waterfilling is another class of power allocation algorithm used when a transmitter communicates with a receiver over multiple channels [29]. The classical waterfilling solution solves the problem of maximizing the data rate between the two over a link composed of several channels (such as a frequency-selective channel, a time-varying channel, or spatial channels arising from the use of multiple antennas on both ends of a link) with a maximum power constraint at the transmitter by appropriately allocating power to each channel [29]. This allocation can be visually interpreted as pouring water over a surface given by the inverse of the effective channel gains, hence the name *waterfilling*.

The aforementioned power control mechanisms let nodes distributedly optimize their point-to-point links. To reiterate, a key difference in our dissertation work and the link-adaptive schemes in [20, 23, 32–34] is that we pursue the framework of local adaptations by using feedback on the dynamic congestion conditions in multihop cellular networks. In heterogenous or multihop networks, optimizing link-layer performance may not always improve the end-to-end data rate when, for instance, a UE is connected to a relay that is experiencing a congested backhaul. Likewise, hitting a fixed target SINR may be a poor strategy if the UE is connected to the base station on a direct link with high channel gain. Thus, unlike [18–23], our work fills in the gap on when and how a UE can switch between different power

allocation algorithms given its current resources.

2.2 Topology Adaptations through Cell Selections

In most current cellular systems the cell selection process is done based on a mobile's observations of the best detected SNR [3]. In 4G wireless networks the UE has the ability to connect to different Points of Access (PoAs) (e.g. base stations, picocells and relays). This opens the possibility of dynamic topology adaptations by mobiles. Good cell section techniques ensure that a UE remains connected to a PoA with good enough signal quality and with a high enough backhaul capacity.

The research on cell selection algorithms grew during the 1990s, with the advent of CDMA networks with focus on handoffs, multiple access techniques and power control. In [36], Hanly proposed a cell selection algorithm where information on channel quality from multiple base stations was fed back to the mobiles to enable them to dynamically switch between cells and to allocate transmit power so as to satisfy target SINR requirements. In [3], Amzallag et al. formulated the cell selection problem as a centralized optimization problem called *all-or-nothing demand maximization* and proposed algorithms to handle load balancing better than the current local mobile SNR-based decision protocol.

However, these schemes were designed either for CDMA systems or have a centralized optimization formulation that reduces their utility for autonomous cell selection in LTE-Advanced networks. Some recent work that focuses on making cell selections more autonomous in heterogeneous networks for the mobiles includes [37–39]. These papers essentially propose load-balancing mechanisms to evenly spread the attachment of mobiles between different PoAs. In [38], macro-cell and pico-cell users make service selection decisions dynamically according to the performance satisfaction level and cost, which in turn depend on the pricing and spectrum sharing between the macrocell and small-cell providers. Similarly, in [37], nodes perform an inter-cell game to first choose their cells; this is in turn followed by channel and transmit power allocation such that the load across the cells is dynamically balanced.

The traditional load-balancing in [3, 36–39] however does not study the effect of having constrained backhaul capacity at the PoAs on the end-to-end data rates. To address this issue, in Chapter 4 we explore (i) the notion of load-balancing as a congestion alleviation mechanism and (ii) how a mobile can prioritize between minimizing its power consumption (which indirectly also reduces the load at its current PoA) or performing a topology adaptation by connecting to a better PoA.

2.3 Channel Aggregation

Carrier or channel aggregation is a simple and effective approach in LTE-Advanced to increase available bandwidth and to boost data rates [40]. However, if the carriers are reused without any restrictions or without careful assignment, then intra-cell interference may adversely affect performance [41] between users at different tiers (i.e. picocells, macrocells or relay nodes etc.). Notwithstanding that there are numerous centralized and distributed implementations of channel assignment algorithms to minimize interference, it is essentially an NP-Hard problem and a viable alternative is to let nodes autonomously perform carrier or channel selections [41].

The autonomous carrier selection algorithm in [41] enables nodes to select channels based on the lowest expected interference levels in the radio spectrum. In [42], nodes aim at choosing a subset of the total channels so that the aggregate interference across the chosen bandwidth is minimized.

Greedy carrier aggregation on the uplink suffers from a few limitations, however. Firstly, if the transmit power available to a UE is limited, then aggregating carriers would diminish the transmit power per channel and thus also adversely affect its data rate. This issue has also been raised in [43], where through a load-balancing mechanism under-utilized carriers within a network are assigned only to those UEs which have sufficient on-board transmit power. Secondly, a greedy carrier aggregation can only improve a UE's link-layer performance. In heterogeneous networks, if carrier aggregation is performed by UEs attached to congested relays then this will not improve their end-to-end data rate and may also create interference

for other links operating on the aggregated carriers. In Chapter 4 we present mechanisms that ensure that carriers are only aggregated by a UE if its end-to-end data rate can be enhanced.

2.4 Multipoint Relay-based Systems

In currently deployed LTE systems, UEs can establish links to individual PoAs only. To reiterate, in conventional cellular topology, nodes maintain connection to a single access point [44] which is often the one with the highest received SNR [3]. However, with the growth in wireless technology, mobiles are increasingly multi-channel and multi-interface capable. In [45], for example, an architecture is proposed where mobiles equipped with multiple network interface cards can establish links on multiple channels. We envision that UEs will be able to transmit multiple parallel data streams, that are controlled by some upper layers (above the link layer) to multiple PoAs.

An area of research adjacent to the aforementioned notion of topology control with parallel links is Coordinated Multi-Point transmission (CoMP) in the LTE uplink. In this field, cooperative MIMO is proposed for dynamic or joint reception of signals at multiple eNodeBs [46][6]. However, CoMP also requires coordination between different mobiles and exchange of channel quality indicators through the X2 back-end link. The alternative to this is to let a mobile make its decisions about its points of attachment at the upper layers of the protocol stack. For instance, a mobile could stream data through a direct link to the base station as well as via a link to a close-by relay or picocell base station without any back-end coordination between the two PoAs.

Another field of research somewhat related to our work is *parallel relay channels* [47] which have been studied from an information-theoretic perspective in the context of: (i) a single source-destination node pair with transmit power resource allocation over the sub-channels without interference from other source nodes [48–52], (ii) a Gaussian interference channel [53] for the two-user case (i.e. two source-destination pairs) where the capacity region is explored with an out-of-band relay [54–58] and (iii) a general multiple access channel from

multiple source nodes to a single shared relay and common destination [54].

The exact capacity for the general n-user parallel relay system is an open problem. Instead we focus on a more basic issue of how nodes can dynamically choose between multiple PoAs and then allocate their transmit power over their parallel links. The cited works either assume a single-user system that has no interference or a multi-user system with interference cancellation capability at the receivers. In contrast, our work focuses on designing practical transmission-receiver protocols suitable for general networks with multiple relays and where interference is treated as noise.

2.5 Conclusion

We have highlighted the major approaches in literature to local adaptations for allocation of transmit power, channel assignment and topology control by autonomous nodes in wireless networks. In Chapter 3, we begin with transmit power control schemes that let nodes take into account both local and network-wide conditions in their adaptations.

Chapter 3

Power Control Adaptations: Marginal Power Efficiency and Power Minimization Considerations

LTE-Advanced networks support the use of relays to provide improvement in system capacity and coverage [1]. When coupled with distributed power control, this motivates the need for adaptive schemes which can support heterogeneous traffic and balance spectral efficiency and energy consumption [59].

In this chapter we first propose a marginal power efficiency-based adaptation algorithm for distributed power control in wireless communication systems: Links autonomously adapt their transmit power keeping a differential measure of power efficiency, defined as the additional capacity obtained per unit of transmit power, at a desirable threshold. This metric is motivated by the inherent tradeoff between the transmit power (cost) and the data rate (utility) of a link with a given bandwidth and effective interference. A marginal power efficiency-based adaptation falls under the category of *opportunistic power control* (OPC) [22, 31, 33, 34], which is suitable for data services where maintaining a constant SINR is not necessary and variation in latency can be tolerated.

We combine the MPEA with the Foschini-Miljanic (FM) scheme [18] into algorithms

for multihop cellular networks where links can dynamically adapt to both local and global conditions. We first propose the Multihop Marginal Power Efficiency-based Adaptation (referred to as MH-MPEA), in which all the links initially try to maintain a target marginal power efficiency. However, if a relay-to-base station link becomes congested, then depending on which UE is instantaneously causing the most congestion, the attached nodes switch to minimizing their transmit power and data rates, subject to a minimum SINR, using the FM power control.

In the later half of the chapter, we then modify MH-MPEA into a more generalized Network-State based Link Adaptive scheme (NSLA). In NSLA nodes are fully autonomous in choosing between the MPEA and FM algorithm so as to balance their data rate maximization and transmit power minimization requirements while taking into account congestion conditions at the relays.

In both the MPEA-based schemes, the power allocation objective of the UEs depends on the current network-wide conditions, unlike in [60] where nodes are only optimizing their link layer goals. We also derive closed-form expressions for the converged transmit power levels of the radios, and show that, under the schemes, the system throughput is increased by at least 200%, at a cost of less than 15% *infeasible* links [19, 30], over a range of simulation scenarios. This is even though UEs adapt to optimize their own local objective instead of some centralized network-wide goal as in [16, 33, 34, 61].

3.1 System Model

Consider a single-cell network serving n user equipment (UEs) that wish to communicate with the Base Station (BS) on the uplink. There are N_r fixed relay stations (RS), which are located towards the edges of the cell to provide coverage for UEs farther away from the base station (see Fig. 3.1 with $N_r = 3$). Each RS receives data from those UEs which fall in its coverage region and decodes-and-forwards the data to the BS. Those UEs which uplink to a relay use a multihop route to connect with the BS. All established uplinks are power- and rate-adaptive and can be represented by a set $\mathcal{L} = \{1, 2, \cdots, L\}$ which is the union of three

subsets $\mathcal{L}_1$ (UE-to-RS), $\mathcal{L}_2$ (RS-to-BS) and $\mathcal{L}_3$ (UE-to-BS).

We assume that there are multiple channels that can be conceptualized over time or frequency, similar to *resource blocks* in LTE [1]. Channel assignments are made with the constraint that all links to and from a given Point of Access (relay or BS) operate on orthogonal channels. With the same constraint for every link, these channels can be *reused* by other links in the cell (e.g. as in Fig. 3.1). We represent the channel assignment of the links as a set $\mathcal{F}(f) \subseteq \mathcal{L}$ for each of the F channels $f \in \{1, 2, \cdots, F\}$. Each link i is associated with a single channel $f_i \in \mathcal{F}$ of bandwidth W Hz, where when $f_i \neq f_j$, we have $\mathcal{F}(f_j) \cap \mathcal{F}(f_j) = \emptyset$ such that $\bigcup_{\forall f_i} \mathcal{F}(f_i) = \mathcal{L}$.

Let $g_{j,i}$ represent the channel gain between the transmitter of link j and the receiver of link i, which depends on factors such as the path loss and fading. Given these gains and the channel assignments, a normalized cross-link gain matrix $\mathbf{F}$ of dimension $L \times L$ is defined as

$$\mathbf{F}(i,j) = \begin{cases} 0 \text{ if } i = j \text{ or } f_i \neq f_j, \\ \frac{g_{j,i}}{g_{i,i}} \text{ otherwise.} \end{cases} \tag{3.1}$$

The transmit powers of all links are represented by the vector $\mathbf{P} = [P_1, P_2, \cdots, P_L]$. The effective interference E_i for link i is defined as [31]

$$E_i = \frac{n_o + \sum_{j \neq i, j \in \mathcal{F}(f_i)} g_{j,i} P_j}{g_{i,i}}, \tag{3.2}$$

where n_o is the total thermal noise power per channel. Let $\mathbf{P}_{\max}$ and $\mathbf{D}$ be $L \times 1$ vectors, where the first vector represents the links' maximum transmit powers and the i^{th} element of the second vector is $\mathbf{D}(i) = n_o / g_{i,i}$. The achieved SINR of link i is $\gamma_i = \frac{P_i}{E_i}$. The corresponding data rate of link i is assumed to be

$$\eta_i = W . \log_2(1 + \gamma_i) \text{ bits/s.} \tag{3.3}$$

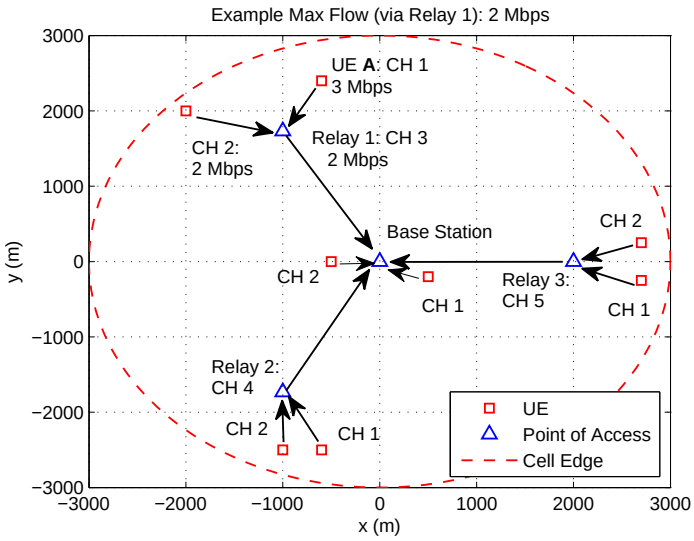

Figure 3.1: A depiction of a multihop cellular network where local adaptations take into account the end-to-end data rate performance.

3.2 Problem Formulation

Consider the aggregate end-to-end data rate, denoted as η_N. Using the Max-Flow Min-Cut Theorem [62], this can be expressed as:

$$\eta_N = \sum_{i \in \mathcal{L}_3} \eta_i + \sum_{r \in \mathcal{L}_2} \min \left(\eta_r, \sum_{j \in \mathcal{L}_1^r} \eta_j \right) \tag{3.4}$$

where $\mathcal{L}_1^r \subseteq \mathcal{L}_1$ denotes the subset of UE-to-RS links forwarding their data via the backhaul RS-to-BS link $r \in \mathcal{L}_2$. The minimum of the outgoing RS-to-BS link data rate η_r ($r \in \mathcal{L}_2$) and the aggregate incoming data rate $\sum_{j \in \mathcal{L}_1^r} \eta_j$ is the maximum aggregate data rate possible for the flows (see Fig. 1 as an example). When $\eta_r < \sum_{j \in \mathcal{L}_1^r} \eta_j$, the backhaul RS-to-BS link becomes the *bottleneck* link for all UEs of relay r, as it constrains their aggregate end-to-end data rate. We define the *rate differential* for each relay r as

$$V_r = \eta_r - \sum_{j \in \mathcal{L}_1^r} \eta_j \tag{3.5}$$

which is broadcast to all its attached UEs. We propose that the objective of direct links to the base station be to maximize data rate. Conversely, for a link to a relay its power control objective should also depend on the backhaul capacity. If the RS-to-BS link is congested (as indicated by V_r), an associated UE-to-RS link could operate in power minimization mode, subject to some SINR constraint, to alleviate the congestion in the backhaul link. Therefore, we define the objective function of the transmitter of each link i as

$$\begin{aligned} &\underbrace{\max}_{P_i} w_i\eta_i + (1-w_i)(P_{max,i} - P_i) \\ &\text{s.t. } (1-w_i)\gamma_i \geq (1-w_i)\beta \\ &w_i\frac{\partial \eta_i}{\partial P_i} \geq w_i\mu_i \\ &P_i \leq P_{\max,i}, \forall i \\ &w_i \in \{0,1\}, \forall i \end{aligned} \tag{3.6}$$

If $w_i = 1$, then link i maximizes its data rate subject to a minimum marginal capacity improvement (denoted as μ_i) with respect to its power, referred to as the *marginal power efficiency*. In contrast, if $w_i = 0$, then link i minimizes its transmit power subject to some minimum SINR threshold β (i.e. feasibility constraint). The power allocations are subject to a maximum transmit power constraint. We illustrate how $w_i \in \{0,1\}$ is determined for each link in the next section.

3.3 Network Adaptation Scheme

The distributed transmit power adaptations by UEs to solve (3.6) occur in time intervals denoted as $k \in \{1,2,..\}$. There is transmitter-side knowledge of the current effective interference $E_i(k)$ on each link i. The determination of w_i for each link i is illustrated in Algorithm 1. Initially, each link sets out to maximize its data rate (i.e. $w_i(0) = 1$ for each link i). However, if there is congestion on an RS-to-BS link, defined as when $V_r(k) < -\tau$ where τ is a positive-valued threshold, some of the UE-to-RS links may instead be selected to switch to power minimization mode to relieve the load on the uplink backhaul. In each

Algorithm 1: The determination of w_i for each link i is based on the network-wide conditions in MH-MPEA.

Initialization: $w_i(0) = 1$, $\forall i$
Iteration k: Link i adapts as per (3.6), $\forall i$
for *Relay* $r = 1$ *to* N_r **do**
    if $V_r(k) < -\tau$ **then**
        $j = \arg\max\{\eta_j(k)\} : w_j(k) = 1, j \in \mathcal{L}_1^r$;
        $w_j(k+1) = 0$;
    else if $V_r(k) \geq 0$ **then**
        $w_j(k+1) = 1$, $\forall j \in \mathcal{L}_1^r$;
    else
        $w_i(k+1) = w_i(k), \forall j \in \mathcal{L}_1^r$
return to Iteration $k = k + 1$.

iteration, the selected link j is the one that has the highest instantaneous data rate. This selection continues iteratively until $V_r(k) \geq -\tau$ or until all UE-to-RS links go into power minimization mode.

Thus, as per Algorithm 1, a UE-to-RS link $j \in \mathcal{L}_1$ may either maximize its data rate or minimize its transmit power, whereas the power control objective of link $i \in \mathcal{L}_2 \cup \mathcal{L}_3$ (i.e. direct links to the BS) is always to maximize its data rate subject to the constraints in (3.6).

3.3.1 Marginal power efficiency-based adaptation

Given $w_i(k+1) = 1$, the objective in (3.6) becomes $\underbrace{\max}_{P_i} \eta_i$ for link i. i for link i. Since transmit power is a limited resource, a UE needs to use it opportunistically and economically for time-varying wireless channels. Marginal power efficiency differs from traditional metrics such as spectral efficiency (data rate per unit bandwidth) and power efficiency (spectrum efficiency per unit of transmit power). The former does not indicate at what cost (i.e. transmit power) a certain data rate is achieved; likewise a high power efficiency may be achieved despite a low data rate [63]. The marginal improvement in the capacity of a link (utility) as a function of transmit power (cost) therefore provides insight into the instantaneous utility-cost tradeoff of a node for a given effective interference. As per the second constraint in (3.6),

to balance the marginal improvement in capacity with the cost of increasing transmit power, a node may set the marginal power efficiency to a desirable threshold such that $\frac{\partial \eta_i}{\partial P_i} = \mu_i$:

$$\begin{aligned} \frac{\partial \eta_i}{\partial P_i} &= \frac{\partial}{\partial P_i} W \cdot \log_2 \left(1 + \frac{P_i}{E_i(k)}\right) \\ &= \frac{W}{\ln(2)(E_i(k) + P_i)}. \end{aligned} \tag{3.7}$$

When the inequality constraint on the marginal power efficiency in (3.6) is active, the transmit power of the link is adjusted so that its marginal power efficiency remains constant: $\frac{\partial \eta_i}{\partial P_i} = \mu_i$. Then its power allocation becomes:

$$P_i + E_i(k) = \frac{W}{\ln(2)\mu_i} \tag{3.8}$$

Link i can be calibrated to transmit at full power if its effective interference tends to zero ($E_i \to 0$). Thus, the allocation becomes $P_i + E_i(k) = P_{\max,i}$ when we set $\mu_i = \frac{W}{\ln(2)P_{\max,i}}$. This results in the *water-filling* approach for distributed power allocation over a single time-varying channel. However, unlike [64], there is no constraint on the average transmit power as the transmitter is not assumed to have channel statistics. To achieve a minimal requisite SINR β, the following condition must hold:

$$\begin{aligned} \gamma_i = \frac{P_i}{E_i(k)} &= \frac{P_{\max,i}}{E_i(k)} - 1 \geq \beta \\ \therefore E_i(k) &\leq \frac{P_{\max,i}}{\beta + 1}. \end{aligned} \tag{3.9}$$

As in [61], to conserve its transmit power resource in response to harsh channel conditions, the node delays its transmission until E_i falls below a threshold. Thus, given $w_i(k+1) = 1$ the transmit power of link i is updated under MPEA as:

$$P_i(k+1) = \begin{cases} P_{\max,i} - E_i(k) \text{ , if } E_i(k) \leq \frac{P_{\max,i}}{\beta+1} \\ 0, \text{ otherwise.} \end{cases} \tag{3.10}$$

The corresponding effective interference in vector notation is

$$\mathbf{E}(k) = \mathbf{D} + \mathbf{F}\mathbf{P}(k). \tag{3.11}$$

Next we establish a sufficient condition for all links to achieve the minimum SINR under MPEA. The condition corresponds to a constraint on the maximum interference in the network, denoted as $\mathbf{E}_{\max} = \mathbf{F}\mathbf{P}_{\max} + \mathbf{D}$.

Theorem 3.3.1. *If* $(\beta+1)\mathbf{D} \leq [\mathbf{I} - (\beta+1)\mathbf{F}]\mathbf{P}_{\max}$ *then all links under MPEA, regardless of the initial transmit power vector, will achieve the minimum SINR* β*.*

Proof. As per (3.10), links transmit with non-zero power in iteration $k+1$ if their current effective interference is less than the cutoff threshold (i.e. $E_i(k) \leq \frac{P_{max,i}}{\beta+1}, \forall i$). We rearrange $(\beta+1)\mathbf{D} \leq [\mathbf{I} - (\beta+1)\mathbf{F}]\mathbf{P}_{\max}$ into $(\mathbf{F}\mathbf{P}_{\max} + \mathbf{D}) \leq \frac{\mathbf{P}_{\max}}{\beta+1}$. The effective interference is maximized ($\mathbf{E}_{\max} = \mathbf{F}\mathbf{P}_{\max} + \mathbf{D}$) when all links transmit at full power. Hence, given the inequality condition (i.e. $\mathbf{F}\mathbf{P}_{\max} + \mathbf{D} = \mathbf{E}_{\max} \leq \frac{\mathbf{P}_{\max}}{\beta+1}$), the maximum effective interference possible (LHS) is always less than $\mathbf{P}_{\max}/(\beta+1)$ (RHS). Since $\beta > 0$, $\mathbf{P}(k+1) = \mathbf{P}_{\max} - \mathbf{E}(k) > \mathbf{0}$ always and it also follows that the SINR of each link remains above β. □

Equivalently, we have $\mathbf{E}_{\max} \leq \frac{\mathbf{P}_{\max}}{\beta+1}$ from the above inequality.

3.3.2 Backhaul Congestion

When $V_r(k) < -\tau$, then the relay indicates congestion to the UE-to-RS link j that currently has the highest data rate among the UE-to-RS links (see Algorithm 1). Then $w_j(k+1) = 0$, and link j switches to the objective $\underbrace{\max}_{P_j}(P_{\max,j} - P_j)$ as per (3.6). Its transmit power is adjusted as follows:

$$\begin{aligned} P_j(k+1) &= \min\left(P_{\max,j}, \beta E_j(k)\right) \\ &= \min\left(P_{\max,j}, \frac{\beta}{\gamma_j(k)} P_j(k)\right) \end{aligned} \tag{3.12}$$

Algorithm 2: Power control updates under MH-MPEA for iteration k.

for *UE* $i = 1$ *to* n **do**
  if $w_i(k) = 0$ **then**
    $P_i(k+1) = \min\left(P_{\max,i}, \beta E_i(k)\right)$;
  else if $w_i(k) = 1$ *and* $E_i(k) \leq \frac{P_{\max,i}}{\beta+1}$ **then**
    $P_i(k+1) = P_{\max,i} - E_i(k)$;
  else if $w_i(k) = 1$ *and* $E_i(k) > \frac{P_{\max,i}}{\beta+1}$ **then**
    $P_i(k+1) = 0$.

which is the well-known Foschini-Miljanic (FM) algorithm [18] to meet the target SINR β [34]. Until the backhaul congestion is alleviated, such that that $V_r > -\tau$, an additional UE-to-RS link will switch from MPEA to the FM algorithm at each iteration. If the backhaul capacity becomes sufficiently high (i.e. $V_r(k) \geq 0$), then all UE-to-RS links to relay r may again adapt under MPEA. In the intermediate case, if $-\tau \leq V_r(k) < 0$, the adaptation objective of each link $j \in \mathcal{L}_1$ remains unchanged (i.e. $w_j(k+1) = w_j(k)$).

3.4 Convergence Conditions

We denote the power adaptation mode of links under MH-MPEA as an $L \times L$ diagonal matrix $\mathbf{W}(k+1) = diag[w_1(k+1), \cdots, w_L(k+1)]$. If the inequality condition in Theorem 3.3.1 holds, then the distributed power allocation for the optimization in (3.6) will become:

$$\begin{aligned} \mathbf{P}(k+1) = &[\mathbf{I} - \mathbf{W}(k+1)][\mathbf{P}_{\max} - \mathbf{E}(k)] \\ &+\mathbf{W}(k+1)\beta\mathbf{E}(k) \\ =&\mathbf{Y} + \mathbf{X}\mathbf{P}(k) \end{aligned} \tag{3.13}$$

where $\mathbf{I}$ is the identity matrix, $\mathbf{Y} = \beta\mathbf{W}(k+1)\mathbf{D} + [\mathbf{I} - \mathbf{W}(k+1)][\mathbf{P}_{\max} - \mathbf{D}]$ and $\mathbf{X} = \beta\mathbf{W}(k+1)\mathbf{F} - [\mathbf{I} - \mathbf{W}(k+1)]\mathbf{F}$.

Lemma 3.4.1. *If* $\mathbf{E}_{\max} \leq \frac{\mathbf{P}_{\max}}{\beta+1}$, *then the spectral radius (maximum absolute eigenvalue) of* $\mathbf{X}$ *is less than* 1.

Proof. We manipulate the given inequality to obtain

$$\begin{aligned} \mathbf{E}_{\max} &\leq \frac{\mathbf{P}_{\max}}{\beta+1} \\ (\beta+1)\left(\mathbf{D}+\mathbf{F}\mathbf{P}_{\max}\right) &\leq \mathbf{P}_{\max} \\ \bar{\mathbf{F}}\mathbf{P}_{\max} &< \mathbf{P}_{\max} \end{aligned} \tag{3.14}$$

where $\bar{\mathbf{F}} = (\beta+1)\mathbf{F}$. Multiplying the last inequality above by $\bar{\mathbf{F}}^k$, where $k \in \mathbb{N}$, we obtain $\bar{\mathbf{F}}^{k+1}\mathbf{P}_{\max} < \bar{\mathbf{F}}^k\mathbf{P}_{\max}$ which implies that $\bar{\mathbf{F}}^{k+1}\mathbf{P}_{\max} < \bar{\mathbf{F}}^k\mathbf{P}_{\max} < \bar{\mathbf{F}}^{k-1}\mathbf{P}_{\max} < \cdots < \bar{\mathbf{F}}\mathbf{P}_{\max} < \mathbf{P}_{\max}$. Only if the spectral radius of $\bar{\mathbf{F}}$ is less than one (and thus that of $\mathbf{F}$ less than $\frac{1}{\beta+1}$), would the inequality chain $\lim_{k\to\infty} \bar{\mathbf{F}}^{k+1}\mathbf{P}_{\max}$ be an all-zeros vector [65, pg. 618]. The non-diagonal matrix elements of row i in $\mathbf{X}$ are either the same as those of $\mathbf{F}$ (if $\mathbf{W}(k+1)(i,i) = 0$) or they are scaled by a factor of β (if $\mathbf{W}(k+1)(i,i) = 1$). The spectral radius of $\mathbf{X}$ is thus also bounded by $\frac{\beta}{\beta+1} < 1$ [65, pg. 498]. □

The convergence analysis in [22, 31, 33, 34] is based on the *two-sided scalability* property. In contrast, we illustrate convergence for our scheme using matrix series expansion.

Theorem 3.4.2. *Given a high enough* τ *and* $\mathbf{E}_{\max} \leq \frac{\mathbf{P}_{\max}}{\beta+1}$*, then* $\left[\mathbf{I}-\mathbf{X}\right]^{-1}\mathbf{Y}$ *represents a fixed point solution to* (3.6) *for all links.*

Proof. Setting a high enough τ, indicating an acceptable congestion level, ensures that $V_r(k) > -\tau$ at each relay. Thus, for some value of τ, not all UE-to-RS links will switch to the FM algorithm and the matrix $\mathbf{W}(k+1)$ will thus become constant. Thus, given Theorem 3.3.1 and Lemma 3.4.1, the transmit power vector converges to:

$$\begin{aligned} \mathbf{P}(k+1) &= \mathbf{X} + \mathbf{Y}\left(\mathbf{X} + \mathbf{Y}\left(\mathbf{Y} + \mathbf{X}\left(\cdots\mathbf{P}(0)\right)\right)\right) \\ &= \left[\mathbf{I} + \mathbf{X} + \mathbf{X}^2 + \mathbf{X}^3 + \cdots\right]\mathbf{Y} + \mathbf{X}^k\mathbf{P}(0) \\ \lim_{k\to\infty} \mathbf{P}(k+1) &= \mathbf{P}^* = \left[\mathbf{I}-\mathbf{X}\right]^{-1}\mathbf{Y} \end{aligned} \tag{3.15}$$

□

In practical wireless systems, estimation error will render transmitter-side knowledge

about channel gain to its receiver imperfect [66]. The transmit power updates will thus be based on inaccurate effective interference values. Given the estimated gain $\widehat{g_{i,i}}$ for link i, the effective interference in (3.2) becomes:

$$\widehat{E_i}(k) = \frac{n_o + \sum_{j \neq i, j \in \mathcal{F}(f)} g_{j,i} P_j(k)}{\widehat{g_{i,i}}},$$

Essentially, the estimation error will project $\mathbf{E}(k)$ into

$$\widehat{\mathbf{E}}(k) = \widehat{\mathbf{D}} + \widehat{\mathbf{F}}\mathbf{P}(k),$$

where $\widehat{\mathbf{D}}(i) = n_o/\widehat{g_{i,i}}$ and $\widehat{\mathbf{F}}\mathbf{P}(k)$ is the received interference vector adjusted for the estimated transmitter-receiver gains on the links. Consequently, corresponding to the imperfect channel knowledge, if the inequality $\mathbf{E}'_{\max} = \widehat{\mathbf{F}}\mathbf{P}_{\max} + \widehat{\mathbf{D}} < \frac{P_{\max}}{\beta+1}$ is satisfied then the results in Lemma 3.4.1 and Theorem 3.4.2 still hold. Therefore, under MH-MPEA, links will converge to (3.15) with the values in $\mathbf{X}$ and $\mathbf{Y}$ adjusted for estimation error.

3.5 Feasibility and Fairness

Note that the inequality condition $\mathbf{E}_{\max} \leq \frac{\mathbf{P}_{\max}}{\beta+1}$ may not always be met in a wireless network and some links may be unable to achieve an SINR of β under MPEA. Conversely, for a feasible system it is sufficient to show the existence of a transmit power vector $\mathbf{P}^* = [P_1^*, P_2^*, \cdots, P_L^*]$, meeting the maximum power constraint, such that all links can achieve an SINR of β [30][19].

Theorem 3.5.1. *The sufficient and necessary condition for system feasibility is that the spectral radius of* $\mathbf{F}$ *be less than* $\frac{1}{\beta}$ *and that there be a transmit power vector* $\mathbf{P}^* = \beta[\mathbf{I} - \beta\mathbf{F}]^{-1}\mathbf{D}$ *such that* $\mathbf{P}^* \leq \mathbf{P}_{\max}$.

Proof. See [30][19] for details. □

It has been shown that if a feasible system exists then the FM power control will be able to achieve the target SINR β for all links with minimum aggregate power [19].

The region of particular interest to us is when the system is feasible but some links fail to realize the minimum acceptable SINR when they use MPEA. When system throughput is preferred over instantaneous fairness, having a few links that are unable to achieve a minimal SINR may be justified if the resultant increase in the network's aggregate end-to-end data rate under MPEA is sufficiently high. For the feasible region, we compute the *throughput gain* as the expected value $\mathbf{E}\left[\frac{\eta_N^{''}-\eta_N^{'}}{\eta_N^{'}}\right]$, where $\eta_N^{''}$ is the aggregate end-to-end data rate of the network under our proposed scheme while $\eta_N^{'}$ is the corresponding system throughput under the FM scheme. The *proportion of links* with an SINR less than β can be defined as the expected value $\mathbf{E}[\frac{L_{IF}}{L}]$ where L_{IF} is the number of links unable to achieve β. We use this expectation to assess relative fairness under our scheme. Moreover, under MH-MPEA, UE-to-relay links with the highest instantaneous data rate switch to the FM power control if the relay backhaul is congested. This mechanism improves fairness between different UEs by enabling advantaged flows to reduce interference and congestion which in turn benefits starving flows without diminishing the system throughput. We subsequently characterize, using Monte-Carlo simulations, the tradeoff between the throughput gain and fairness.

3.6 Simulation Results

We consider a multihop network with $N_r = 3$ relays separated by 120^o from the BS at a distance of 2000 m from it. We assume that the link gains are of the form $g_{j,i} = k_{j,i}d_{j,i}^{-\alpha}$, where α is the path loss exponent, $k_{j,i}$ and $d_{j,i}$ are the exponential fading gain (due to Rayleigh block fading) and the distance between the transmitter of link j and the receiver of link i respectively. The gains remain constant for 15 power control iterations. We have $\alpha = 3.0$ for all RS-to-BS links and $\alpha = 3.6$ for all UE links. The maximum transmit power of a UE is 0.5 Watt, that of RS-to-BS links is 3.0 Watts, $\beta = 1.59$ (2 dB), $W = 1$ MHz and $n_o = -120$ dBW.

We first verify (3.15) for the sample network as shown in Fig. 3.1. For this network, we generate random fading coefficients for all links such that $\mathbf{E}_{\max} \leq \frac{\mathbf{P}_{\max}}{\beta+\mathbf{1}}$. All links have a randomly selected initial transmit power level and adapt under MH-MPEA. With $w_1(k+1) =$

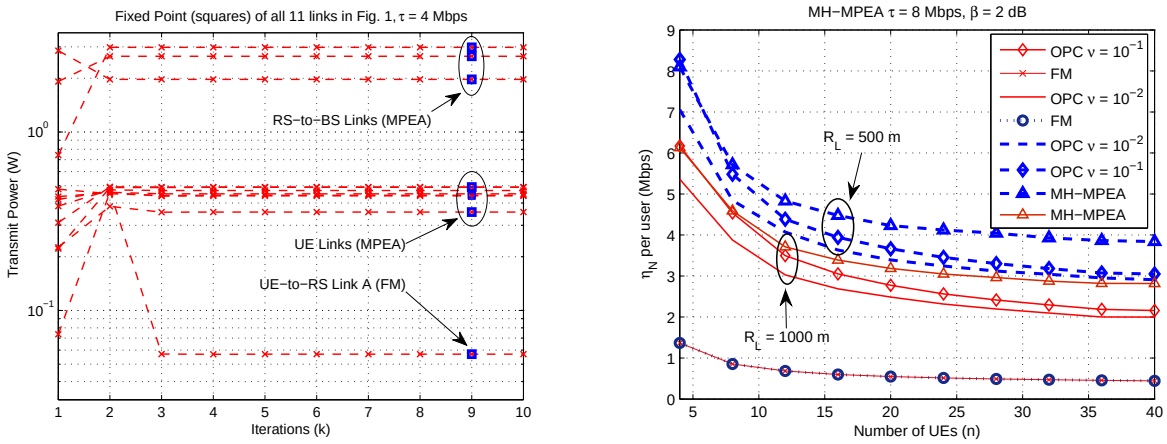

(a) (b)

Figure 3.2: (a) Random initial transmit power levels of links in the sample network converge to the vector in (5.16) (superimposed at $k = 9$), which is a solution of (3.6). (b) MH-MPEA enables better system throughput performance than both the FM and OPC algorithms with increasing n. At $v = 10^{-1}$, links are almost always transmitting at maximum power under OPC.

0 for UE-to-RS link A and $w_j(k+1) = 1$ for the remaining links in Fig 3.1, the transmit powers converge to the corresponding (3.15) as shown in Fig. 3.2a.

Next we simulate the impact of the number of UEs n and of how closely these UEs are clustered around the Points of Access (i.e. one BS and three RS) on the system's aggregate end-to-end data rate. The n UEs in the cell are randomly distributed within circular regions around the Points of Access according to a uniform distribution. The radius of the circular region around each of the four Points of Access is R_L m. For performance comparison, we benchmark against two schemes: (1) all links use the FM algorithm with target SINR β and (2) each link uses the OPC algorithm. The OPC algorithm has been adopted in [22, 31, 33, 34]. Under OPC, each link i adapts as:

$$P_i(k+1) = \min\left(P_{\max,i}, \frac{\nu}{E_i(k)}\right) \tag{3.16}$$

to maintain a constant *Signal-to-Interference-Product* (SIP $\nu = P_i \cdot E_i$) [31]. For the simulation trials, we plot the system throughput performance by averaging the aggregate end-to-end data rate η_N. In Fig. 3.2(b) and Fig. 3.3 we observe that MPEA provides better performance than both FM and OPC algorithms (with different values of ν). The performance

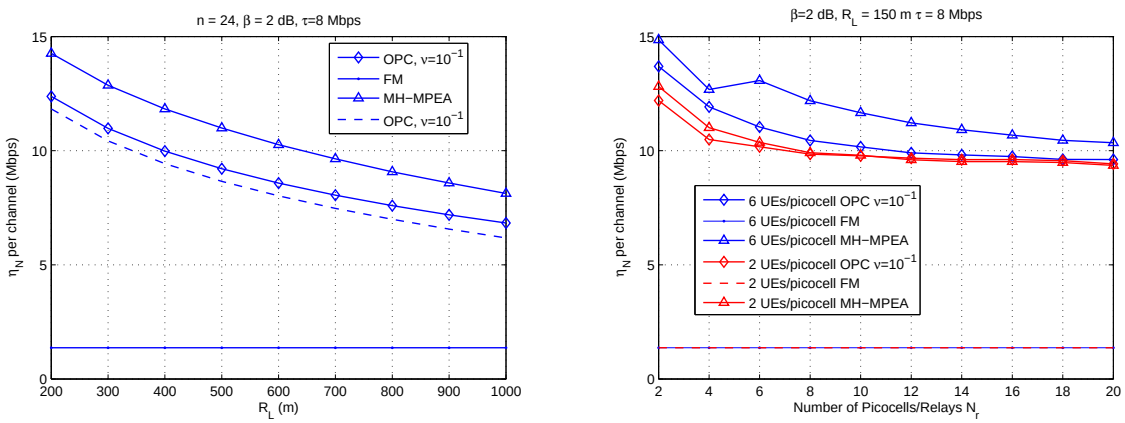

(a) (b)

Figure 3.3: (a) MH-MPEA has the best system throughput performance over the range of cluster radii R_L.(b) With increasing number of relays that have UEs clustered close to them, the multihop network approximates picocell networks overlaid within a macro-cell.

improvement is more pronounced when n is large or when R_L is small (i.e. UEs are clustered closely around their Point of Access). If the UEs are dispersed over a smaller region, the mutual interference between co-channel links becomes smaller and correspondingly the system throughput is higher. In Fig. 3.3b we consider the case when a large number of relays are randomly and uniformly located within the cell in a 2 km $\times$ 2 km square region and the UEs are clustered close to them. The 2-hop network could resemble the situation when picocells with wireless backhaul links coexist within a macro-cellular system [67]. We again observe performance improvement under MH-MPEA, as compared to other schemes.

Next we assess the throughput-fairness tradeoff for MH-MPEA for both the multihop scenario and with only UE nodes in the network. In the single-hop (no relay) scenario, all UEs communicate directly with the BS and lie within a radius R_L m around the BS (i.e. MH-MPEA becomes an all-MPEA scheme). Considering the simulation trials when the system is feasible, in Fig. 3.4a we produce scatter plots of the sample mean of $\left[\frac{\eta_N'' - \eta_N'}{\eta_N'}\right]$ (throughput gain) against the sample mean of $[\frac{L_{IF}}{L}]$ (proportion of infeasible links). The scatter plot is derived by varying R_L from 200m to 1000m for both the multihop and single-hop scenarios. We observe that the throughput gains are at least 200% whereas a maximum of 15% of the links are unable to meet the minimum target SINR. Also note that MH-MPEA is adept at bringing substantial throughput gains as the fairness penalty (i.e. *proportion* of links that

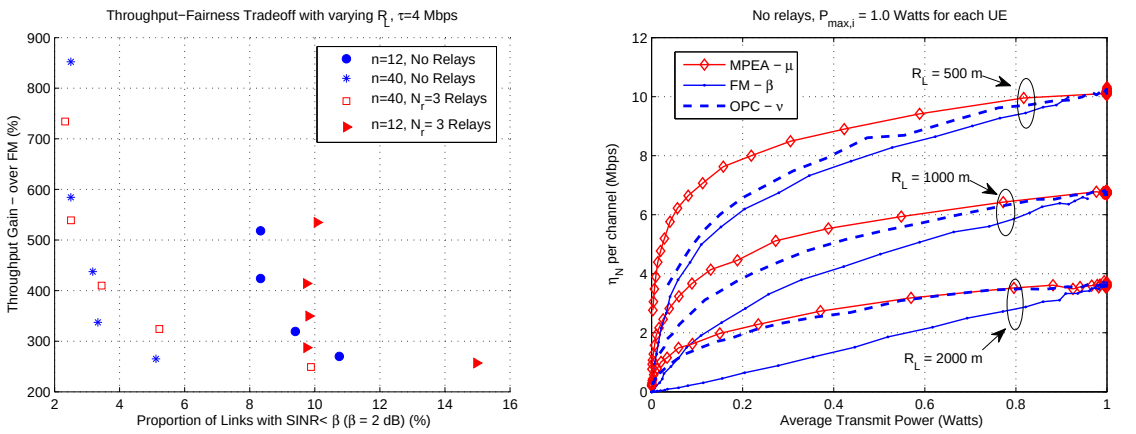

(a) (b)

Figure 3.4: (a) Note the significant throughput gains under MH-MPEA; the relative decrease in the *fraction* of infeasible links with more UEs implies that these gains are robust even with high traffic volume. (b) The average data rate achieved per link is higher for MPEA than that for either OPC or FM algorithms for the same average transmit powers.

are infeasible) becomes relatively smaller with a larger n.

Finally in Fig. 3.4b, we compare the average data rate of a link with MPEA against FM and OPC algorithms in terms of the average transmit power in a network with only UEs (i.e. no relays) and with $P_{\max,i} = 1.0$ Watts for each node. For the FM algorithm, the curve is obtained by adjusting the target SINR over $\beta \in [-10, 30]$ dB. For MPEA we adjust the value of marginal power efficiency as defined in (3.8) over $\mu \in [10^{-3}, 10^{3}]$ whereas the curve for the OPC algorithm is obtained by adjusting the target SIP over $\nu \in [10^{-4}, 10^{0}]$. The larger the values of ν or β, the more is the consumed power and higher is the throughput. We can observe that over the range of parameters, the achieved data rates are larger for MPEA than for FM and OPC algorithms.

3.7 Network State-based Link Adaptations

We now modify the MH-MPEA into a new network state-based link adaptive (NSLA) scheme where nodes are fully autonomous and all have a minimum SINR requirement. Bottleneck links in a multihop wireless network limit the maximum rate achieved by users along their routes [68]. A multihop cellular network can thus be viewed as having two kinds of links:

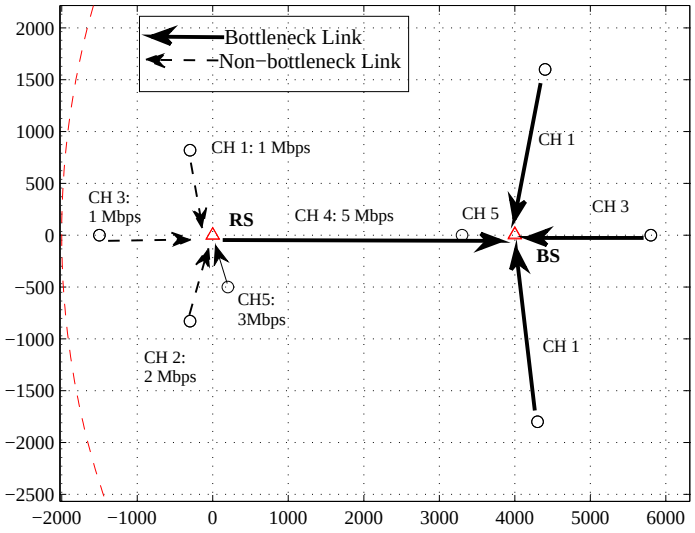

Figure 3.5: In the above multihop cellular network, the RS-to-BS link is a bottleneck link since it is receiving a higher aggregate data rate (7 Mpbs) than its capacity (5 Mbps).

bottleneck and non-bottleneck. For instance, when a large number of nodes are forwarding their data via a relay, the relay-to-base station link can become a bottleneck and is thus more critical to the flows' end-to-end performance. Under the NSLA scheme a link dynamically switches between the MPEA and FM algorithms based on whether it is currently a bottleneck or a non-bottleneck link. Specifically, all non-bottleneck links iteratively reduce their transmit powers until the congestion is alleviated, whereas the bottleneck links aim to improve their SINRs.

In contrast to MH-MPEA, the NSLA scheme has three key features: (i) all links have a minimum target SINR, (ii) whenever congestion is detected at a relay, all its attached UEs can prioritize transmit power-saving instead of one UE being selected at a time, and (iii) if the backhaul link is under-utilized by UEs attached to the relay, then the relay-to-base station link can also reduce its transmit power. Under NSLA we again show substantial system throughput performance gain as compared to related power control schemes with a local scope, and under certain scenarios, we derive a closed-form expression for the converged transmit power levels regardless of their initial values. Through simulation we also compare and weigh the relative performance advantages of NSLA and MH-MPEA.

3.8 Problem Formulation

We associate with each link $i \in \mathcal{L}$ an indicator function w_i such that $w_i = 1$ when the link is a bottleneck link and $w_i = 0$ otherwise. The determination of w_i is based only on whether it is a bottleneck link or not. Recall that under MH-MPEA, in contrast, the value of w_i was fixed for all links except the UE-to-RS links. The *rate differential* V_r between the data rates of all incoming links and the outgoing link for the relay has already been defined in (3.5). When $V_r < 0$, then the RS-to-BS (bottleneck) link limits the total end-to-end data rates of UEs connected through links in $\mathcal{L}_1^r$. The indicator function for an RS-to-BS link $r \in \mathcal{L}_2$ is defined as

$$w_r = \begin{cases} 1 \text{ , if } V_r < 0, \\ 0, \text{ otherwise.} \end{cases} \tag{3.17}$$

Conversely, the indicator function for a UE-to-RS link i attached to the RS is always $w_i = 1 - w_r$, $i \in \mathcal{L}_1^r$. Note that if the RS-to-BS link r is a bottleneck, then all UE-to-RS links in $\mathcal{L}_1^r$ must correspondingly be non-bottleneck, and vice versa. As the links adapt their transmit power and data rates, the rate differential at a relay will change. Consequently, its associated links may switch from bottleneck to non-bottleneck (or vice versa), which will be reflected in their respective indicator values. As for a UE-to-BS link $q \in \mathcal{L}_3$ (the set of all UE-to-BS links), it is always a bottleneck ($w_q = 1, \forall q \in \mathcal{L}_3$) as it directly links to the BS. The dynamic determination of the values w_i is also provided in Algorithm 3.

The local adaptation goal of link $i \in \mathcal{L}$ is stated as an optimization problem

$$\begin{aligned} &\underbrace{\max}_{P_i} w_i\eta_i + (1 - w_i)(P_{max,i} - P_i) \\ &\text{s.t. } \gamma_i \geq \beta \\ &w_i \frac{\partial \eta_i}{\partial P_i} \geq w_i \mu_i \\ &P_i \leq P_{\max,i}, \forall i \\ &w_i \in \{0, 1\}, \forall i \end{aligned} \tag{3.18}$$

In contrast to (3.6), all links have a minimum SINR requirement β (i.e. feasibility constraint)

Algorithm 3: NSLA: The dynamic determination of w_i for each link i.

```
Initialization: w_i(0) = 1, ∀i
Iteration k: Link i adapts as per (3.18), ∀i
for Relay r = 1 to N_r do
    if V_r(k) < 0 then
        w_j(k+1) = 0, ∀j ∈ L_1^r;
        w_i(k+1) = 1, i ∈ L_2;
    else if V_r(k) ≥ 0 then
        w_j(k+1) = 1, ∀j ∈ L_1^r;
        w_i(k+1) = 0, i ∈ L_2;
return to Iteration k = k + 1.
```

given a limit on the maximum transmit power. Each bottleneck link needs to meet the marginal power efficiency threshold as well. Note that the aggregate end-to-end data rate in the network that was defined earlier in eq. (5.4) is equivalently the sum data rate of all bottleneck links:

$$\eta_N = \sum_{\forall i} w_i \eta_i. \tag{3.19}$$

3.9 Network-wide Adaptations Algorithm

In NSLA, distributed power control is performed to heuristically approach a solution to the optimization problem in (3.18). The determination of bottleneck and non-bottleneck links is made by tracking rate differentials at the relays and disseminating this information to the attached UEs in each iteration $k \in \{1, 2, ..\}$. As the network adapts, the values of w_i can dynamically change and thus link i would also correspondingly update its adaptation algorithm depending on whether it is currently a bottleneck link or not.

3.9.1 Bottleneck Links

If link i is a bottleneck in iteration k (i.e. $w_i(k) = 1$) then its transmit power is updated according to:

$$P_i(k+1) = \begin{cases} P_{\max,i} - E_i(k), \text{ if } E_i(k) \leq \frac{P_{\max,i}}{\beta+1} \text{ (a)} \\ \min\left(P_{\max,i}, \frac{\beta}{\gamma_i(k)} P_i(k)\right), \text{ otherwise (b).} \end{cases} \tag{3.20}$$

As reflected in (3.20a), the power control for a bottleneck link corresponds to the Marginal Power Efficiency-based Adaptation (MPEA) with the substitution of $\mu_i = \frac{W}{\log(2) P_{\max,i}}$ into (3.18). Under unfavorable channel conditions, (3.20a) will be unable to achieve the minimum SINR β (i.e. if the effective interference becomes larger than $\frac{P_{\max,i}}{\beta+1}$). To satisfy the minimum SINR constraint in (3.18), the transmitter can switch to the FM algorithm (3.20b) [18]. Thus, the two-mode power control for bottleneck links in (3.20) combines the advantageous features of both algorithms.

3.9.2 Non-bottleneck Links

When congestion is detected at a relay, each of its associated non-bottleneck links switches to a transmit power minimization mode. In contrast to MH-MPEA, where the power-minimizing links always had a fixed target SINR β, under NSLA their target SINRs are iteratively reduced to this minimum acceptable SINR threshold. Given that the current SINR of non-bottleneck link j is $\gamma_j(k)$ and the rate differential at its RS r is $V_r(k)$, the link's target SINR $\overline{\gamma_j}(k+1)$ is dynamically revised via:

$$\overline{\gamma_j}(k+1) = \begin{cases} \max(\beta, z\gamma_j(k)), \text{ if } V_r(k) < -\tau \text{ , (a)} \\ \max(\beta, \gamma_j(k)), \text{ if } -\tau \leq V_r(k) < 0 \text{ , (b)} \end{cases} \tag{3.21}$$

where $0 < z < 1$ and $\tau \geq 0$. Given the target SINR $\overline{\gamma_j}(k+1)$, link j then uses the FM algorithm of [18] to update its transmit power:

$$P_j(k+1) = \min\left(P_{\max,j}, \frac{\overline{\gamma_j}(k+1)}{\gamma_j(k)} P_j(k)\right). \tag{3.22}$$

Algorithm 4: Power control updates under NSLA for iteration k for link i.

```
if w_i(k) = 0 then
    if V_r(k) < −τ then
        γ̄_i(k+1) = max(β, z.γ_i(k));
    else if −τ ≤ V_r(k) < 0 then
        γ̄_i(k+1) = max(β, γ_i(k));
    P_i(k+1) = min(P_max,i, γ̄_i(k+1).E_i(k));
else if w_i(k) = 1 then
    if E_i(k) > P_max,i/(β+1) then
        P_i(k+1) = min(P_max,i, βE_i(k));
    else if E_i(k) ≤ P_max,i/(β+1) then
        P_i(k+1) = P_max,i − E_i(k).
```

Effectively, the transmit power (and data rate) of a non-bottleneck link is iteratively decreased until the congestion is alleviated (while ensuring that the achieved SINR is always equal to or more than β). If the congestion drops to an acceptable level (i.e. $-\tau \leq V_r(k) < 0$), the transmit power of the non-bottleneck link is maintained in the next iteration as per (3.21b).

Note that if a bottleneck and non-bottleneck link are on the same channel (see Fig. 3.5 as an example) this iterative transmit power reduction also decreases interference for the bottleneck link. Thus, a bottleneck link can benefit from this interference reduction and correspondingly also increase its transmit power as per (3.20a). These twin factors will thus result in a higher SINR for the bottleneck link. In Algorithm 4, the transmit power update for all UEs is stated in pseudo-code form.

3.10 Convergence

Now we consider convergence under the NSLA scheme. We define $\mathbf{W}(k+1) = diag[w_1(k+1), w_2(k+1), \cdots w_L(k+1)]$ where $w_i(k+1) \in \{0, 1\}$. To reiterate, under NSLA, each transmitter adapts to always achieve the minimum target SINR on its link regardless of whether it is a bottleneck or non-bottleneck link.

Proposition 3.10.1. *Under NSLA, if* $\mathbf{E}_{\max} \leq \frac{\mathbf{P}_{\max}}{(\beta+1)}$ *then the minimum target SINR* β *can be met by all links and the bottleneck links adapt as per MPEA.*

Proof. Given that $\mathbf{E}_{\max} = \mathbf{F}\mathbf{P}_{\max} + \mathbf{D} \leq \frac{\mathbf{P}_{\max}}{\beta+1}$, the maximum possible network-wide effective interference is always less than the threshold $\mathbf{P}_{\max}/(\beta+1)$ for all links (see Algorithm 4). It follows that under both the MPEA and FM algorithms, the transmitter i has sufficient transmit power to achieve the minimum SINR β. □

If $\mathbf{E}_{\max} \leq \frac{\mathbf{P}_{\max}}{\beta+1}$, then each bottleneck link is operating with MPEA whereas each non-bottleneck link is operating with the variant-FM algorithm in (3.21). The power control updates of all the L links is then

$$\mathbf{P}(k+1) = \mathbf{W}(k+1)[\mathbf{P}_{\max} - \mathbf{E}(k)] + [\mathbf{I} - \mathbf{W}(k+1)]\mathbf{\Gamma}(k+1)\mathbf{E}(k) \tag{3.23}$$

where $\mathbf{E}(k) = \mathbf{D} + \mathbf{F}\mathbf{P}(k)$ and $\mathbf{\Gamma}(k+1) = diag[\gamma_1(k+1), \cdots \gamma_L(k+1)]$ is the $L \times L$ diagonal matrix of target SINRs of the non-bottleneck links.

Theorem 3.10.2. *If* $\mathbf{E}_{\max} \leq \frac{\mathbf{P}_{\max}}{\beta+1}$*, then for a high enough* τ *the transmit power vector converges under NSLA.*

Proof. With the constraint on the maximum interference, the minimum requisite SINR can be met by all links as per Theorem 3.10 and the spectral radius of $\mathbf{F}$ is less than one as per Lemma 3.4.1. Moreover, given a high enough τ, a bottleneck link adapts under MPEA as per (3.20a) whereas a non-bottleneck link will maintain its transmit power from a preceding iteration as per eq. (3.21b) since the congestion level is within the tolerable range. Thus, eq. (3.23) reduces to

$$\begin{aligned} \mathbf{P}(k+1) &= \mathbf{W}(k+1)[\mathbf{P}_{\max} - \mathbf{E}(k)] + [\mathbf{I} - \mathbf{W}(k+1)]\mathbf{P}(k) \\ &= \mathbf{W}(k+1)[\mathbf{P}_{\max} - \mathbf{F}\mathbf{P}(k) - \mathbf{D}] + [\mathbf{I} - \mathbf{W}(k+1)]\mathbf{P}(k) \end{aligned} \tag{3.24}$$

where $\mathbf{W}(k+1)$ is the quasi-identity matrix. The evolution of transmit powers above is essentially equivalent to all links either updating their transmit power according to MPEA

or maintaining it (i.e. their transmit power levels are based on an update from an earlier iteration). The power updates can therefore be described as an *asynchronous iterative* system [69][70]. It is known that such a system converges if the iterative matrix $\mathbf{F}$ in (3.24) has a spectral radius less than one [70]. □

Limited Backhaul Capacity

We next derive a closed-form expression for a convergence point of transmit power levels under NSLA (similar to what we had for MH-MPEA), for when the network is rate-limited by the RS-to-BS backhaul links. For instance, this would be when the number of UEs each relay has to serve is sufficiently large such that even if the SINR of each UE-to-RS link is the minimum β and the RS-to-BS links operate at full power with no interference, there is still congestion at each relay r (i.e. $V_r(k) \leq W\left(\log_2(1+\frac{g_{r,r}P_{\max,r}}{n_o}) - |\mathcal{L}_1^r|\log_2(1+\beta)\right) < 0$, where $g_{r,r}$ is the gain of the RS-to-BS link).

Thus, under NSLA, if network performance is rate-limited by the RS-to-BS links, then the dynamically-updated target SINR $\overline{\gamma}_i(k+1)$ converges to β for each UE-to-RS link $i \in \mathcal{L}_1$ if we set $\tau = 0$ to minimize congestion at the relays. Hence, we will have $\lim_{k\to\infty} \mathbf{\Gamma}(k+1) = \mathbf{\Gamma}_\beta = diag[\beta, \cdots, \beta]$ and we can replace $\mathbf{W}(k+1)$ with an $L \times L$ diagonal matrix $\mathbf{W}_a$ where

$$\mathbf{W}_a(i,i) = \begin{cases} 0 \text{ , if } i \in \mathcal{L}_1, \\ 1, \text{ otherwise.} \end{cases} \tag{3.25}$$

Given that $\mathbf{E}_{\max} \leq \frac{\mathbf{P}_{\max}}{\beta+1}$, we can then modify (3.23) to obtain:

$$\begin{aligned} \mathbf{P}(k+1) &= \mathbf{W}_a[\mathbf{P}_{\max} - \mathbf{E}(k)] + [\mathbf{I} - \mathbf{W}_a]\mathbf{\Gamma}_\beta(k+1)\mathbf{E}(k) \\ &= \mathbf{Y}_a + \mathbf{X}_a\mathbf{P}(k) \end{aligned} \tag{3.26}$$

where $\mathbf{Y}_a = \beta\mathbf{W}_a\mathbf{D} + [\mathbf{I} - \mathbf{W}_a][\mathbf{P}_{\max} - \mathbf{D}]$ and $\mathbf{X}_a = \beta\mathbf{W}_a\mathbf{F} - [\mathbf{I} - \mathbf{W}_a]\mathbf{F}$.

Theorem 3.10.3. *In a network where performance is rate-limited by RS-to-BS links, then with* $\mathbf{E}_{\max} \leq \frac{\mathbf{P}_{\max}}{\beta+1}$*, the transmit power vector converges to* $[\mathbf{I} - \mathbf{X_a}]^{-1}\mathbf{Y}_a$.

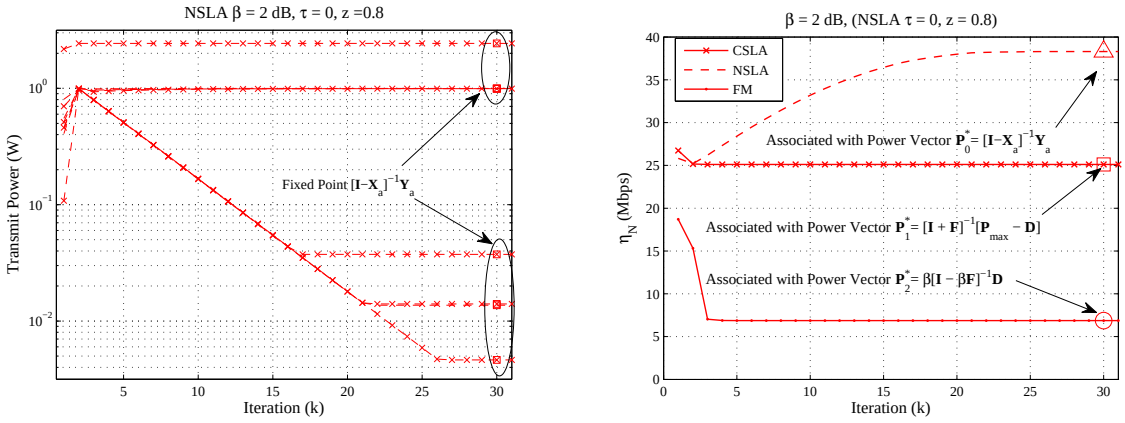

(a) (b)

Figure 3.6: (a) Evolution of transmit powers and convergence to the vector predicted by (3.27) for the network in Fig. 3.5. (b) Taking into account end-to-end goals via NSLA correspondingly enables the best performance.

Proof. The spectral radius of $\mathbf{X}_a$ is less than one (see Lemma 3.4.1). Moreover, with $\tau = 0$ then the target SINR of all non-bottleneck links becomes β. Hence, the transmit power levels in (3.26) evolve to:

$$\begin{aligned} \mathbf{P}(k) &= \mathbf{Y}_a + \mathbf{X}_a\left(\mathbf{Y}_a + \mathbf{X}_a\left(\mathbf{Y}_a + \mathbf{X}_a\left(\cdots \mathbf{P}(0)\right)\right)\right) \\ &= \left[\mathbf{I} + \mathbf{X}_a + \mathbf{X}_a^2 + \mathbf{X}_a^3 + \cdots\right]\mathbf{Y} + \mathbf{X}_a^{k-1}\mathbf{P}(0) \qquad (3.27) \\ \lim_{k\to\infty} \mathbf{P}(k) &= \mathbf{P}_0^* = \left[\mathbf{I} - \mathbf{X}_a\right]^{-1}\mathbf{Y}_a \end{aligned}$$

□

We can verify the above derivation in Fig. 3.6a, where we plot the evolution of transmit powers under NSLA given a set of randomly selected initial transmit powers for the network shown in Fig. 3.5. We assume that the gain is of the form $g_{j,i} = d_{j,i}^{-\alpha}$, where α is the path loss exponent ($\alpha = 3.0$ in Fig. 1), $W = 1$ MHz and $d_{j,i}$ is the distance between the transmitter of link j and the receiver of link i. The maximum transmit power of UEs is 1 Watt, that of the relay-to-BS link is 2.5 Watts, while the noise power is set as $n_o = -120$ dBW. Given $\beta = 1.59$ (2 dB), the inequality $\mathbf{E}_{\max} \leq \frac{\mathbf{P}_{\max}}{(\beta+1)}$ is satisfied. With $z = 0.8$ and $\tau = 0$, we observe that the transmit powers for NSLA converge to the vector predicted by (3.27).

3.10.1 Benchmark Power Control Schemes

We compare the performance of NLSA with that of other power control schemes with only a link layer objective:

1. Channel State-based Link Adaptation (CSLA): Each link uses the power control in eq. (3.20) only. In CSLA, each transmitter either adapts with the FM algorithm to achieve the minimum target SINR when channel conditions are harsh or it waterfills with the MPEA when the channel is good. Note that the CSLA scheme is similar to the two-mode power control scheme in [34] where a link switches between the FM algorithm and the *opportunistic* power control of [31] depending on its instantaneous effective interference.

2. FM algorithm: Each link simply tries to maintain a target SINR β.

In Fig. 3.6b, we plot the evolution of the aggregate user data rate for the three power control schemes. Given the system parameters used in Fig. 3.6a, all links adapt as per MPEA under the CSLA scheme. Thus, we set $\mathbf{W}_a = \mathbf{I}$ (i.e. no link uses the FM algorithm) to obtain $\mathbf{X}_a = -\mathbf{F}$ and $\mathbf{Y}_a = \mathbf{P}_{\max} - \mathbf{D}$ in eq. (3.27). The converged transmit power vector is then $\mathbf{P}_1^* = [\mathbf{I} + \mathbf{F}]^{-1} [\mathbf{P}_{\max} - \mathbf{D}]$. In contrast, with the FM algorithm, we set $\mathbf{W}_a = 0.\mathbf{I}$ (i.e. no link uses the MPEA algorithm). Since $\mathbf{X}_a = \beta\mathbf{F}$ and $\mathbf{Y}_a = \beta\mathbf{D}$, then the converged transmit power vector in eq. 3.27 is $\mathbf{P}_2^* = \beta [\mathbf{I} - \beta\mathbf{F}]^{-1} \mathbf{D}$.

Observe that the transmit power levels converge to the aggregate user data rate corresponding to the vectors $\mathbf{P}_0^*$, $\mathbf{P}_1^*$ and $\mathbf{P}_2^*$ (plotted for $k = 30$). Also note that NSLA outperforms both these schemes that only optimize link layer performance.

3.11 Simulation Results

We consider a multihop network with $N_r = 3$ relays separated by 120^o from the BS at a distance of 2000 m from it. We assume that the link gains are of the form $g_{j,i} = k_{j,i} d_{j,i}^{-\alpha}$, where α is the path loss exponent, $k_{j,i}$ and $d_{j,i}$ are the exponential fading gain (due to Rayleigh block fading) and the distance between the transmitter of link j and the receiver

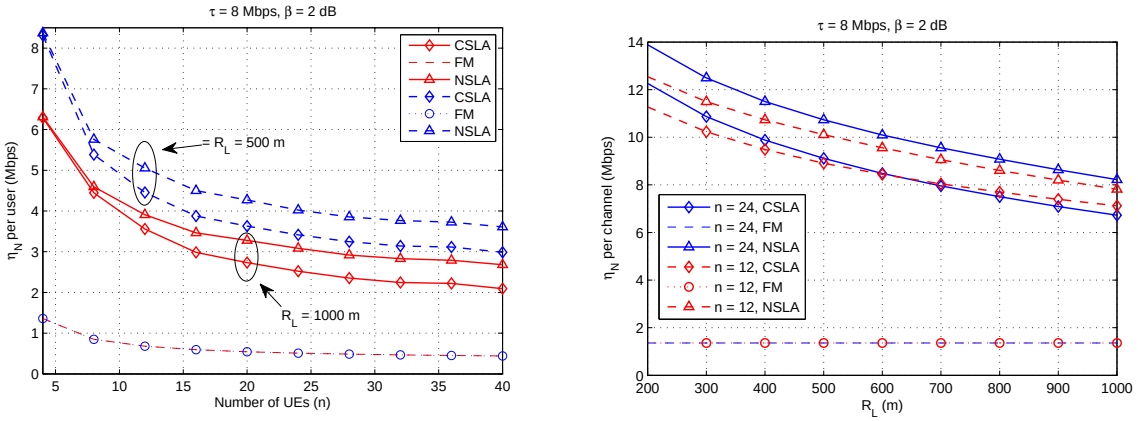

(a) (b)

Figure 3.7: (a) We observe that NLSA outperforms CSLA and FM algorithm over the range of n (the latter schemes only optimize link layer metrics). (b) The performance advantage of NSLA over CSLA and FM increases when R_L becomes smaller and UEs are clustered closer.

of link i respectively. The gains remain constant for 25 power control iterations. We have $\alpha = 3.0$ for all RS-to-BS links and $\alpha = 3.6$ for all UE links. The maximum transmit power of a UE is 0.5 Watt, that of RS-to-BS links is 3.0 Watts, $\beta = 1.59$ (2 dB), $W = 1$ MHz and $n_o = -120$ dBW. The transmit powers of downlink pilot signals from the BS and RS are assumed equal. There are a total of n UEs in the cell, again randomly distributed within circular regions of radii R_L m around the four receiver stations (i.e. one BS and three RS) according to a uniform distribution. Unless stated otherwise, the NSLA parameter is set as $z = 0.9$ and $R_L = 1000$ m. We average the corresponding value of η_N for an appropriate number of trials.

In Fig. 3.7a we plot the aggregate end-to-end data rate in the network against the total number of UEs n. We see that NSLA outperforms CSLA and the FM algorithm over the range of n. In Fig. 3.7b, we plot the average aggregate user data rate as a function of how closely the UEs are dispersed across the receiver stations. When R_L is large, the UEs are dispersed over wider regions while, conversely, when R_L is small, the UEs are clustered more closely. We observe a significant gap between the system throughput achieved by NSLA over both CSLA and the FM algorithm over the range of R_L. If the UEs around the receiver stations are clustered more closely, the advantage afforded by NSLA increases. In other words, NSLA becomes more advantageous in interference-limited regimes.

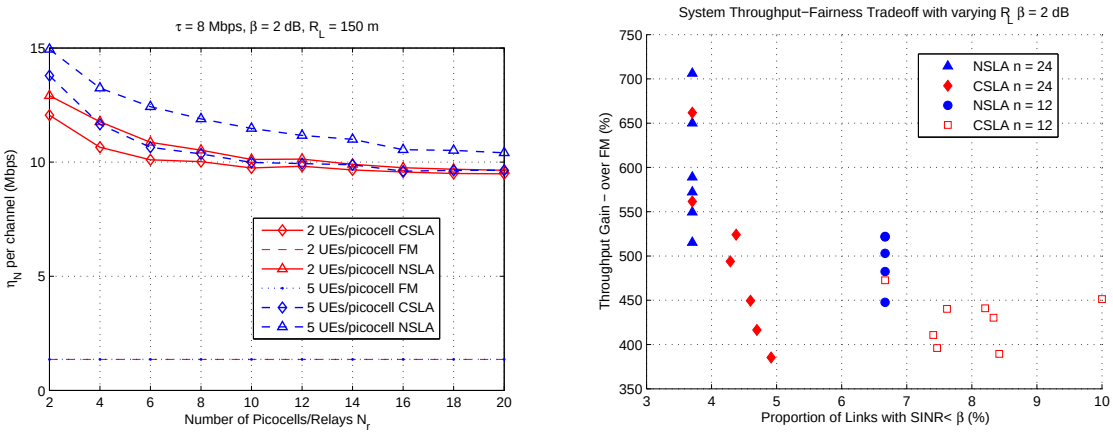

(a) (b)

Figure 3.8: (a) With a large number of relays that approximate overlaid picocell networks, we observe that NSLA yields a better performance than CSLA and FM algorithm. (b) NSLA has a higher throughput gain and fewer infeasible links than CSLA.

In 3.8a, we observe the superior system performance with NSLA against other schemes over the range of N_r that indicates the number of randomly located relays within a 2 km $\times$ 2 km square region. The UEs are also located randomly within $R_L = 150$ m of each PoA. To plot the results in 3.8b, we consider the simulation trials when all links' SINR can converge to β under the FM scheme (i.e. the system is feasible) but when either NSLA or CSLA may not reach a feasible solution. We produce a scatter plot of the sample mean of $\mathbf{E}\left[\frac{\eta_N'' - \eta_N'}{\eta_N'}\right]$ against the sample mean of $\mathbf{E}[\frac{L_{IF}}{L}]$ (see Section 3.6: Feasibility and Fairness above). We can observe that the proportion of inadmissible links may range between 3-7% for NSLA while it ranges between 3-10% for CSLA. Likewise, the throughput gain in the user data rate varies between 450-730% for CSLA but it is 350-660% for NSLA. Thus, NSLA does better than CSLA in terms of both system throughput and relative feasibility.

3.12 NSLA versus MH-MPEA

Recall that in MH-MPEA, if a RS-to-BS link suffers congestion, the associated UE-to-RS links sequentially switch to transmit power minimization, whereas under NSLA their reduction is in parallel. In Fig. 3.9, we compare MH-MPEA and NSLA in terms of system

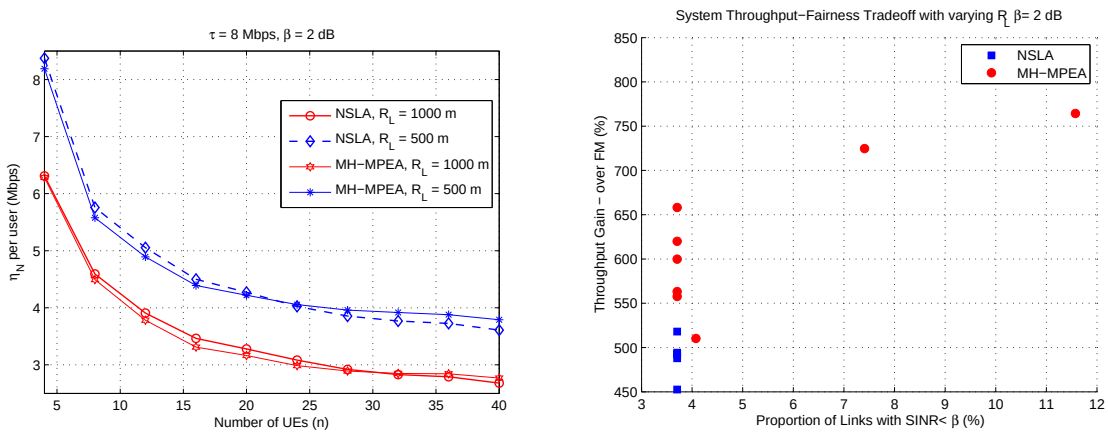

(a) (b)

Figure 3.9: (a) In terms of system throughput, the NSLA and MH-MPEA are not much different. (b) However, in terms of system feasibility NSLA has an advantage owing to its constraint in meeting the minimum SINR requirement by all links.

throughput and feasibility. While we note that there is not much of a difference between the two with regards to η_N, NSLA has a feasibility advantage as links switch to the FM algorithm to ensure that the minimum target SINR is met. In Fig. 5.9, we plot the results by varying the rate differential threshold τ. We observe that too low a τ can lead to instability and therefore a low system throughput whereas too high a τ can ensure convergence albeit at the cost of tolerance for congestion for both MPEA-based schemes. Finally in Fig. 3.11, we plot the average transmit power consumption in a network, for the two schemes. For these plots, we have 100 power control iterations per simulation trial and set $z = 0.8$ for NSLA. We observe that MH-MPEA generally has better energy consumption performance than NSLA over the range of simulated parameters. In contrast, note that nodes have a greater degree of autonomy under NSLA.

3.13 Conclusions

We have proposed two marginal power efficiency-based power control schemes that can be used in conjunction with the FM algorithm for cellular systems, taking into account network-wide conditions to regulate each link's transmit power. We have derived closed-form expressions for fixed points of the transmit power levels under either adaptation approach and have

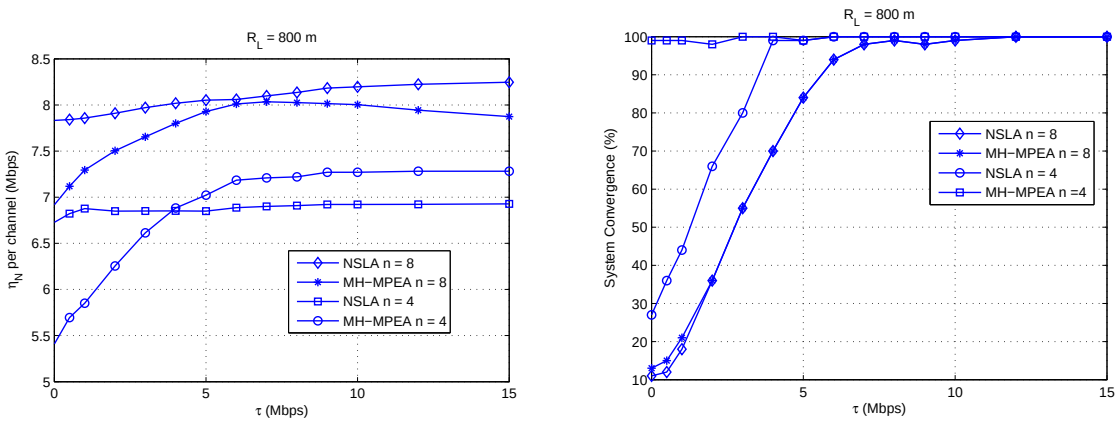

(a) (b)

Figure 3.10: (a) The effect of τ on system throughput and in (b) as τ increases the likelihood of convergence increases under both NSLA and MH-MPEA.

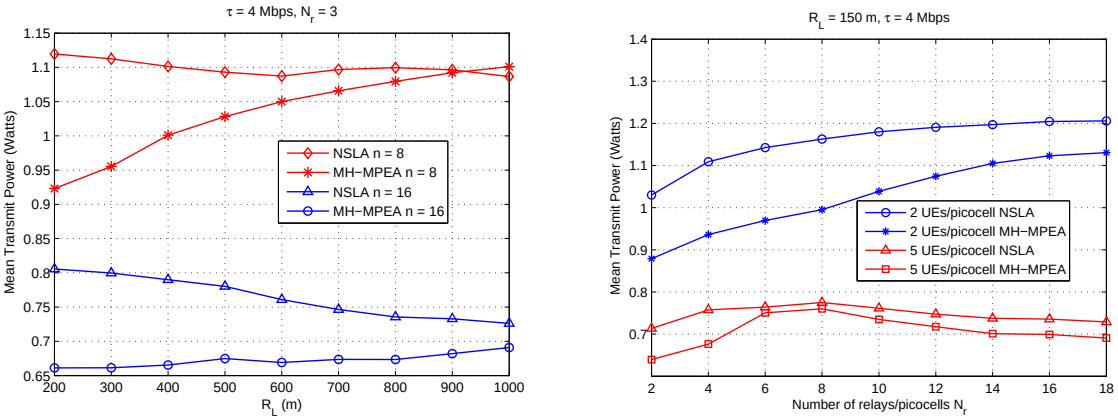

(a) (b)

Figure 3.11: The energy consumption of MH-MPEA is more attractive than of NSLA over the shown range of (a) cluster radius and (b) number of relays.

found a significant benefit to overall network performance in terms of both system throughput and relative fairness. We observe that the proposed adaptation schemes are particularly suitable for LTE-Advanced networks that deploy relays to improve coverage. In the next chapter we extend our analysis to when nodes can also aggregate additional channels and adapt their PoA within the network in response to the current congestion conditions.

Chapter 4

Transmit Power, Carrier Aggregation and Topology Adaptations

Carrier aggregation (CA) is a feature of LTE-Advanced that enables mobiles to support high data rates by aggregating additional channels that lie in contiguous or non-contiguous frequency bands [1]. In this chapter, we study the problem of carrier aggregation with power control for multihop cellular networks as envisioned in LTE-Advanced, where mobiles have the additional flexibility to dynamically change their point of access in the network (between the base station or the relays). We adopt the NSLA power control scheme presented in the preceding chapter into a mechanism that incorporates bandwidth and topology adaptations so that a mobile can optimize a combination of achieved data rate and power consumption.

We consider cellular systems with multiple relays where each relay periodically broadcasts feedback on the current traffic volume supported on its backhaul uplink. A UE that is connected to a relay which is suffering congestion cannot increase its end-to-end data rate by simply increasing its transmit power. Under our adaptive scheme, when faced with a congested relay, the UE either minimizes its transmit power (to conserve battery life and to reduce interference) or connects to a better access point (with sufficient backhaul capacity) to improve its data rate performance. Conversely, when the system offers sufficient resources, the node can maximize its data rate using power control and by aggregating additional

channels.

We compare our proposed approach to the case when UEs cannot dynamically select their points of access to the network, simply associating with the point of access with the strongest received signal strength, and perform greedy power and channel aggregation adaptations. We show that our approach results in a significant improvement in system throughput.

4.1 System Model

Consider a single-cell network serving n user equipment (UEs) from a set $\mathcal{N} = \{1, 2, \cdots, n\}$ that wish to communicate with the Base Station (BS) on the uplink. There are N_r fixed relays (RS), which are located towards the edges of the cell to provide coverage for the UE nodes located farther away from the base station (see Fig. 4.1 with $N_r = 1$). All Points of Access (PoA) are denoted by a set $\mathcal{R} = \{1, 2, \cdots, N_r, N_r + 1\}$ where elements 1 to N_r indicate an RS and the BS is represented by element $N_r + 1$. A subset of UEs uplink to the BS directly, whereas other UEs uplink to one of the RSs. The RS decodes-and-forwards the data from these UEs to the BS. We denote the PoA that node i connects to as $r_i \in \mathcal{R}$.

We assume that there are multiple orthogonal channels, each of bandwidth W Hz. Each UE is initially assigned a single communication channel. Channel assignments are made such that nodes transmitting to a given PoA operate on orthogonal channels. Each of these channels can be *reused* by nodes attached to other PoAs (see Fig. 4.1(a) for example). We represent the set of channels as $\mathcal{F} = \{1, 2, \cdots, F\}$. We use an indicator function to denote whether UE i is communicating on channel f:

$$c_{if} = \begin{cases} 1 \text{ if } i \text{ uses } f \in \mathcal{F} \\ 0 \text{ otherwise.} \end{cases} \tag{4.1}$$

A node may operate over multiple channels, for which it has to allocate its transmit

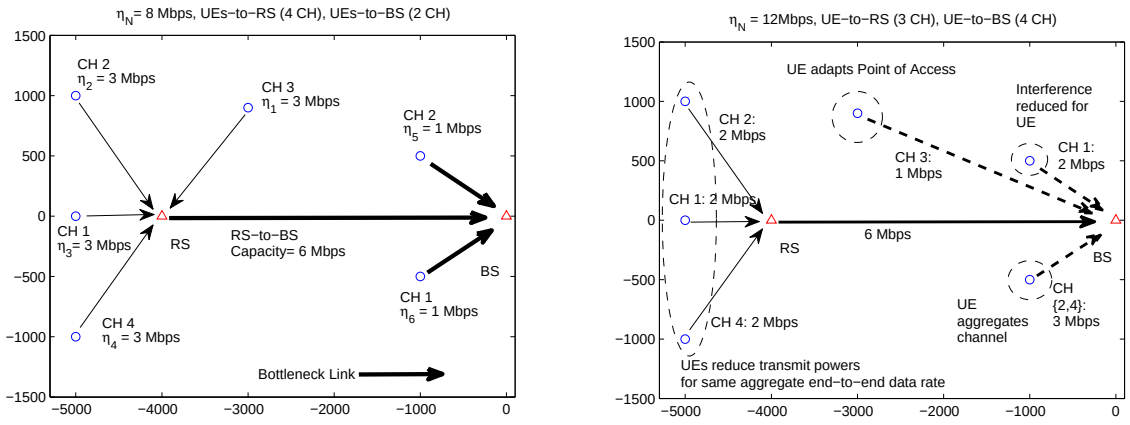

(a) (b)

Figure 4.1: (a) A depiction of the initial topology and channel assignments where the performance of all UE-to-RS links is limited to 6 Mbps. (b) Each node makes its adaptation based on its reading of the latest network-wide conditions.

power. Given a maximum available transmit power $P_{\max,i}$, the total consumed power is

$$P_i = \sum_{\forall f} c_{if} P_{if} \leq P_{\max,i} \tag{4.2}$$

where P_{if} is the transmit power of node i on channel f. Let g_{fir_i} and g_{fjr_i} represent the channel gains between the nodes $i, j \in \mathcal{N}$ and node i's receiver $r_i \in \mathcal{R}$ on channel f, which depend on several factors such as the path loss and fading. In the sequel, with a slight abuse of notation, we refer to these gains as g_{fir} and g_{fjr} respectively. The effective interference E_{if} suffered by node i on channel f (for which $c_{if} = 1$) is defined as

$$E_{if} = \frac{n_o + \sum_{j \neq i, j \in \mathcal{N}} c_{jf} g_{fjr} P_{jf}}{g_{fir}}, \tag{4.3}$$

where n_o is the total thermal noise power per channel and P_{jf} is the transmit power allocated by node $i's$ co-channel interferer $j \in \mathcal{N}$. Thus, the signal-to-interference-and-noise ratio (SINR) of i on channel f is

$$\gamma_{if} = \frac{P_{if}}{E_{if}} = \frac{g_{fir} P_{if}}{n_o + \sum_{j \neq i, j \in \mathcal{N}} c_{jf} g_{fjr} P_{jf}}. \tag{4.4}$$

The corresponding data rate of the link of node i is assumed to be

$$\eta_i = W. \sum_{\forall f: c_{if}=1} \log_2(1+\gamma_{if}) \text{ bits/s.} \tag{4.5}$$

We assume that each RS-to-BS link has a capacity η_r bps and operates on out-of-band channels with fixed bandwidth. We then define the *rate differential* across the RS $r \in \{1, 2, \cdots N_r\}$ as

$$V_r = \eta_r - \sum_{\forall i: r_i = r} \eta_i \tag{4.6}$$

which denotes the difference between the aggregate incoming data rate from its UEs and the capacity of the outgoing RS-to-BS link. When $V_r \geq 0$, the corresponding UE-to-RS links are considered *bottleneck links*, as they constrain the end-to-end performance. Conversely, when $V_r < 0$, the RS-to-BS link becomes the bottleneck. Note that the UE-to-BS links are also deemed as bottleneck for those respective nodes. Finally, we use an indicator function w_i to denote whether the link of node i to its receiver is a bottleneck link:

$$w_i = \begin{cases} 1 \text{ node } i \text{ has a bottleneck link} \\ 0 \text{ otherwise.} \end{cases} \tag{4.7}$$

4.2 Problem Formulation

The aggregate end-to-end data rate in the network, denoted as η_N, is the sum of the data rates of all bottleneck links. Using the Max-Flow Min-Cut Theorem [62], this is expressed as:

$$\eta_N = \sum_{\forall i: r_i = N_r+1} \eta_i + \sum_{r=1}^{N_r} \min\left(\eta_r, \sum_{\forall m: r_m = r} \eta_m\right). \tag{4.8}$$

Since nodes are autonomous, we propose that the local adaptation objective of a node should depend on the current network-wide conditions: if node i has a bottleneck link to its receiver r_i ($w_i = 1$), it should try to maximize its data rate. Conversely, with a non-bottleneck link ($w_i = 0$), it should either maximize its battery life subject to some minimum SINR or connect to another PoA to improve its end-to-end data rate. Node i's local objective

function is therefore:

$$\begin{aligned}
\underbrace{\max}_{P_{i1},..,P_{if},c_{i1},..,c_{if},r_i} \quad & w_i\eta_i - (1-w_i)v_i \sum_{\forall f} c_{if}P_{if} \\
\text{s.t. } & \gamma_{if} \geq \beta, \forall i, \forall f : c_{if} = 1 \\
& \sum_{\forall f} c_{if}P_{if} \leq P_{\max,i}, \forall i \\
& \sum_{\forall f} c_{if} \geq 1, \forall i \\
& (r_i - r_j)^2 + (2 - c_{if} - c_{jf}) > 0, \forall r_i, r_j, \forall i, \forall j : i \neq j \\
& w_i \in \{0, 1\}, \forall i
\end{aligned} \tag{4.9}$$

where v_i is a positive constant defined by the UE i. Since the choice of PoA by the UE can affect w_i, this constant reflects the relative weight the node assigns to the two objectives. For instance, if v_i is large, the UE prioritizes maximizing battery life, whereas, conversely it prefers maximizing its data rate if v_i is small. The first two constraints reflect a need to meet some minimal SINR threshold β for each channel a link uses (i.e. feasibility constraint), given a limit on the maximum transmit power of each node. The third reflects that a UE may operate over multiple (and possibly non-contiguous) channels. The fourth *channel assignment* constraint ensures that node i does not transmit on the same channel as node j to communicate to a common PoA.

Defining which link is a bottleneck a priori is impractical (except for the UE-to-BS links) since resource allocations also affect whether a node has a bottleneck link (by determining the link data rates and rate differentials). To get around this, we next propose a distributed algorithm where the initial resource allocations by the nodes determine which are the bottleneck links in the network. This in turn lets the UEs update their transmit powers, channels and topology assignments accordingly. As each UE i adapts, w_i may dynamically change and therefore the node would correspondingly switch between maximizing its end-to-end data rate and minimizing its power as per (4.9).

4.3 Link Adaptation Phases

In the initial topology, a UE establishes a link with the PoA from which it receives the strongest pilot signals on a downlink control channel [3]. Each UE is assigned a single channel and its initial transmit power is set at $P_{\max,i}$. Transmitter-side channel state information (CSI) on the effective interference is assumed available to each UE.

Each relay determines its current rate differential based on the latest incoming link data rates and disseminates this information to the UEs in the network. The periodic network feedback through the broadcast of V_r enables each node i to locally determine its current w_i (note that $w_i = 1$ always if the UE is connected to the BS).

We propose that adaptations occur in a two-phase cycle, represented as Algorithm 5. In the first phase, based on their current bottleneck values and the effective interference on their channels, all UEs perform transmit power control to realize the objective in (4.9). After the power control phase, which spans K iterations, as the link data rates evolve, the updated relay differentials are again broadcast to the UEs. In the second phase, a UE i can then appropriately adapt its PoA or aggregate an available channel given its latest w_i. This cycle repeats as relays broadcast rate differential updates in time intervals identified by $t \in \{1, 2, \cdots\}$.

As in LTE-Advanced [3][1], to aggregate a new channel, a UE would send a request to its current PoA. The PoA could then assign it an available channel, under the constraints set in (4.9). Alternatively, the node may send a request to connect to another PoA if that access point can support this UE. Unlike the power control phase, where all UEs adapt their transmit power in parallel, in the second phase only one node can aggregate an additional channel or connect to another PoA within an interval t. This constraint prevents two nodes from selecting the same channel to a common receiver. Thus, over time, as the UEs sequentially aggregate additional channels or change their PoAs, the available system resources diminish. This process converges when nodes can no longer acquire new channels or change their PoA.

As an illustration we consider Fig. 4.1a, where the RS-to-BS link is a bottleneck link

Algorithm 5: In the link adaptation cycle, resource allocations by an individual UE affect subsequent adaptations by other nodes.

```
UE i uplinks to PoA with highest strength of pilot signals
PoA assigns i a channel as per (4.9)
interval t = 1
Step A: Given transmit powers/data rates on links
V_r(t) disseminated/ w_i(t) determined, ∀i, ∀R
  for k = 1 to K iterations
     Power control by all links as per (4.10)(4.12)
  end
t = t+1
V_r(t) disseminated/w_i(t) determined, ∀i, ∀R
If channels available
    Select UE i randomly
       If w_i(t) = 1
         UE i acquires a channel as per Proposition 4.5.1
       elseif w_i(t) = 0
      UE i re-connects to another PoA as per Proposition 4.6.1
end
t = t+1
Go to step A
```

limiting the current end-to-end performance. With rate differential broadcasts, the UEs can decide to bypass this link and directly connect to the BS. Alternatively, they can reduce their transmit powers to a point without reducing their end-to-end performance. In contrast, the UE-to-BS links can aggregate available channels to boost their data rates. As shown in Fig. 4.1b, such local adaptations also lead to an improvement in the network-wide performance.

4.4 Power Control Phase

Our power adaptation scheme is a multi-channel version of the NSLA scheme, presented in Chapter 3, where each UE adapts as per MPEA if it currently has a bottleneck link and good channel conditions. Otherwise, it reduces its transmit power subject to a minimum SINR requirement. In the current formulation, each UE i splits its available power equally among its current aggregated channels such that the power per channel $P_{if}^{\max}(t) = \frac{P_{\max,i}}{c_i(t)}$ in

interval t, where $c_i(t) = \sum_{\forall f} c_{if}(t)$ is the current number of channels in use by node i. To re-iterate, all UEs perform a total of K power control iterations every other interval t.

Bottleneck Links

At the start of a power control phase, if UE i is connected to the BS or to relay R with $V_r(t) \geq 0$, then its weight $w_i(t) = 1$. The transmit power for each of its channels is updated for each iteration $k : \{1, 2, \cdots, K\}$ as per:

$$P_{if}(k+1) = \begin{cases} P_{if}^{\max}(t) - E_{if}(k), \text{ if } E_{if}(k) \leq \frac{P_{if}^{\max}}{\beta+1} \text{ (a)} \\ \min\left(P_{if}^{\max}(t), \frac{\beta}{\gamma_{if}(k)} P_{if}(k)\right), \text{ else (b).} \end{cases} \tag{4.10}$$

given that $c_{if}(t) = 1$. As reflected in (4.10a) the power control for a bottleneck link is a waterfilling-like allocation for time-varying channels. However, under unfavorable channel conditions, when the effective interference becomes large, the transmitter switches to the Foschini-Miljanic (FM) power control (4.10b), which is a well-known algorithm for converging to a fixed target SINR with minimum power if the allocation is feasible [18].

Non-bottleneck Links

If UE i is connected to relay r with $V_r(t) < 0$ then it has a non-bottleneck link and $w_i(t) = 0$. In this case, increasing its transmit power would not help improve its end-to-end data rate. Hence, given an SINR of $\gamma_{if}(k)$ on channel f in iteration k, the node sets itself a revised target SINR $\overline{\gamma_{if}}(k+1)$ such that:

$$\overline{\gamma_{if}}(k+1) = \begin{cases} \max\left(z.\gamma_{if}(k), \beta\right), \text{if } V_r(t) < -\tau, \text{ (a)} \\ \max\left(\gamma_{if}(k), \beta\right), \text{else, (b)} \end{cases} \tag{4.11}$$

where $0 < z < 1$. In the first case above, the UE iteratively decreases its target SINR on all its channels if the backhaul capacity of its current relay is insufficient to support the incoming data rate. Otherwise, it maintains its target SINR if $V_r(t)$ is above some threshold where τ has a positive value. The UE then uses the FM algorithm [18] to update its transmit

power as follows:

$$P_{if}(k+1) = \min\left(P_{if}^{\max}(t), \frac{\overline{\gamma_{if}}(k+1)}{\gamma_{if}(k)} P_{if}(k)\right). \tag{4.12}$$

Thus, this iterative approach by a non-bottleneck link also helps reduce interference in the network for co-channel links without affecting the node's end-to-end performance.

4.5 Bandwidth Adaptations

LTE-Advanced offers UEs in the network the ability to aggregate and transmit over multiple carriers [1]. We propose that a UE i aggregate a new channel only if it currently has a bottleneck link to its PoA. Thus, a UE should be able to acquire additional channels if either it has a direct link to the BS or if it is forwarding its data to an RS that already has a large enough capacity on the backhaul uplink (i.e. $V_r(t) \geq 0$). Under our approach, the PoA would assign the UE a new channel if: (1) this will produce an improvement in the data rate achieved by the UE, (2) the minimum SINR can be met on all the UE's channels and (3) the channel is not already allocated to another UE j where $r_j = r_i$.

Based on the three criteria above, we will subsequently derive an effective interference threshold which the PoA can use to determine whether to assign an additional channel from the available pool to the UE. We assume that the PoA compares the instantaneous effective interference levels of a UE corresponding to the start of the interval t (i.e. $E_{if}(t)$) against this threshold. Note that once UE i is allocated a new channel q, it will then have less peak power available per channel. Hence the effective interference on each channel must be less than the threshold to offset the reduction in data rate.

Suppose that on each channel f where node i operates, the effective interference is such that $E_{if}(t) \leq \frac{P_{max,i}}{(1+\beta)c_i(t)} : \forall f$ such that $c_{if}(t) = 1$. Given the effective interference threshold in the inequality, the node can use the waterfilling-like power control of (4.10a) on all its channels. Since $P_{\max,i}/c_i(t)$ is the peak power per channel, where $c_i(t) = \sum_{\forall f} c_{if}(t)$ is the current number of acquired channels, the power allocated as per (4.10a) is then $P_{if}(t) =$

$\frac{P_{\max,i}}{c_i(t)} - E_{if}(t)$. Thus, the corresponding current data rate of node i is

$$\begin{aligned}\eta_i(t) &= \sum_{\forall f: c_{if}(t)=1} W.\log_2\left(1+\frac{\frac{P_{\max,i}}{c_i(t)}-E_{if}(t)}{E_{if}(t)}\right)\\ &= \sum_{\forall f: c_{if}(t)=1} W.\log_2\left(\frac{P_{\max,i}}{c_i(t)E_{if}(t)}\right).\end{aligned} \tag{4.13}$$

A node would be allocated an available channel q if the node can still meet the minimum SINR on all its current channels despite the reduction in its peak power per channel.

Proposition 4.5.1. *UE i can acquire channel q when $w_i(t) = 1$ and if*
(a) $E_{iq}(t), E_{if}(t) \leq \frac{P_{max,i}}{(1+\beta)(1+c_i(t))} : \forall f$ such that $c_{if} = 1$ and
(b) $E_{iq}(t) \leq \frac{P_{max,i}c_i(t)^{c_i(t)}}{(1+c_i(t))^{c_i(t)+1}} \leq \frac{P_{max,i}}{(1+\beta)(1+c_i(t))}$.

Proof. When $E_{if}(t), E_{iq}(t) \leq \frac{P_{max,i}}{(1+\beta)(1+c_i(t))} : \forall f$ such that $c_{if} = 1$ then node i will allocate $P_{if} \geq \frac{P_{max,i}}{(1+c_i(t))} - \frac{P_{max,i}}{(1+\beta)(1+c_i(t))}$ as per the water-filling principle in (4.10a). Thus, the SINR on each channel will be at least $P_{if}(t)/E_{if}(t), P_{iq}/E_{iq}(t) \geq \beta$ based on the instantaneous observations. Thus, while acquiring channel q will be feasible in terms of meeting the minimum SINR requirement on all channels, the achieved data rate on the current channels is reduced.

The transmit power available on each channel drops from $P_{if}^{\max}(t) = \frac{P_{\max,i}}{c_i(t)}$ to $P_{if}^{\max}(t) = \frac{P_{\max,i}}{1+c_i(t)}$ if channel q is aggregated by node i in interval $t+1$. As per (4.13), this leads to a reduction in the data rate on the current channels which is $W.\sum_{\forall f: c_{if}(t)=1}\log_2\left(\frac{c_i(t)+1}{c_i(t)}\right) = W.c_i(t)\log_2\left(\frac{c_i(t)+1}{c_i(t)}\right)$. Hence, the data rate achieved over channel q must be sufficiently high to offset this decrease. Thus, the effective interference on channel q must be such that

$$\begin{aligned}W.c_i(t)\log_2\left(\frac{c_i(t)+1}{c_i(t)}\right) &< W\log_2\left(\frac{P_{\max,i}}{(c_i(t)+1)\,E_{iq}(t)}\right)\\ E_{iq}(t) &< \frac{c_i^{c_i(t)}(t)P_{\max,i}}{(c_i(t)+1)^{c_i(t)+1}}.\end{aligned}$$

Finally, by acquiring channel q, we have $c_i(t+1) = c_i(t)+1$. □

The PoA allocates channel q to the UE if the effective interference is below the stated threshold.

4.6 Topology Adaptations

When a relay is supporting heavy traffic volume, the end-to-end data rate of the UEs connected to it will be limited by the capacity of the RS-to-BS backhaul link. In response, either the UEs can minimize their transmit power as in (4.12) or alternatively migrate to better access points. Under our approach, UE i with a non-bottleneck link to a relay ($w_i(t) = 0$), sends a request to establish a link to another PoA if the relay is suffering congestion such that $V_{r_i}(t) \leq -\tau$. Recall that otherwise if $V_{r_i}(t) > -\tau$ then the UE operates in the power minimization mode as per (4.11). The alternative PoA could be the BS or any other relay $y \neq r_i(t)$ with a high enough backhaul capacity such that $V_y(t) > \tau$. The PoA y will confirm the request of the UE and allocate it a channel q for uplink communication if (1) no other node is currently transmitting to PoA y on channel q and (2) if the current effective interference observed at y for UE i is below a selected threshold.

Note that in a network with many access points, multiple PoAs may satisfy the above criteria. As in [3], UE i will establish an uplink to the first PoA that positively confirms its request. When the UE connects to the new PoA, it relinquishes control of channels used on the link to its current access point. If, however, no alternative PoA is available to support this UE then it will only adapt its transmit power according to (4.11).

Proposition 4.6.1. *When $V_r(t) < -\tau$ UE i may establish an uplink to the BS or any relay $y : y \neq r_i(t)$ $(r = r_i)$ where $V_y(t) > \tau$, if there is an available channel q such that $E_{iq}(t) \leq \frac{P_{\max,i}}{\beta+1}$ on the link to PoA y.*

Proof. The PoA determines the current $E_{iq}(t)$ that node i experiences and then allocates channel q to UE i if the effective interference is below $\frac{P_{\max,i}}{\beta+1}$. The choice of the effective interference threshold is such that the link can satisfy the minimum SINR as per (4.10). Since node i relinquishes all other channels to the previous PoA, it has $c_i(t+1) = 1$. □

Note that over time, UE i may later also aggregate additional channels on its link to the latest access point. Setting τ to a large value reduces the likelihood of nodes switching back and forth between PoAs. Hence, for a large enough τ, the topology and bandwidth

adaptations will terminate within $t \leq N_r \cdot C$ intervals where $C = \underbrace{\max}_{\forall r \in \mathcal{R}} \sum_{\forall i: r_i = r} c_{ir}$. Note that C is the minimum number of channels to satisfy the channel assignment constraint in (4.9) and equals the maximum number of nodes connected to a PoA in the system. In each interval, since only one node will either aggregate a new channel or adapt its PoA, as per (5), it would take at most $N_r \cdot C$ intervals for all nodes connected to the N_r PoAs to acquire new channels or connect to other PoAs.

4.7 Discussion

In the preceding sections, we have presented a heuristic implementation of (4.9) through transmit power, bandwidth and topology adaptations (i.e. channel-and-topology adaptive NSLA), where each UE maximizes its own objective by taking into account network-wide conditions. We next compare it against a few benchmark schemes where a node has the same constraints as in (4.9) but where it makes local adaptations and does not have any feedback on traffic conditions:

a. Channel State-based Link Adaptations (CSLA): Each node that operates on a single channel that is assigned to it initially uses the power control algorithm as per (4.10) to improve its own data rate (i.e. $\underbrace{\max}_{P_{i1},.,P_{if}} \eta_i$).

b. CSLA + Greedy Channel Aggregation (CA): Each node only uses the CSLA power control as per (4.10) and always tries to acquire additional channels to greedily maximize its data rate (i.e. $\underbrace{\max}_{P_{i1},.,P_{if},c_{i1},.,c_{if}} \eta_i$).

c. Foschini-Miljanic (FM) power control: Each node uses the FM power control in (4.12) to maintain a fixed target SINR β given a single channel assigned initially.

d. FM + Greedy CA: Each node uses the FM power control on all its channels to maintain SINR at β and tries to greedily maximize the number of its acquired channels.

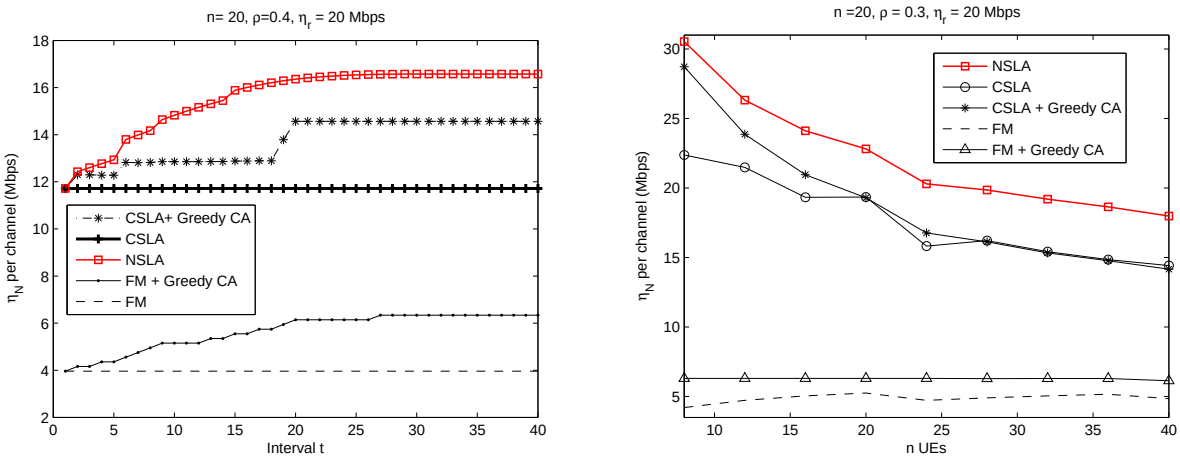

(a) (b)

Figure 4.2: (a) We observe convergence of the adaptations for a sample network. (b) With increasing traffic n, NSLA offers relatively increasing improvement over other schemes.

4.8 Simulation Results

We now consider a multihop cellular network with $N_r = 3$ relays that are angularly separated by 120^o and located 2000m from the base station. We assume $n_o = -140$ dBW, $W = 1$ MHz, $\alpha = 4.0$, $\beta = 3$ dB, the maximum transmit power of UEs as 1.0 W, and the cross-link gains of the form $g_{fji} = d_{jr_i}^{-\alpha}$, where d_{j,r_i} is the distance from node j to the PoA of node i. The transmit powers of downlink pilot signals from the BS and RS are assumed equal. There are a total of n UEs in the cell, randomly distributed within circular regions of radius R_L m around each of the four PoAs (i.e. one BS and three RS) according to a uniform distribution.

Recall that as per (4.9), all links to a given PoA need to be on orthogonal channels. Thus, to vary the number of channels required for an n-user system, or generate uneven traffic at the relays, we define a variable $0 < \rho < 1$ which determines the proportion of nodes clustered around each PoA. The number of UEs located around the first RS $r = 1$ is $n_1 = \lceil n\rho \rceil$, while around each relay $y \in \{2, \cdots, N_r\}$, the number of nodes is $n_y = \lceil \rho(n - \sum_{m=1}^{y-1} n_m) \rceil$ and finally around the BS it is $n_{N_r+1} = n - \sum_{m=1}^{N_r} n_m$. For instance, when $\rho = 0.3$, $n = 10$ UEs and $N_r = 3$, there will be 3, 3, 2, and 2 UEs located randomly within R_L m around each of the four PoAs respectively and the requisite bandwidth is $C = |\mathcal{F}| = 3$ channels.

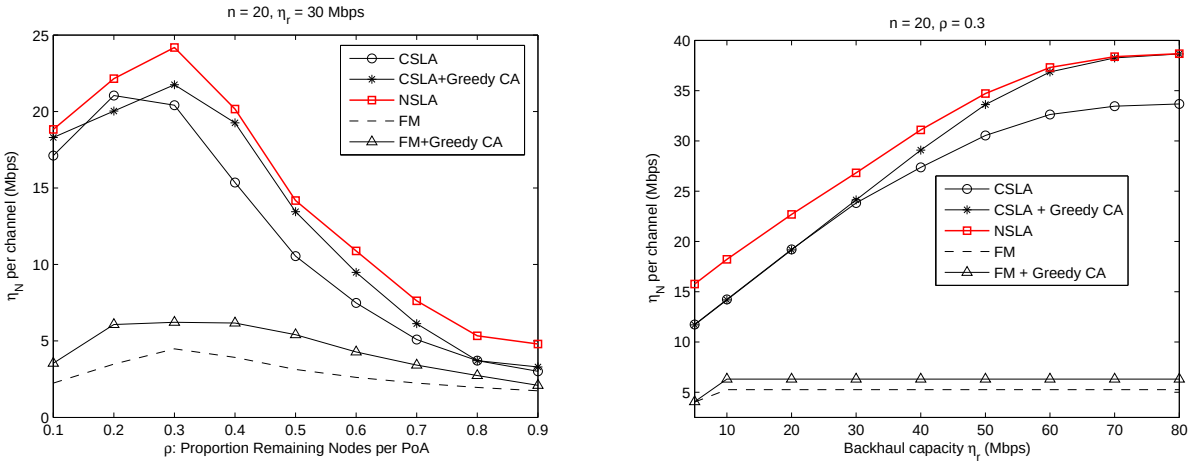

(a) (b)

Figure 4.3: (a) Topology adaptations and power minimization by the UEs enables NSLA the best performance over the range of ρ. (b) The greedy approach matches NSLA only when η_r is large.

Unless stated otherwise, we set $\tau = W \log_2(1+\beta)$, $v_i = \frac{\tau}{WP_{\max,i}} : \forall i$ and $K = 4$ when the nodes adapt as per NSLA. We plot aggregate end-to-end data rate normalized with system bandwidth, $\frac{\eta_N}{|\mathcal{F}|}$, against a range of parameters. In Fig. 4.2(a), we plot the evolution of $\frac{\eta_N}{|\mathcal{F}|}$ against time for a sample network with 20 UEs and observe that NSLA yields the best performance. Likewise in Fig. 4.2(b), we plot the performance against n, and observe that it declines under all schemes. However, under NSLA, since topology adaptations enable UEs to select better access points at $n = 40$, the scheme's offered performance is still almost 25% higher than the next best scheme.

In the Fig. 4.3a, when ρ is closer to one, the UEs are concentrated mostly around the relays. In this case, the relays are overloaded with traffic and topology adaptations under NSLA yield the best performance. Conversely, when ρ is closer to zero, the majority of UEs are clustered around the BS. In this case, the performance gain under NSLA over other schemes comes from the power minimization by nodes with non-bottleneck links (using (4.12)) which in turn also helps reduce network-wide interference for co-channel links. We can thus conclude that power minimization and topology adaptation approaches under NSLA offer significant performance improvement. In contrast, in Fig. 4.3b only when the backhaul capacity is large does the performance under CSLA with greedy channel aggregation match

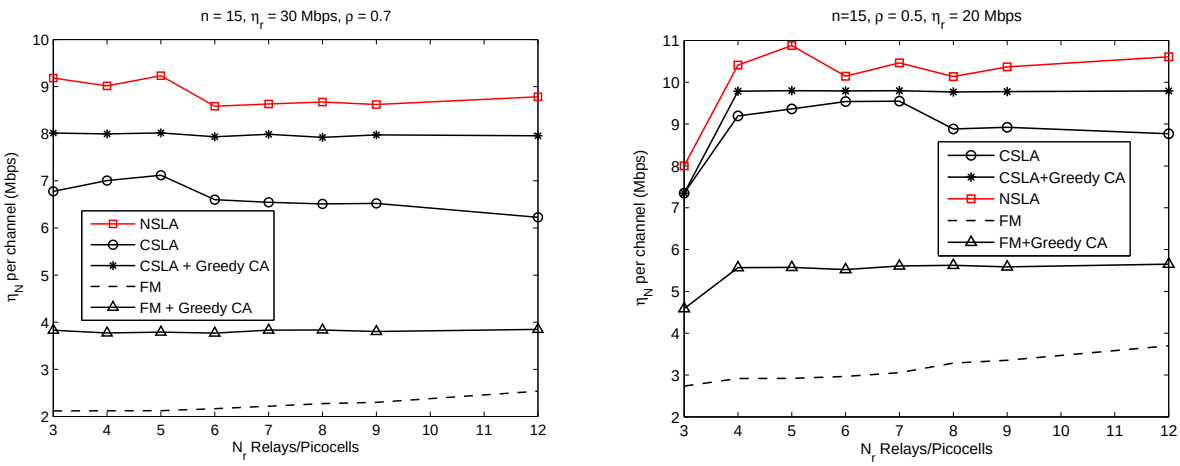

(a) (b)

Figure 4.4: (a) Topology adaptations under NSLA enable nodes to have a better performance when ρ is large whereas in (b) power minimizations by UEs with non-bottleneck links help reduce interference in the network when ρ is moderate.

that of NSLA.

In Fig. 4.4 we plot the system performance as a function of the number of relays randomly located within a 2 km $\times$ 2 km region within the cell. Since the backhaul links of these PoAs operate on out-of-cell bands as the UEs, these relay nodes can approximate picocell networks. In these results, we set $R_L = 150$ m, $\tau = 8$ Mbps and $K = 3$. We can observe that the NSLA scheme yields the best performance as it enables nodes to make transmit power, channel aggregation and topology adaptations based on the congestion conditions at the PoAs.

4.9 Conclusions

We have considered distributed power, bandwidth and topology adaptations in a cellular multihop network. Nodes with bottleneck links to their receivers maximize their data rate using power control and channel aggregation. Conversely, the nodes with non-bottleneck links can either minimize their transmit power to reduce network-wide interference or they can connect to alternative access points. We have shown significant improvement in the network's aggregate end-to-end data rate under the proposed adaptation scheme, as com-

pared to greedy adaptations, especially when greater traffic volume requires efficient use of resources. In the next chapter we extend the analysis of power allocation and topology adaptations when nodes have parallel links to multiple Points of Access within a network.

Chapter 5

Soft Topology Adaptations with Power Allocation

In the currently deployed LTE architecture, each UE can only connect to a single access point at a given time, despite the availability in the cellular system of multiple access points such as relays and eNodeBs [71]. In such a topology, a mobile can either establish a direct link to the base station or a link to a relay, but not both. In this chapter, we consider the benefit in allowing UEs to split their transmit power over simultaneous links to the base station and a relay (i.e. *dual connectivity* [7]), in effect transmitting two parallel flows. In a multihop cellular network, the flexibility to forward the data via multiple access points that are spatially separated would enable nodes to better overcome the resource limitations induced by the wireless channel and traffic conditions.

If not adequately balanced, a relay-to-eNodeB backhaul link may limit the end-to-end data rate of UEs connected to the relay, especially if there is a large number of attached UEs. To support high traffic volume via the relay, a network operator may allocate a larger bandwidth to the wireless relay-to-eNodeB backhaul to increase the uplink's capacity. However, in LTE-Advanced, the channels used for the relay backhaul and for the UEs come from the same pool [1][72]. Hence, such bandwidth re-allocation to the backhaul links would also reduce the system bandwidth available to the UEs and thus this approach may not

help increase the network-wide end-to-end performance. Therefore, in lieu of increasing the bandwidth of the relay backhaul, our focus in this chapter is to allow UEs maintain dual connections to relays and to the base station, and can transmit independent data streams on two separate channels.

We model decisions by the UEs as to: (i) which points of access to attach to (either a relay or a relay and the BS or only the BS); and (ii) how to allocate transmit power over these links so as to maximize data rate. We devise a link-adaptive scheme where, given knowledge of the current congestion conditions in the backhaul link, each UE adapts to maximize its own achievable rate by appropriately selecting its access points, followed by transmit power allocation over its links. The power allocation essentially works in two modes: (1) waterfilling or (2) the UE iteratively re-allocates more power on its link to the base station whenever there is congestion on the backhaul link between the relay and the base station.

We show that the additional flexibility in the selection of multiple access points leads to substantial aggregate throughput increase as compared to when nodes operate in a fixed network topology. Individual adaptations by UEs, in terms of both point of access and transmit power, are inter-dependent due to interference effects and to the possibility of congestion in the relay-to-base station link. We show that these decisions converge (under certain conditions) and derive a closed-form expression for the transmit power at the point of convergence.

We also consider the case when, due to insufficient bandwidth resources, some UEs can only connect to a single access point. We show that under our scheme, when the congestion on the relay backhaul increases, some of these UEs will switch from maximizing data rate to minimizing transmit power (and thereby reduce interference). Therefore, our scheme can translate into a range of adaptation strategies depending on the resources available to the UEs.

5.1 System Model

We consider a single-cell network with a set $\mathcal{N} = \{1, 2, \cdots, n\}$ of User Equipment (UEs) that want to send their data to a base station (BS). Located towards the edges of the cell are N_r fixed relays (RS) that provide coverage for UEs located farther away from the base station (see Fig. 5.1 with $N_r = 3$). All Points of Access (PoA) are denoted by a set $\mathcal{R} = \{1, 2, \cdots, N_r, N_r + 1\}$, where elements 1 to N_r indicate an RS and the BS is represented by element $N_r + 1$. The RS decodes the data it receives from the UE and forwards it to the BS (i.e. a decode-and-forward scheme).

With *dual connectivity*, a UE can have parallel links to two different PoAs. A node i maintains its connection to a PoA $r_i \in \mathcal{R}$ on its first link, which is referred to as the *dedicated-PoA* link. The PoA chosen by each UE on its dedicated-PoA link is the one with the highest received pilot signal strength on a downlink control channel. On its second link (referred to as the *adaptive-PoA* link), node i may choose to send data to the same PoA or to an alternative PoA. The possible choices of $r_i^A \in \mathcal{R}$ on its adaptive-PoA link are such that the UE can transmit either to the BS or to an RS.

In general, only a subset of m UEs ($m \leq n$) may have the dual connectivity, whereas the remaining $n - m$ UEs will only have a dedicated-PoA link. We shall subsequently analyze different approaches to determine which of the UEs should have an adaptive-PoA link. We assume that the dedicated-PoA link of a node may experience interference, but its adaptive-PoA link is orthogonal in time or frequency with respect to all other links, so that it does not suffer any intra-cell interference. All links operate on a set of channels $\mathcal{F} = \{1, 2, \cdots, F\}$, where each channel has a bandwidth W Hz. The assignment of each channel f to nodes is represented as a set $\mathcal{A}(f) \subseteq \mathcal{N}$.

The power gain between the UE node $j \in \mathcal{A}(f)$ and the intended receiver (PoA) of node $i \in \mathcal{A}(f)$ is represented as $g_{j,r_i}^{(f)}$, which depends on several factors such as shadowing, path loss and fading on channel $f \in \mathcal{F}$. We define for the dedicated-PoA links a normalized

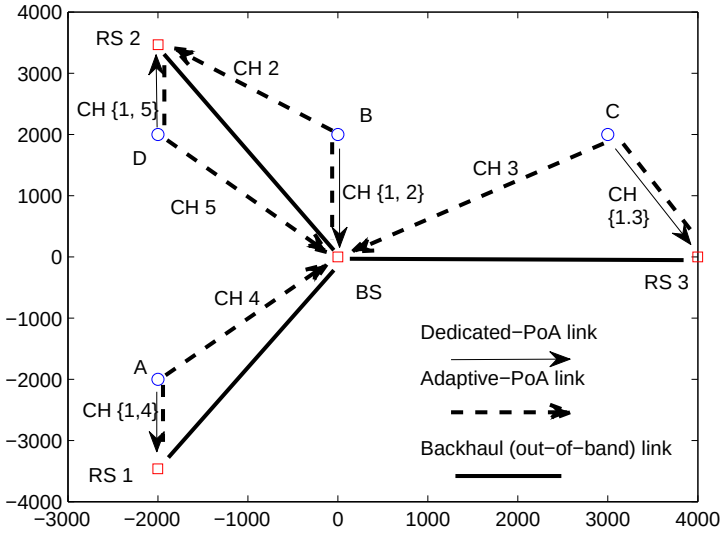

Figure 5.1: A depiction of a network with parallel links when nodes have dual connectivity. While all the UEs transmit data on Channel 1 to their respective relays, they can send data to either the BS or to the RS on their other channel.

cross-link gain matrix $\mathbf{F}$ of dimension $n \times n$ as

$$\mathbf{F}(i,j) = \begin{cases} 0 \text{ if } i = j \text{ or } i,j \text{ orthogonal} \\ \frac{g_{j,r_i}^{(f)}}{g_{i,r_i}^{(f)}} \text{ otherwise,} \end{cases} \tag{5.1}$$

where i, j are orthogonal if their links operate on different channels in $\mathcal{F}$. For the adaptive-PoA link of UE i, we denote as $g_{i,r}^{(q)}$ and $g_{i,b}^{(q)}$ its gain to the selected RS and to the BS, respectively, on channel $q \in \mathcal{F}$. As an example of parallel links, consider Fig. 5.1, where each node has a dedicated-PoA link on channel 1. With $m = 4$, each node has an adaptive-PoA link as well.

Given n_o as the total thermal noise power per channel, we define $\mathbf{D}_d$, $\mathbf{D}_r$ and $\mathbf{D}_b$ as $n \times 1$ vectors, which represent normalized noise powers on the dedicated-PoA links and the adaptive-PoA links (to RS and BS) respectively. The i^{th} elements of these vectors are such that $\mathbf{D}_d(i) = n_o/g_{i,r_i}^{(f)}$, $\mathbf{D}_r(i) = n_o/g_{i,r}^{(q)}$ and $\mathbf{D}_b(i) = n_o/g_{i,b}^{(q)}$. All links in the network (i.e., UE-to-RS and UE-to-BS) can adapt their transmit power and, consequently, their data rate. Given the UEs' available power vector as $\mathbf{P}_{\max}$ Watts, the transmit power of nodes on

their first link are represented by the vector $\mathbf{P}_d = \left[P_1^{(d)}, P_2^{(d)}, \cdots, P_n^{(d)}\right]$ and those on their adaptive-PoA links as $\mathbf{P}_a = \left[P_1^{(a)}, P_2^{(a)}, \cdots, P_n^{(a)}\right]$ where $P_i^{(d)} + P_i^{(a)} \leq P_{\max,i}$. The effective interference for node i on its dedicated-PoA link and on its adaptive-PoA link is then defined as [31]:

$$E_i^{(d)} = \frac{n_o + \sum_{j \neq i, j \in \mathcal{A}_r(f)} g_{j,r_i}^{(f)} P_j^{(d)}}{g_{i,r_i}^{(f)}}, \tag{5.2}$$

dedicated-PoA link

$$E_i^{(b)} = \frac{n_o}{g_{i,b}^{(q)}}, \text{ if adaptive-PoA link to BS}$$

$$E_i^{(r)} = \frac{n_o}{g_{i,r}^{(q)}}, \text{ if adaptive-PoA link to RS.}$$

With transmitter-side channel state information (CSI), each UE knows these effective interferences. The corresponding SINRs are:

$$\gamma_i^{(d)} = \frac{P_i^{(d)}}{E_i^{(d)}} = \frac{P_i^{(d)}}{\frac{n_o + \sum_{j \neq i, j \in \mathcal{A}_r(f)} g_{j,r_i}^{(f)} P_i^{(d)}}{g_{i,r_i}^{(f)}}} \tag{5.3}$$

$$\gamma_i^{(b)} = \frac{P_i^{(a)}}{E_i^{(b)}} = \frac{P_i^{(a)}}{\frac{n_o}{g_{i,b}^{(q)}}}$$

$$\gamma_i^{(r)} = \frac{P_i^{(a)}}{E_i^{(r)}} = \frac{P_i^{(a)}}{\frac{n_o}{g_{i,r}^{(q)}}}$$

where either $\gamma_i^{(b)}$ or $\gamma_i^{(r)}$ will be the achieved SINR depending on the choice of PoA by the UE on its adaptive-PoA link, and $\gamma_i^{(d)}$ will be the SINR on the dedicated-PoA link. Note that for a single-cell system, the dedicated-PoA links are interference-limited while the adaptive-PoA links are noise-limited. We define the achievable rate as a function $\eta(\cdot)$ of SINR γ such that $\eta(\gamma) = W \log_2(1 + \gamma)$.

Finally, the RS-to-BS links operate on *out-of-band* channels from the UEs, and are assumed to have a fixed capacity η_r bps.

Table 5.1: Symbol definitions: Subscript i denotes UE i.

c_i	adaptive-PoA link indicator
a_i	adaptive-PoA link to the BS indicator
$P_i^{(d)}$	dedicated-PoA link transmit power
$P_i^{(a)}$	adaptive-PoA transmit power
$E_i^{(d)}$	effective interference dedicated-PoA link
$E_i^{(b)}$	effective interference adaptive-PoA (BS)
$E_i^{(r)}$	effective interference adaptive-PoA (RS)
$\gamma_i^{(d)}$	SINR dedicated-PoA link
$\gamma_i^{(b)}$	SNR adaptive-PoA link to BS
$\gamma_i^{(r)}$	SNR adaptive-PoA link to RS
$\zeta_i^{(br)}$	peak data rate BS-RS transmission
$\zeta_i^{(rr)}$	peak data rate RS-RS transmission
$\zeta_i^{(bb)}$	peak data rate BS-BS transmission
V_r	rate differential at RS r
τ	rate differential threshold
r_i	dedicated-PoA link receiver
$\eta(\gamma)$	achievable data rate $W \log_2(1+\gamma)$

5.2 Problem Formulation

With dual connectivity, if UE i has a dedicated-PoA link to an RS then it has the choice of (a) either transmitting both its data streams to the same RS or (b) sending one stream to the RS and the other one to the BS. Conversely, if UE i has a dedicated-PoA link to the BS, then it can also send one stream to an RS and the other one to the BS or (c) it can transmit both its data streams to the BS. Henceforth, we denote (a),(b) and (c) as RS-RS, BS-RS and BS-BS transmissions, respectively.

We next define two indicator variables $c_i, a_i \in \{0, 1\}$ for a UE i. The indicator c_i is an input to the problem, where when the system has enough bandwidth resources for all nodes to have dual connectivity, we set $c_i = 1, \forall i$. Conversely, with limited bandwidth, some nodes will only have a dedicated-PoA link; we set $c_i = 0$ for each such node i. Moreover, given $c_i = 1$, if UE i transmits to the BS on the adaptive-PoA link, then $a_i = 1$; otherwise, if the PoA is a relay, $a_i = 0$. Using the Max-Flow Min-Cut Theorem [62], the aggregate end-to-end

data rate in the network (system throughput), denoted as η_N, is formally defined in equation (5.4).

$$\eta_N = \sum_{r=1}^{N_r} \min \left(\eta_r, \sum_{\forall i: r_i = r} \eta \left(\gamma_i^{(d)} \right) + \sum_{\forall i: r_i^A = r} c_i \left(1 - a_i \right) \eta \left(\gamma_i^{(r)} \right) \right) + \sum_{\forall i} c_i a_i \eta \left(\gamma_i^{(b)} \right) + \sum_{\forall i: r_i = N_r + 1} \eta \left(\gamma_i^{(d)} \right) \tag{5.4}$$

This expression represents the achievable sum rate in the network when interference is treated as noise. Next, we define the *rate differential* across the RS $r \in \{1, 2, \cdots N_r\}$ as

$$V_r = \eta_r - \sum_{\forall i: r_i = r} \eta \left(\gamma_i^{(d)} \right) - \sum_{\forall i: r_i^A = r} c_i \left(1 - a_i \right) \eta \left(\gamma_i^{(r)} \right) \tag{5.5}$$

which denotes the difference between the outgoing RS-to-BS link capacity and the aggregate incoming data rate of associated UEs at relay r. When $V_r < 0$, the RS-to-BS link represents a *bottleneck* link that limits the end-to-end data rate for the UEs sending data to BS via RS r. Conversely, $V_r \geq 0$ indicates that the capacity of the RS-to-BS link is high enough to support all traffic coming via the relay. Note that the UE-to-BS links (i.e. when nodes transmit directly to the BS) are also deemed to be bottleneck links. The aggregate end-to-end data rate η_N in equation (5.4) is the sum of the data rates of all bottleneck links in the network.

When UEs use power control or change their Points of Access, the data rates at which they can transmit to their RS will vary, thereby causing a change in the rate differential. When $V_r \geq 0$, there is room for UE i to send at a higher data rate to its RS. Conversely, when $V_r < 0$, the UE cannot increase its end-to-end rate by forwarding its data exclusively through the relay. In this case, it may choose to transmit some of its data to the BS directly and allocate its transmit power accordingly. We denote V_r^+ as the unused backhaul capacity at relay r, which indicates how much improvement in a UE's total rate is achievable given the current congestion level. We therefore set the adaptation objective of each node i as

given by (5.6).

$$f_i(a_i, P_i^{(d)}, P_i^{(a)}) =$$
$$\begin{cases} (1-a_i)\min\left(V_{r_i}^+, \eta\left(\gamma_i^{(d)}\right) + \eta\left(\gamma_i^{(r)}\right)\right) + a_i\left(\eta\left(\gamma_i^{(b)}\right) + \min\left(V_{r_i}^+, \eta\left(\gamma_i^{(d)}\right)\right)\right), \; c_i = 1 \text{ and } r_i \leq N_r \\ (1-a_i)\min\left(V_{r_i^A}^+, \eta\left(\gamma_i^{(r)}\right)\right) + a_i\eta\left(\gamma_i^{(b)}\right) + \eta\left(\gamma_i^{(d)}\right), \; c_i = 1 \text{ and } r_i = N_r + 1 \\ \min(V_{r_i}^+, \eta(\gamma_i^{(d)})), \; c_i = 0 \text{ and } r_i \leq N_r \\ \eta(\gamma_i^{(d)}), \; c_i = 0 \text{ and } r_i = N_r + 1 \end{cases} \tag{5.6}$$

$$\begin{aligned} \underbrace{\max}_{a_i, P_i^{(d)}, P_i^{(a)}} \quad & f_i(a_i, P_i^{(d)}, P_i^{(a)}) \\ P_i^{(d)} + P_i^{(a)} &\leq P_{\max,i} \\ P_i^{(d)}, P_i^{(a)} &\geq 0 \\ a_i &\in \{0, 1\} \end{aligned} \tag{5.7}$$

The total transmit power of node i is constrained by $P_{\max,i}$ over either of its channels. While it may appear complex, the function (5.6) reduces to simpler expressions for individual UEs in the following manner:

$c_i = 1$ **and** $r_i \leq N_r$

UE i has dual connectivity and has a dedicated-PoA link to an RS r_i with rate differential V_{r_i}. In an RS-RS transmission, the UE transmits on both links to RS r_i only. We thus have $a_i = 0$ and (5.6) equals $\min\left(V_{r_i}^+, W\log_2\left(1 + \frac{P_i^{(d)}}{E_i^{(d)}}\right) + W\log_2\left(1 + \frac{P_i^{(a)}}{E_i^{(r)}}\right)\right)$. Conversely, when node i transmits to the BS on the adaptive-PoA link (i.e. BS-RS transmission), we have $a_i = 1$ and (5.6) becomes $W\log_2\left(1 + \frac{P_i^{(a)}}{E_i^{(b)}}\right) + \min\left(V_{r_i}^+, W\log_2\left(1 + \frac{P_i^{(d)}}{E_i^{(d)}}\right)\right)$.

$c_i = 1$ **and** $r_i = N_r + 1$

UE i has dual connectivity and has a dedicated-PoA link to the BS. When the UE transmits on both links to the BS (i.e. BS-BS transmission), we have $a_i = 1$ and (5.6) equals $W\log_2\left(1 + \frac{P_i^{(d)}}{E_i^{(d)}}\right) + W\log_2\left(1 + \frac{P_i^{(a)}}{E_i^{(b)}}\right)$. Conversely, when the UE transmits to an RS on its adaptive-PoA link, we have $a_i = 0$. This RS is one from which it receives the highest

pilot signals. Thus, in a BS-RS transmission, equation (5.6) becomes $W \log_2 \left(1 + \frac{P_i^{(d)}}{E_i^{(d)}}\right)$ $+ \min \left(V_{r_i^A}^+, W \log_2 \left(1 + \frac{P_i^{(a)}}{E_i^{(r)}}\right)\right)$, where $V_{r_i^A}^+$ is the rate differential at the RS.

$c_i = 0$ **and** $r_i \leq N_r$

The UE only has a single (dedicated-PoA) link to an RS. Then (5.6) reduces to $\min \left(V_{r_i}^+, W \log_2 \left(1 + \frac{P_i^{(d)}}{E_i^{(d)}}\right)\right)$.

$c_i = 0$ **and** $r_i = N_r + 1$

The UE only has a single (dedicated-PoA) link to the BS, and (5.6) equals $W \log_2 \left(1 + \frac{P_i^{(d)}}{E_i^{(d)}}\right)$.

We assume that the relays can broadcast the current values of the rate differentials on a downlink control channel, which the UEs then use to make adaptations. Each UE's decision can then be expressed as the optimization problem in (5.7).

5.3 Transmission Strategy

5.3.1 UEs with dual connectivity

All nodes with dual connectivity have to make corresponding transmit power allocations on the dedicated-PoA and the adaptive-PoA links. By using the available CSI, UEs can estimate the peak (maximum) data rate they can achieve through BS-RS, RS-RS or BS-BS transmissions. Under our strategy, a node selects its receiver on the adaptive-PoA link by comparing the rate differential against these peak data rates. For example, if the peak data rate achievable through an RS-RS transmission is larger than that of a BS-RS transmission and the rate differential is sufficiently large, then the node should transmit to the RS only. Conversely, a node that is currently transmitting only to the BS can switch to a BS-RS transmission if the corresponding peak data rate is more than that of the BS-BS transmission and the rate differential at the relay is above some threshold. We will subsequently show

that the strategy we have proposed results in better network-wide performance than a *greedy* maximization of the local objective in (5.7) by the nodes.

We next define expressions for the transmit power allocations that result in the peak data rates in (5.8) for all possible transmission configurations.

$$\begin{aligned}
\zeta_i^{(rr)} &= \underbrace{\max}_{P_i^{(d)},P_i^{(a)}} W\log_2\left(1+\frac{P_i^{(d)}}{E_i^{(d)}}\right)+W\log_2\left(1+\frac{P_i^{(a)}}{E_i^{(r)}}\right), \text{ RS-RS transmission } r_i \le N_r \\
\zeta_i^{(bb)} &= \underbrace{\max}_{P_i^{(d)},P_i^{(a)}} W\log_2\left(1+\frac{P_i^{(d)}}{E_i^{(d)}}\right)+W\log_2\left(1+\frac{P_i^{(a)}}{E_i^{(b)}}\right), \text{ BS-BS transmission } r_i = N_r+1 \\
\zeta_i^{(br)} &= \underbrace{\max}_{P_i^{(d)},P_i^{(a)}} W\log_2\left(1+\frac{P_i^{(d)}}{E_i^{(d)}}\right)+W\log_2\left(1+\frac{P_i^{(a)}}{E_i^{(x)}}\right), \text{ BS-RS transmission } x\in\{b,r\} \\
&\qquad x=b \text{ if } r_i \le N_r,\ x=r \text{ if } r_i = N_r+1
\end{aligned} \tag{5.8}$$

Theorem 5.3.1. *Given $E_i^{(d)}$, $E_i^{(b)}$ and $E_i^{(r)}$, the peak data rate $\zeta_i^{(rr)}$, $\zeta_i^{(br)}$ or $\zeta_i^{(bb)}$ for UE i is achieved with a water-filling power allocation such that $P_i^{(d)} = \min\left(P_{\max,i}, \frac{1}{2}\left(P_{\max,i}+E_i^{(x)}-E_i^{(d)}\right)^+\right)$ and $P_i^{(a)} = P_{\max,i}-P_i^{(d)}$, where $x\in\{b,r\}$ denotes the adaptive-PoA link to either BS or RS.*

The proof of this theorem and the corollary below are in the Appendix. Note that the above may also represent the power allocation strategy of a UE when it does not have any information about the rate differential and tries only to maximize its data rate on its two links.

Corollary 5.3.2. *The peak data rate $\zeta_i^{(br)} > \zeta_i^{(rr)}$ if $E_i^{(b)} < E_i^{(r)}$, and $\zeta_i^{(br)} > \zeta_i^{(bb)}$ if $E_i^{(r)} < E_i^{(b)}$.*

The peak data rate achievable for UE $i : r_i \le N_r$ through a BS-RS transmission is higher than that via RS-RS transmission if the effective interference to the BS is lower than that to the RS on the adaptive-PoA link. The same result applies for UE $i : r_i = N_r+1$ in relation to the peak data rate via BS-BS transmission.

5.3.2 Single-Link UEs

The UEs that do not have dual connectivity can only adapt their transmit power on their dedicated-PoA links. When the UE has a bottleneck link it can transmit at full power to maximize its data rate. Conversely, if it connected to an RS that is suffering congestion (i.e. $V_r < 0$), the allocation in (5.7) requires the UE to switch to transmit power minimization to match the rate differential.

5.4 Network state-based Distributed Transmission

Based on the above discussion, we propose an adaptation algorithm, which we call Network state-based Distributed Transmission (NDT). We assume that adaptations occur in time intervals denoted as $k \in \{1, 2, ..\}$. In interval k, the effective interferences $E_i^{(b)}(k)$, $E_i^{(d)}(k)$, $E_i^{(r)}(k)$ and the rate differential $V_r(k)$ at its associated relay are available to each UE i. We further assume that a positive-valued constant τ, known to all UEs, is a rate differential threshold that represents some tolerable level of congestion at the relays.

5.4.1 UEs with Dual Connectivity

If $c_i(k+1) = 1$, then UE i will have dual connectivity.

UE $i : r_i \leq N_r$

We propose that UE i, which has a dedicated-PoA link to an RS, update its adaptive PoA as follows:

$$a_i(k+1)=$$

$$\begin{cases} 0, \text{ if } V_{r_i}(k) \geq \zeta_i^{(br)}(k) \text{ and } \zeta_i^{(rr)}(k) \geq \zeta_i^{(br)}(k) & \text{(5.9a)} \\ 1, \text{ if } \zeta_i^{(rr)}(k) < \zeta_i^{(br)}(k) \text{ or } V_{r_i}(k) \leq -\tau & \text{(5.9b)} \\ a_i(k), \text{ otherwise.} & \text{(5.9c)} \end{cases}$$

When $V_{r_i}(k)$ is sufficiently high, the choice of PoA between (5.9a) and (5.9b) depends only on which transmission (BS-RS or RS-RS) can achieve a higher peak data rate. In contrast, in (5.9b), the UE chooses BS-RS transmission if this has a higher peak data rate than RS-RS transmission or if $V_{r_i}(k) \leq -\tau$. The latter condition is active when the congestion at the relay exceeds the threshold τ. For all intermediate cases, in (5.9c), the PoA on the adaptive-PoA channel remains unchanged. Corresponding to its choice of access point in iteration $k+1$ in (5.9), UE i allocates transmit power to the dedicated-PoA link as shown in (5.10).

$$P_i^d(k+1) =$$

$$\begin{cases} \min\left(P_{\max,i}, \left(\dfrac{P_{\max,i} - E_i^{(d)}(k) + E_i^{(r)}(k)}{2}\right)^+\right), \text{ if } a_i(k+1)=0 & \text{(5.10a)} \\ \min\left(P_{\max,i}, \left(\dfrac{P_{\max,i} - E_i^{(d)}(k) + E_i^{(b)}(k)}{2}\right)^+\right), \text{ if } a_i(k+1)=1 \text{ and } V_{r_i}(k) \geq 0 & \text{(5.10b)} \\ P_i^{(d)}(k), \text{ if } a_i(k+1)=1 \text{ and } -\tau \leq V_{r_i}(k) < 0 & \text{(5.10c)} \\ z \cdot P_i^{(d)}(k), \text{ if } a_i(k+1)=1 \text{ and } V_{r_i}(k) < -\tau & \text{(5.10d)} \end{cases}$$

The first two cases (5.10a) and (5.10b) correspond to the waterfilling allocation for RS-RS and BS-RS transmissions, respectively, as indicated in Theorem 5.3.1. Given $z : 0 < z < 1$, (5.10d) is the power allocation on the dedicated-PoA (UE-to-RS) link when the relay backhaul link is overloaded with traffic. The node iteratively reduces its transmit power on its UE-to-RS link and re-allocates this power to its link to the BS. This continues until the congestion level drops to an acceptable level such that $-\tau \leq V_{r_i}(k) < 0$. As per (5.10c) then the UE can maintain its transmit power. Given its transmit power on the dedicated-PoA

link, the remaining power is allocated by node i to the adaptive-PoA link such that:

$$P_i^{(a)}(k+1) = P_{\max,i} - P_i^{(d)}(k+1) \tag{5.11}$$

UE $i : r_i = N_r + 1$

Next consider a UE i that has a dedicated-PoA link to the BS. As before, its decision to select the RS on its adaptive-PoA link depends on whether the peak data rate via BS-RS transmission is higher than that via BS-BS transmission and on whether there is sufficient backhaul capacity:

$$a_i(k+1) =$$

$$\begin{cases} 0, \text{ if } V_{r_i^A}(k) \geq \tau \text{ and } \zeta_i^{(br)}(k) \geq \zeta_i^{(bb)}(k) & \text{(5.12a)} \\ 1, \text{ if } \zeta_i^{(bb)}(k) > \zeta_i^{(br)}(k) \text{ or } V_{r_i^A}(k) \leq -\tau & \text{(5.12b)} \\ a_i(k), \text{ otherwise.} & \text{(5.12c)} \end{cases}$$

If $a_i(k+1) = 1$, then node i performs BS-BS transmission with the corresponding transmit power allocation on the dedicated-PoA as (5.10b). Conversely, if $a_i(k+1) = 0$ then the node performs BS-RS transmission and allocates its power as per (5.10a). As before, the remaining power is allocated to the adaptive-PoA link as per (5.11).

5.4.2 Single-Link UEs

If $c_i(k+1) = 0$, then the UE only has a single (dedicated-PoA) link. In this case, it will adapt its transmit power such that:

$$P_i^d(k+1) =$$

$$\begin{cases} P_{\max,i}, \text{ if } V_{r_i}(k) \geq 0 \text{ or } r_i = N_r + 1 & \text{(5.13a)} \\ z.P_i^d(k), \text{ if } V_{r_i}(k) < -\tau & \text{(5.13b)} \\ P_i^d(k), \text{ otherwise.} & \text{(5.13c)} \end{cases}$$

In the above, if the node is connected to the BS or to an RS with sufficient backhaul capacity, then it will transmit at maximum power to achieve its objective in (5.7). However, if there is congestion such that $V_{r_i}(k) < -\tau$, then as described earlier the node iteratively decrements its transmit power by some scaling factor z so that its data rate reduces. If the congestion at the relay decreases to some acceptable threshold such that $-\tau \leq V_{r_i}(k) < 0$, then the node simply maintains its transmit power.

The key feature of the NDT algorithm is that it gives UEs the flexibility to switch between different transmission modes (i.e. RS-RS versus BS-RS transmission) based on both link-layer and congestion-based conditions. In contrast, in a fixed single connection (RS-RS and BS-BS) or dual connection (BS-RS) topology, the UEs cannot adapt to dynamic traffic and link layer conditions. Moreover, when the traffic load on the backhaul links is large, conventional waterfilling on the links is not an optimal allocation. Under NDT the UEs re-allocate more transmit power (and data rate) on the direct link to the BS until the backhaul link is load-balanced.

5.5 Convergence

We analyze the conditions under which the distributed adaptations performed by the nodes under our NDT mechanism will converge to a solution of (5.7). We first show convergence under certain conditions when all n UEs have dual connectivity (i.e. there is sufficient bandwidth to have $m = n$). We will later show that even when $m \leq n$, then under the same conditions the system will still reach convergence.

Suppose $n = m$. We define matrix $\mathbf{A}(k) = diag([a_1(k), a_2(k), \cdots, a_n(k)])$ which is an $n \times n$ diagonal matrix where element $a_i(k)$, as defined earlier, represents whether node i is connected to the BS or to an RS on its adaptive-PoA link. We let $\overline{\mathbf{A}} = \mathbf{I} - \mathbf{A}$ where $\mathbf{I}$ is the identity matrix. For example, $\mathbf{A}(0) = \mathbf{I}$ implies that all UEs initially transmit to the BS on their adaptive-PoA links. The vector representation of the effective interference in (5.2) in iteration k is then

$$\begin{aligned} \mathbf{E}_d(k) &= \mathbf{D}_d + \mathbf{F}\mathbf{P}_d(k), \text{ (dedicated-PoA links)}, \\ \mathbf{E}_a(k) &= \mathbf{A}\mathbf{D}_b + \overline{\mathbf{A}}\mathbf{D}_r, \text{ (adaptive-PoA links)} \end{aligned} \tag{5.14}$$

where $\mathbf{E}_a(k)(i) = \mathbf{D}_b(i)$ when $a_i(k) = 1$ and $\mathbf{E}_a(k)(i) = \mathbf{D}_r(i)$ when $a_i(k) = 0$.

5.5.1 High η_r regime

Note that under NDT when the capacity of the RS-to-BS backhaul links is sufficiently high, the choice of PoA of UEs depends only on the peak data rates achievable through the BS-RS, RS-RS or BS-BS transmissions. As per Corollary 5.3.2, this in turn depends on the effective interferences on their adaptive-PoA links.

Corollary 5.5.1. *Given a large enough RS-to-BS link capacity η_r, $a_i = 1$ when $\mathbf{D}_b(i) < \mathbf{D}_r(i)$ for each UE i and conversely $a_i = 0$ when $\mathbf{D}_b(i) \geq \mathbf{D}_r(i)$, regardless of the initial PoA assignments.*

Proof. Suppose that there is some η_r which is more than the maximum aggregate data rate the UEs can ever forward through the relay. Under NDT, the choice of a PoA by each UE depends on the peak data rate it can achieve via waterfilling allocation on the two links. Recall that as per Corollary 5.3.2, $\zeta_i^{(rr)} < \tau_i^{br}$ when $E_i^{(b)} < E_i^{(r)}$ for UE $i : r_i \leq N_r$. Likewise, $\zeta_i^{(bb)} < \tau_i^{br}$ when $E_i^{(b)} < E_i^{(r)}$ for UE $i : r_i = N_r + 1$. If $\mathbf{D}_b(i) < \mathbf{D}_r(i)$ for UE i then $E_i^{(b)}(k) < E_i^{(r)}(k)$ always. Hence the UE chooses the BS as the PoA under NDT on the adaptive-PoA link. Conversely, $E_i^{(b)}(k) \geq E_i^{(r)}(k)$ when $\mathbf{D}_b(i) \geq \mathbf{D}_r(i)$ and the UE will choose the RS. This applies regardless of which PoA the UE initially attaches to. □

Given a high enough backhaul capacity, we now derive a solution of (5.7) for each UE in the network under NDT. Corresponding to Corollary 5.5.1, the choice of PoAs of all UEs on their adaptive-PoA links can be represented by $\mathbf{A}^* = diag[a_1, a_2, \cdots, a_n]$.

Theorem 5.5.2. *The transmit powers converge to* $\mathbf{P}_d^* = \frac{1}{2}\left[\mathbf{I} + \frac{\mathbf{F}}{2}\right]^{-1}\left[\mathbf{P}_{\max} - \mathbf{D}_d + \mathbf{A}^*\mathbf{D}_b + \overline{\mathbf{A}}^*\mathbf{D}_r\right]$ *given a large enough RS-to-BS link capacity* η_r *if* $\mathbf{0} \leq \mathbf{P}_d^* \leq \mathbf{P}_{\max}$.

Proof. For some large η_r, the rate differential at each relay is larger than the thresholds set in (5.9a) and in (5.9b). Hence, the choice of PoA on the adaptive-PoA link depends only on the peak data rates $\zeta_i^{(rr)}$ and $\zeta_i^{(br)}$ if $r_i \leq N_r$. Conversely, if $r_i = N_r + 1$ then the choice is between $\zeta_i^{(bb)}$ and $\zeta_i^{(br)}$. Hence, regardless of the transmit powers, as per Corollary 5.5.1, let $\mathbf{A}^*$ represent the choice of PoAs given the normalized noise powers on the channels for adaptive-PoA links: the nodes allocate transmit power according to either (5.10a) or (5.10b). We represent the power updates for the dedicated-PoA links in matrix notation as

$$\begin{aligned}
\mathbf{P}_d(k+1) &= \frac{1}{2}\left[\mathbf{P}_{\max} - \mathbf{E}_d(k) + \mathbf{E}_a(k)\right] \\
&= \frac{1}{2}[\mathbf{P}_{\max} - \mathbf{D}_d - \mathbf{F}\mathbf{P}_d(k) + \mathbf{A}^*\mathbf{D}_b + \overline{\mathbf{A}^*}\mathbf{D}_r] \\
&= \frac{1}{2}[\mathbf{P}_{\max} - \mathbf{D}_d + \mathbf{A}^*\mathbf{D}_b + \overline{\mathbf{A}}^*\mathbf{D}_r] - \frac{1}{2}\mathbf{F}\mathbf{P}(k) \\
&= \mathbf{N} - \mathbf{M}\mathbf{P}_r(k)
\end{aligned} \tag{5.15}$$

where $\mathbf{N} = \frac{1}{2}[\mathbf{P}_{\max} - \mathbf{D}_d + \mathbf{A}^*\mathbf{D}_b + \overline{\mathbf{A}}^*\mathbf{D}_r]$ and $\mathbf{M} = -\frac{1}{2}\mathbf{F}$. The above evolves to:

$$\begin{aligned}
\mathbf{P}_d(k) &= \mathbf{N} - \mathbf{M}\left(\mathbf{N} - \mathbf{M}\left(\mathbf{M} + \mathbf{M}\left(\cdots\mathbf{P}(0)\right)\right)\right) \\
&= [\mathbf{I} + \mathbf{M} - \mathbf{M}^2 - \cdots]\mathbf{N} + \mathbf{M}^{k-1}\mathbf{P}(0) \\
\lim_{k\to\infty}\mathbf{P}_d(k) &= \mathbf{P}_d^* = [\mathbf{I} - \mathbf{M}]^{-1}\mathbf{N} \\
&= \frac{1}{2}\left[\mathbf{I} + \frac{\mathbf{F}}{2}\right]^{-1}\left[\mathbf{P}_{\max} - \mathbf{D}_d + \mathbf{A}^*\mathbf{D}_b + \overline{\mathbf{A}}^*\mathbf{D}_r\right]
\end{aligned} \tag{5.16}$$

where $\mathbf{P}_d(0)$ is the initial transmit power vector of the dedicated-PoA links. Likewise, the corresponding transmit powers on the adaptive-PoA channels are simply the difference be-

tween $\mathbf{P}_{\max}$ and (5.15). They evolve to $\lim_{k\to\infty} \mathbf{P}_a(k) = \mathbf{P}_a^* = \mathbf{P}_{\max} - \mathbf{P}_d^*$. □

5.5.2 Limited η_r regime

Next we consider the general case where the backhaul capacity is limited.

Theorem 5.5.3. *Given a large enough tolerable τ, NDT adaptations will converge if the spectral radius of $\mathbf{F}$ is less than two.*

Proof. According to Corollary 5.5.1 the inequality between the peak data rates $\zeta_i^{(rr)}$, $\zeta_i^{(br)}$ or $\zeta_i^{(bb)}$ always holds given the inequality relationship between $\mathbf{D}_b(i)$ and $\mathbf{D}_r(i)$ for each UE i. Thus, given a high enough τ, the nodes will not cycle back and forth their links between different PoAs as per (5.9) and (5.12). The power allocation of UE $i : r_i = N_r + 1$ will only follow the waterfilling allocation either in (5.10b) or (5.10a). Likewise, if UE $i : r_i \leq N_r$, then this node will either perform waterfilling allocation as per (5.10a)(5.10b) or maintain its transmit power from the preceding iteration as per (5.10c). Thus, the evolution of transmit power for the system is equivalent to that in (5.16) except that some nodes may not update their transmit power every iteration (i.e. their transmit power level is based on an update from an earlier iteration). The power updates can therefore be described as an *asynchronous iterative* system [69][70]. It is known that such a system converges if the iterative matrix $\mathbf{M}$ in (5.16) has a spectral radius less than one [70] (corresponding to a spectral radius of less than 2 for $\mathbf{F}$). □

5.5.3 $m \leq n$

Lemma 5.5.4. *If the conditions in Theorems 5.5.2 and 5.5.3 hold, then the system converges when $m \leq n$.*

Proof. Consider the case when only $m \leq n$ of the UEs have an adaptive-PoA link . (i) In the high η_r regime, since there is high backhaul capacity, the remaining single-link UEs will also always transmit at a maximum power level as per (5.13a). (ii) Given a limited η_r, for

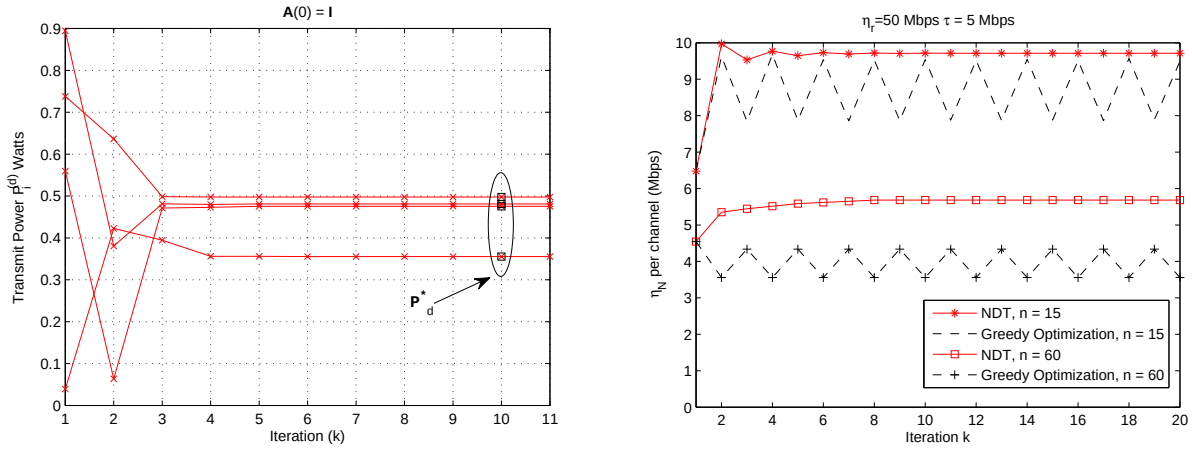

(a) (b)

Figure 5.2: (a) We observe for the network shown in Fig. 5.1, the convergence of the transmit power vector $\mathbf{P}_d$ to the fixed point (superimposed on $k = 10$) predicted in (5.16) regardless of the initial power and PoA assignments. (b) For sample networks, we plot the system throughput and see that NDT converges within a few iterations whereas a greedy optimization results in unstable performance.

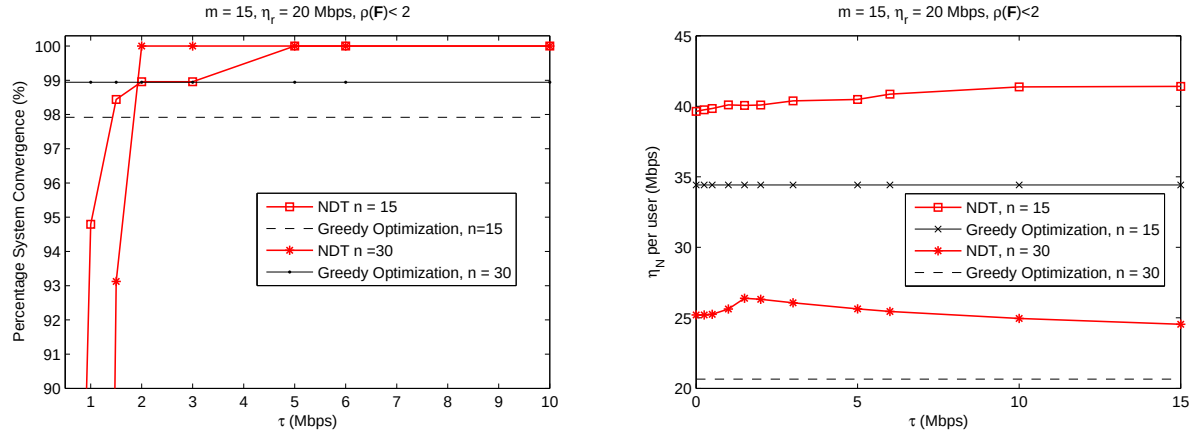

(a) (b)

Figure 5.3: (a) With a higher τ, the system always converges if the spectral radius constraint on $\mathbf{F}$ holds. The corresponding system throughput is shown in (b).

a large enough τ single-link UEs will again always maintain some constant transmit power level as per (5.13c)(5.13a). In either scenario, the interference caused by the single-link UEs to the UEs with parallel links is always constant. Since this is akin to only an increase in the noise level, the adaptations by the UEs with dual connectivity remain unaffected. The system converges under these conditions. □

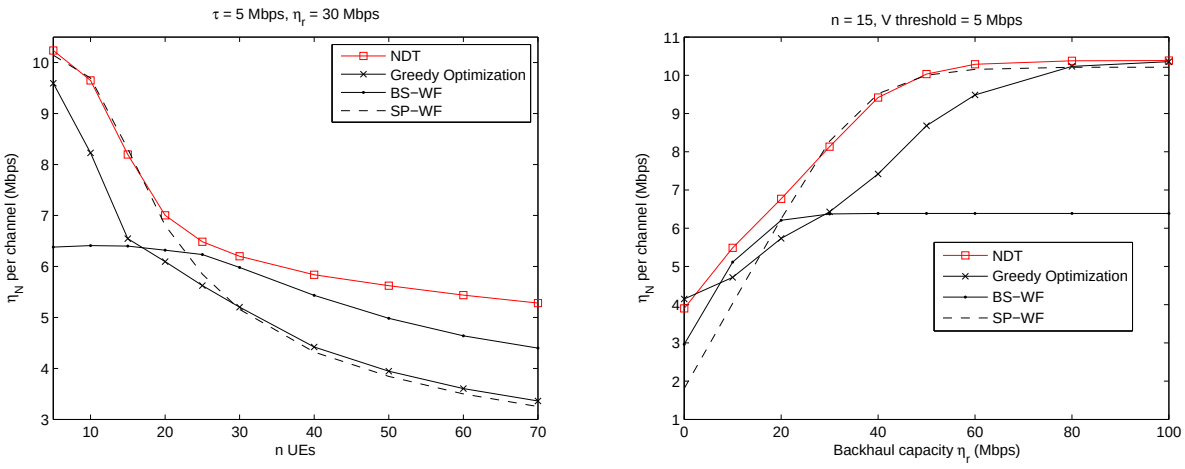

(a) (b)

Figure 5.4: Over the range of (a) n or (b) η_r, BS-WF or SP-WF schemes have good performance over certain regions only. In contrast, NDT enables nodes to benefit from the best of both schemes and adapt to the network-wide conditions.

5.6 Simulation Results

In this section, for a multihop cellular network we use Matlab-based simulation to determine the aggregate end-to-end data rate η_N over a range of control parameters. We assume $n_o = -140$ dBW, $W = 1$ MHz and $P_{\max,i} = 1.0$ Watts for all UEs. We assume that the cross-link gains ($g_{i,r_i}^{(f)}, g_{i,b}^{(q)}$, etc.) are of the form $\kappa_{j,i}^{(f)} \cdot d_{j,i}^{-\alpha}$ where $\kappa_{j,i}^{(f)}$ is an exponentially distributed random variable with unit variance (due to Rayleigh fading) on channel f. The fading gains are assumed independent and identically distributed for all links. There are 50 power control iterations in each simulation trial. The transmit powers of pilot signals from the BS and RS on the downlink control channel are assumed equal. The UEs are randomly and uniformly located in cluster regions of radius R_L around each of the N_r relays.

Unless otherwise stated, we assume the following: $N_r = 4$ where the relays are at 90^o from one another at $R = 2000$ m from the BS, cluster radius $R_L = 1000$ m, path loss exponent $\alpha = 4.0$. For NDT we set $z = 0.8$ in all simulation trials. We first plot results with $m = n$ and will later look at the case when $m \leq n$.

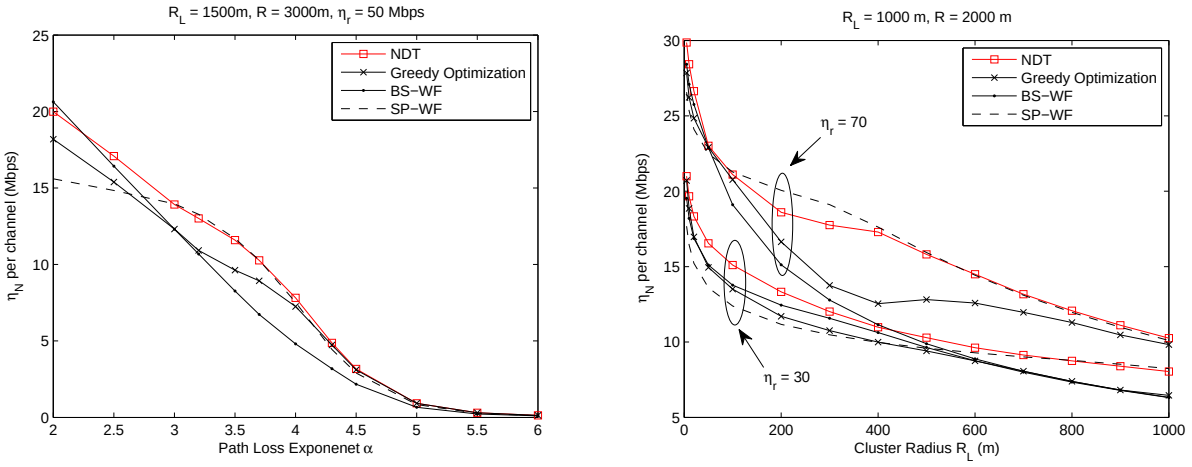

(a) (b)

Figure 5.5: (a) With increasing α or (b) when the cluster radius R_L is larger so that the UEs are dispersed over a wider region, the path loss is increased, thereby leading to a performance decline for all schemes. NDT enables the nodes to better adapt to both high and low path loss conditions.

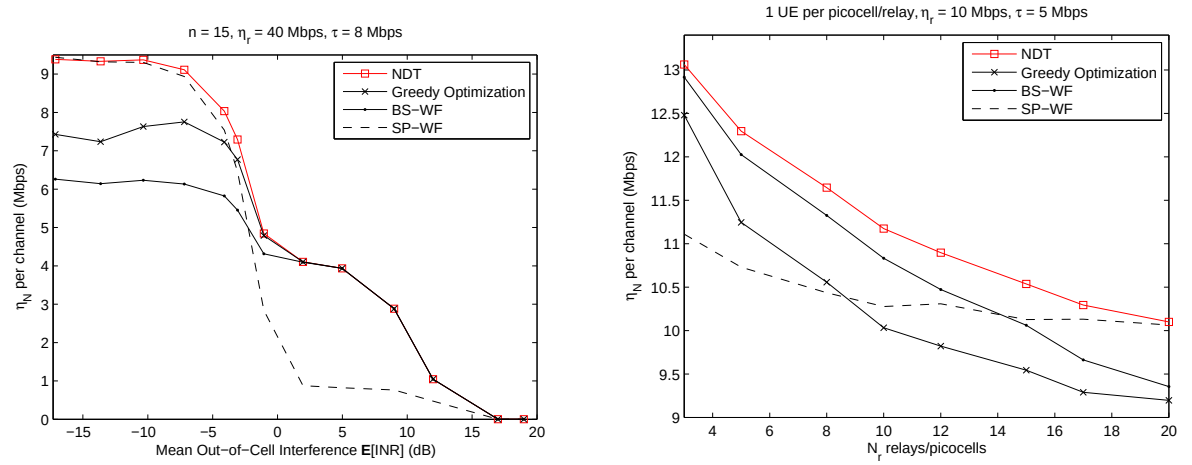

(a) (b)

Figure 5.6: (a) NDT has the best performance over the range of out-of-cell interference. (b) With increasing number of relays that have UEs clustered close to them, the multihop network approximates the case of picocell networks overlaid within a macro-cell.

5.6.1 Convergence

As an example of convergence, we first consider the network in Fig. 5.1 with $n = 3$ UEs located in the positions shown. We plot the evolution of transmit powers given that initially all UEs transmit on their adaptive-PoA link to their relays with a randomly chosen

initial vector $\mathbf{P}_d(0)$. In Fig. 5.2a, we observe that the transmit powers converge to the vector predicted in (5.16) where $\mathbf{A}^* = diag[0, 0, 0, 1]$. In Fig. 5.2b, we plot network-wide performance η_N normalized per UE for sample networks with $n = 15$ and $n = 60$ nodes. We compare NDT against *greedy optimization*, which represents an immediate solution of (5.7) by each node i for $a_i(k+1), P_i^{(d)}(k+1)$ and $P_i^{(a)}(k+1)$. The greedy approach, in contrast to NDT, results in an erratic evolution of the transmit powers, which correspondingly causes an unstable and lower system throughput over time.

In Fig. 5.3 we plot the effects of the rate differential threshold τ on system throughput and corresponding likelihood of convergence for those trials where the spectral radius of $\mathbf{F}$ is less than 2 (recall Theorem 5.5.3). With a higher τ, NDT will convergence 100% of the time. In contrast, convergence under greedy optimization occurs much less frequently and results in lower performance. With $n = 30$, we randomly pick 15 UEs for parallel links in each trial.

Note that in the intermediate case, when the backhaul capacity is limited and τ is small, then convergence cannot always be guaranteed as shown in Fig. 5.3a. For instance, to alleviate the backhaul congestion, UEs can send more data rate directly to the BS and less via the relay backhaul links. Thus, as the congestion levels decrease, the traffic at the relays drops and the backhaul links become under-loaded when τ is set too small. If the RS-to-BS links are not the bottleneck links anymore then this induces the nodes to switch back and send all their data via the relays. Thus, with a small τ, nodes may oscillate between congesting the backhaul links or under-utilizing them as they make local adaptations with instantaneous knowledge of the network-wide conditions. Nonetheless, we observe in Fig. 5.3b that even in these cases the likelihood of non-convergence is still relatively small.

5.6.2 System Throughput

We compare NDT against when nodes perform the well-known waterfilling power allocation [29] with two channels: (1) *Single-PoA Waterfilling (SP-WF):* The node attached to a relay allocates transmit power as per (5.10a)(5.11). Conversely, a node attached to the BS

allocates transmit power as per (5.10b)(5.11). (2) *BS-PoA Waterfilling (BS-WF):* Each node transmits to the BS on at least one of its channels. A node may have both channels to the BS or if it initially attached to an RS, then it also has a channel to the BS. The node allocates its transmit power as per (5.10b) and (5.11) in either case.

Fig. 5.4 shows that, in contrast to BS-WF or SP-WF, NDT offers the best of both approaches over the entire range of the parameters n and η_r. Under NDT, when the traffic load is lighter (either η_r is larger or n is smaller), the nodes only transmit to a single PoA whereas, conversely, they switch to transmitting to the BS on their adaptive-PoA links when the load is heavier. Another observation is that, when the traffic load is large, under NDT the network performance is better than for BS-WF. This is because under NDT, a UE uses power control in (5.10d) and iteratively re-allocates more power on the direct link to the BS, instead of simply waterfilling over its channels.

In Fig. 5.5, we plot the performance for $n = 15$ and $\tau = 5$ Mbps, by varying the path loss exponent α and cluster radius R_L. We observe that, while performance for all schemes declines with an increase in either parameter, NDT still offers the best of any of the schemes. In Fig. 5.5b, with increasing R_L, the inter-UE distance grows and the nodes become dispersed over a wider region, and thus more distant from their receivers. While the performance for NDT declines with increasing R_L (due to greater path loss), it is still better than that of other schemes.

In Fig. 5.6a, we consider the impact of out-of-cell interference on performance. In a single-cell system, the adaptive-PoA links are assumed to be noise-limited. However, in a multi-cellular network, all links will also experience some interference from outside the cell. As in [73], we assume that the out-of-cell interference can be modeled as additional noise with lognormal distribution across each channel such that:

$$n_o^{'} = n_o(1 + INR) \tag{5.17}$$

where INR is interference-to-noise ratio. The interference received at the BS will be weaker than at the relays which lie closer to cell edge. We have μ_1 as the first cumulant of INR

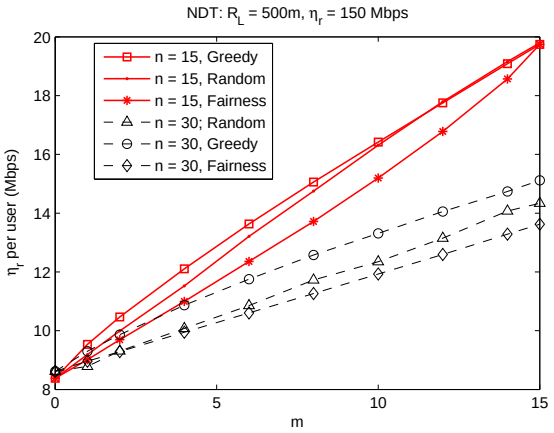

Figure 5.7: When $m \leq n$, the greedy policy enables dual connectivity to nodes with good channels. Note that even a random allocation policy does fairly well.

at each relay whereas for the links to the BS this would be $\widehat{\mu}_1 = \mu_1 \times (\frac{R_L}{R_L+R})^{\alpha}$. The corresponding derivation of the second-order cumulant μ_2 is explained in [73]. In Fig. 5.6a, we observe that NDT has the highest performance over the entire range of the out-of-cell interference.

In Fig. 5.6b we consider the case when a large number of relays are randomly and uniformly located within the cell and the UEs are clustered close to them. Since the RS-to-BS links operate on non-UE channels, the 2-hop network would resemble the situation when picocells coexist within a macro-cellular system. Moreover, the wireless backhaul capacity of the picocell networks might be limited or constrained [5]. Hence, in this scenario the relays of the 2-hop network could resemble picocell base stations. We consider a network with one UE attached to each relay/picocell and where the maximum RS-BS separation is $R = 1000$ m and $R_L = 200$ m. An implication from the results is that if UEs can transmit to both the macro-cellular BS and the picocell BS under the limited backhaul capacity scenario then there are performance gains over when they are constrained to transmit only to picocell base stations.

In Fig. 5.7a, we consider the impact of limited bandwidth such that $m \leq n$ and consider several policies for deciding which UEs should have dual connectivity:

Random allocation

The m UEs are randomly chosen from among the n nodes.

Greedy allocation

In each iteration k, UE j which has the lowest effective interference from among the UEs without dual connectivity is allocated a channel to establish an adaptive-PoA link (i.e. $j = \arg\min[E_1^{(d)}(k), \cdots, E_n^{(d)}] : c_j(k) = 0$). This is to maximize the system throughput by allocating additional links to those UEs which already have good channels.

Fairness-based allocation

In each iteration k, the UE which has the highest instantaneous effective interference from among the UEs without dual connectivity is allocated a channel to establish an adaptive-PoA link (i.e. $j = \arg\max[E_1^{(d)}(k), \cdots, E_n^{(d)}] : c_j(k) = 0$). In contrast to the greedy approach, the fairness-based assignment allocates bandwidth to the nodes which are currently disadvantaged. We can note that the greedy assignment policy has the best performance, the random assignment policy also comes reasonably close to it, and the fairness-based policy yields the poorest performance.

5.6.3 Effect of τ on system throughput

Note that a high rate differential threshold τ does not imply a high congestion load on the backhaul links. This threshold only determines how sensitive nodes are between switching between dual connection mode (i.e. BS-RS transmission) and single connection mode (i.e. RS-RS or BS-BS transmission). In Fig. 5.8 we plot the evolution of the system throughput for a sample network over time. We assume that the initial set of receivers for the UEs with dedicated-PoA links to the relays is randomly selected for the adaptive-PoA links. The UEs are located within $R_L = 250$ m of the PoAs. We note that at $\tau = 0$ the system throughput under NDT does not converge. In contrast a moderate τ leads to a stable and high system

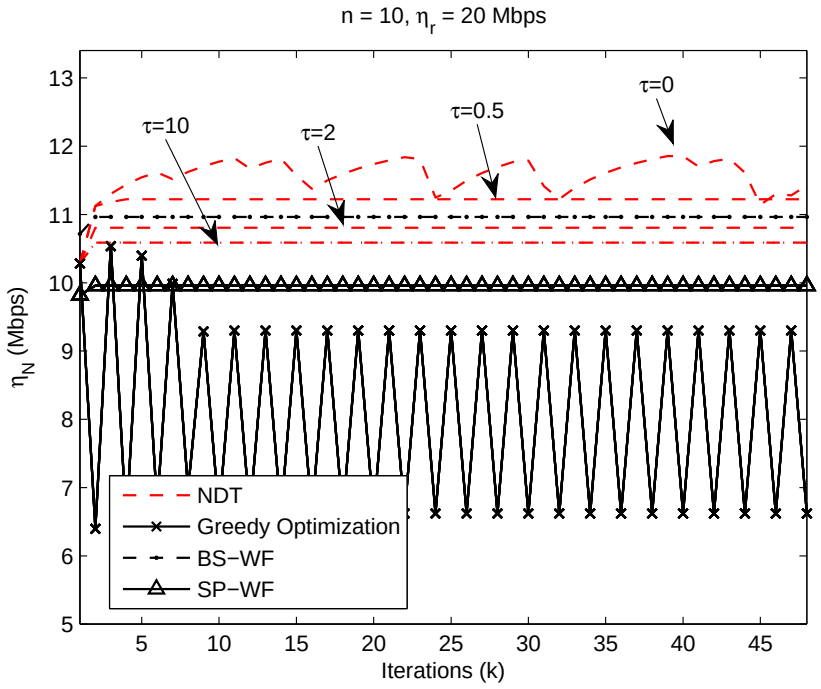

Figure 5.8: Evolution of system throughput in a sample network. A small τ can provide convergence under NDT but increasing it to a high value leads the nodes to only optimize link layer within a fixed topology.

throughput. Increasing τ to a high value also leads to a stable operating point but eventually reduces system throughput (comparable to that between SP-WF and BS-WF).

In the extreme case when τ is set at infinity, then as per (5.12)(5.9) nodes will have fixed transmission mode and will only use waterfilling as per either (5.10a) or (5.10b). In this case, under NDT the system will be equivalent to when a subset of nodes adapt as per SP-WF and the remaining as per BS-WF. In other words, with a high τ, nodes are reduced to only optimizing their link layer performance. While a high τ will contribute to hysteresis in the NDT adaptations of the nodes, it will not affect system performance by much, especially when the backhaul links offer a high enough capacity.

We illustrate this in Fig. 5.9 by plotting the system throughput while varying τ as a factor of the given backhaul capacity η_r. We note that when the backhaul capacity is relatively low, as shown in Fig. 5.9(a)(b), the system is fairly sensitive to the choice of the rate differential threshold. Setting τ to either a low or a high value can result in a drop in the

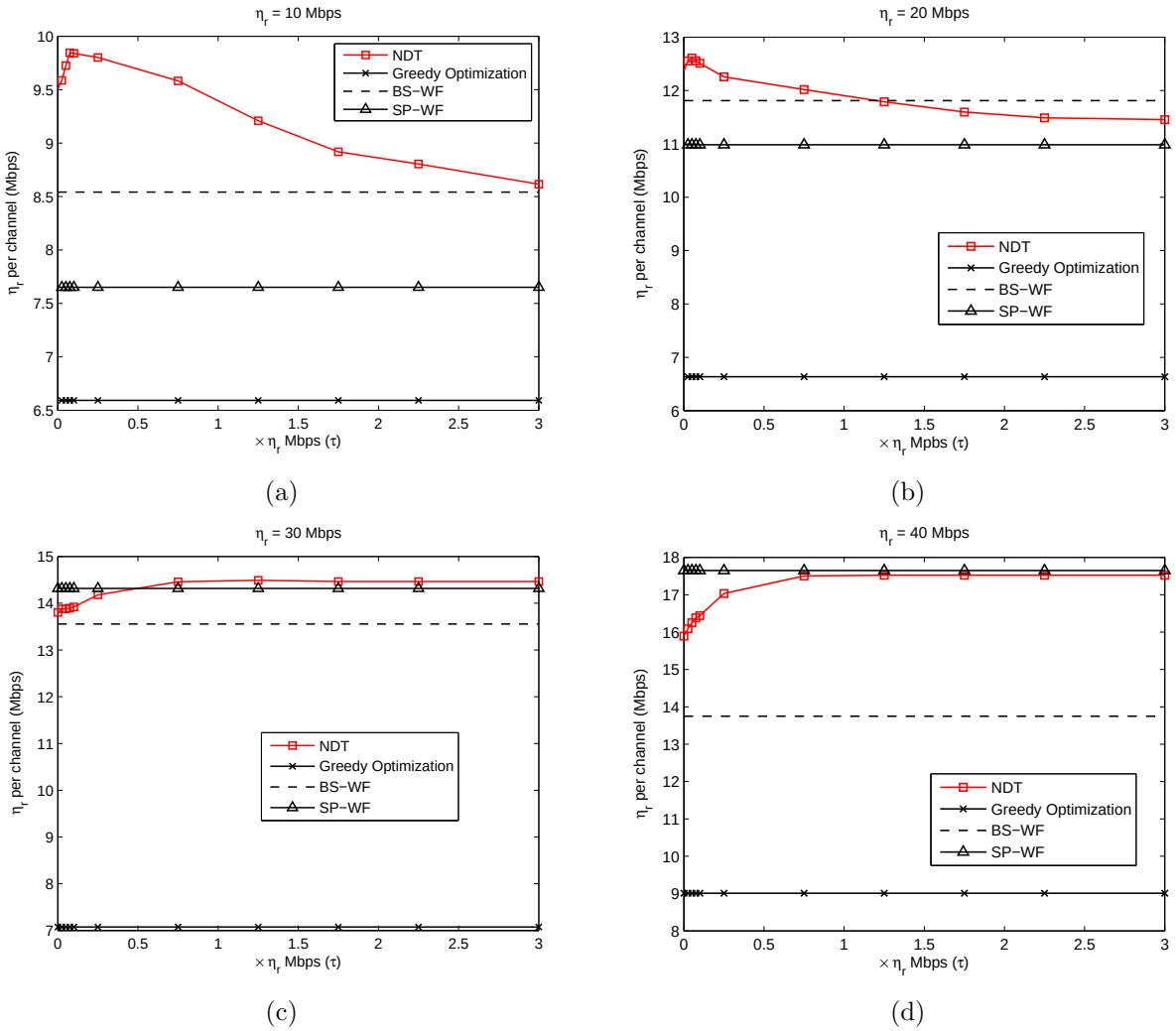

Figure 5.9: We set $n = 10$ UEs, $R_L = 250$ m and vary τ as a fraction of the backhaul capacity η_r in all above results. When the backhaul capacity is low, adaptations are sensitive to local adaptations and the choice of τ can significantly influence system throughput.

system performance. In particular, a high τ can lead to a significant decline in NDT's system throughput. In contrast, when the backhaul capacity is large, Figs. 5.9(c)(d) illustrate that a high τ does not adversely affect the system throughput.

These results are intuitive: when η_r is low, the end-to-end performance of nodes suffers from congestion which in turn makes τ a bigger factor in influencing the optimal system throughput. System stability or equilibrium can only be achieved by regulating τ to a high enough value and consequently paying a price in terms of system throughput loss. Conversely, when η_r is large, there is minimal congestion and the nodes tend to only optimize their link

layer performance. Thus, a high τ then no longer incurs the same system throughput penalty for NDT.

5.7 Conclusion

We have proposed for a 2-hop cellular uplink network a link adaptive scheme where nodes have the flexibility to transmit to multiple Points of Access. Under our scheme, the nodes can split their data streams to either a single access point or transmit to the base station and to a relay using knowledge about channel state information and traffic condition. We demonstrate a significant improvement in the aggregate end-to-end data rate in the network due to the proposed adaptation scheme over greedy optimization. In the next chapter, we provide an overview of the link-adaptive schemes which we have proposed and assess future directions for further research.

Chapter 6

Conclusions

In this dissertation we have focused on how mobiles can act as a decentralized set of autonomous decision-makers that optimize their own local objectives by adapting their transmit power or Point of Access (PoA) or by aggregating carriers. We first provide a summary of our contributions and then present avenues for further research based on our proposed ideas.

6.1 Dissertation Evolution

Wireless communication networks are complex and large systems which are difficult to optimize with conventional cross-layer optimization frameworks. These approaches aim to optimize some network-wide goal or utility and have been widely researched in the past decade. In contrast, multi-agent approaches (e.g. using game theory etc.) have also been widely studied where nodes aim to maximize their local utility or link-layer objectives. However, there has been a gap in addressing the issues which arise when nodes transmit information over multihop networks or when end-to-end performance deviates from link-layer performance.

This dissertation fills in this area by proposing schemes for emerging multihop cellular networks where nodes can adapt to both local and global conditions. We have provided a systematic approach in both defining the notion of global conditions in terms of congestion levels at PoAs and in proposing several schemes for how nodes can consider this information

in their autonomous transmit power, channel and topology adaptations. Over a range of simulation scenarios, we have illustrated the significant gains in system throughput by the proposed approach as opposed to schemes which only consider link-state information. Since the proposed adaptations are dynamic due to the inter-dependence between interference and congestion levels at the PoAs, we have proposed mechanisms to ensure convergence and provided corresponding analytical proofs.

Following is an overview and evolution of how we developed our answers to the research questions which were posed in Chapter 1.

- In Chapter 3 we began by considering link-adaptive schemes where nodes can only adapt transmit power control. We proposed a marginal power efficiency-based adaptation (MPEA) for time-varying wireless channels which enables link SINRs to be dynamically adjusted. We have combined our proposed MPEA with the FM algorithm, resulting in power control schemes for multihop cellular networks where nodes can dynamically adapt to both local and global conditions by taking into account dynamic congestion conditions at the relays. We have proved convergence of the power control adaptations and have derived closed-form expressions to which the transmit power levels converge. Our numerical results showed that, despite the lack of cooperation among users, the power allocation policy is also able to improve the global system performance.

- In Chapter 4 we then extended the range of adaptations to when nodes could also aggregate channels and change their PoAs in the network in addition to performing transmit power control. Our adaptation mechanism enabled the UEs to distributedly optimize a combination of achieved data rate and power consumption by appropriate local adaptations. Simulation results showed these adaptations to yield a better system performance than when nodes simply consider current channel quality indicators, combined with greedy channel aggregation.

- In Chapter 5 we then expanded on the notion of topology adaptations by considering an adaptive scheme for multihop cellular networks where nodes have (i) dual connections

to relays and the base station and (ii) allocate transmit power to optimize data rate on these links. Under our scheme, nodes have the flexibility to stream data via a single PoA (either a single relay or the base station) or through multiple PoAs (e.g. both a relay and the base station) depending on the current congestion conditions. We showed in simulation results that this additional flexibility in topology adaptations with power allocation yields significant system performance improvement, as compared to when nodes operate in a fixed network topology. We also demonstrated convergence of the scheme under a variety of scenarios and derived a closed-form expression for the transmit power at the point of convergence.

6.2 Answers to Research Questions

In Chapter 1, we asked 5 questions on how nodes could perform autonomous link adaptations by taking into account network-wide or end-to-end conditions. While each of the questions is open-ended by its nature, the dissertation addresses them in the context of transmit power, channel aggregation and topology adaptations for multihop cellular networks in the following way:

1. Under what conditions is it beneficial to make local adaptation decisions based on network-wide conditions or end-to-end goals?

The dissertation showed that the benefit of taking into account end-to-end conditions arises when UEs are operating in multihop networks and the traffic load on the relays is large. We have demonstrated that simply optimizing link layer performance is not an optimal strategy especially when the (i) the number of users is large or (ii) when the backhaul capacity is insufficient, as this leads the relay-to-base station links to suffer from a heavy traffic load. Instead, under the proposed schemes MH-MPEA, NSLA and NDT, when nodes take into account these congestion conditions, they are able to autonomously conserve transmit power resource in a way which minimizes network-wide interference and congestion. Thus, this adaptation strategy leads to a better system throughput. In short, we demonstrate that as

a multihop cellular network becomes large and more complex, the proposed schemes enable increasing performance improvement over greedy local adaptations.

2. What is an appropriate link adaptation algorithm?

The dissertation has explored a framework where the network is viewed in terms of a dynamic set of bottleneck links and non-bottleneck links. The appropriate link adaptation algorithm is selected by each node based on which of the two sets it belongs to. To improve their performance, nodes with bottleneck links adopt transmit power allocation algorithms which use the waterfilling principle in either the time domain (i.e. MH-MPEA or NSLA) or across the frequency domain (in NDT) so as to boost their data rates. In contrast, we propose the use of resource-conserving adaptation algorithms for nodes with non-bottleneck links. In particular, the well-known FM power control algorithm has been employed in the proposed schemes so as to enable non-bottleneck links to achieve some minimum SINR with the least transmit power.

3. How is the conflict between different adaptation choices resolved?

When a node can adapt in a variety of ways given the current link layer and end-to-end conditions, we have explored mechanisms to resolve the conflict between the adaptation choices. In Chapter 3, we compared MH-MPEA and NSLA schemes, in which transmit power of non-bottleneck links was updated in a complementary fashion. On the one hand, in NSLA we explored the case where all nodes could reduce their transmit power levels in parallel when the backhaul link was congested. On the other hand, in MH-MPEA we explored the complementary case when nodes reduced their transmit power levels sequentially. Using simulation, we illustrated that while the system throughput performance of the two approaches was somewhat similar, the latter approach resulted in a better power consumption.

In Chapter 4, we also considered for a node with a non-bottleneck link the conflict between transmit power minimization and a topology adaptation. We proposed that whenever the backhaul congestion is above a certain threshold and connection to a better PoA is fea-

sible, a node should prioritize the latter. Otherwise, it can continue to reduce its transmit power level. In Chapter 5, we similarly explored the choice for a node between having a single connection and a dual connection in a flexible topology. We illustrated that a good strategy for a node in terms of achieving a stable performance is to switch from single connection mode to the dual mode or vice versa by comparing its possible achievable rates using a threshold-based approach instead of a greedy approach.

4. Can the link adaptations converge to a stable transmit power selection and topology? Since nodes are assumed autonomous, the proposed adaptive schemes need to ensure convergence so as to prevent erratic changes in system throughput. We have illustrated that all the proposed schemes MH-MPEA, NSLA and NDT can achieve convergence in terms of transmit power levels and topology adaptations. The basic mechanism for convergence in all these schemes essentially relies on two system properties: (i) that the maximum interference experienced by each link in the network be less than some threshold, and (ii) the rate differential threshold at the relays be set high enough. This mechanism adds hysteresis into the autonomous adaptations of the nodes and prevents them from cycling between different adaptation choices.

5. What is the impact of global knowledge as opposed to local knowledge? We have characterized local knowledge of each node in terms of the effective interference level on its link and the global knowledge in terms of the rate differential at its PoA. Using simulation, we have demonstrated that when nodes adapt using global knowledge (i.e. taking into account current congestion levels) the proposed schemes result in a consistent 10% to 25% system throughput improvement over the range of simulation parameters.

6.3 Future Directions: An Eye Towards 5G

The adaptive framework which we have explored in this dissertation can be extended to emerging communication technologies and networks. Researchers have already begun considering the paradigm of 5G networks, which will require fundamental changes in the design of future cellular systems. In particular, 5G networks are envisioned to include (i) device-centric architectures, (ii) millimeter-wave systems, and (iii) massive-MIMO technologies [74]. The mechanisms which we have have proposed to take into account network-wide conditions can be applied in the following ways to such networks:

- In device-centric architectures, nodes will have parallel connections to multiple heterogeneous radio access networks and will need to route information flows with different priorities [74]. In this context, a UE of the future will need to consider the feedback on the congestion levels at the backhaul/back-end of the PoA at all these connections as it makes its adaptations.

- In heterogeneous networks, we could consider the case when UEs operate in certain bands as primary/incumbent users and as opportunistic/secondary users in other frequencies while accounting for current congestion conditions at their PoAs. For instance, a UE may opportunistically transmit more data rate to a lightly loaded PoA in secondary-user bands if its current primary-band link to a PoA is suffering backhaul congestion.

  With an evolving FCC spectrum policy which allows devices to communicate in the higher 5 GHz and 60 GHz bands, the achievable rates on different bands will be significantly varied due to the underlying propagation properties. Thus, another possibility is to extend the work in Chapter 5 and consider using channels for the dedicated-PoA and adaptive-PoA links in different frequencies with significantly different bandwidths.

  In short, there are numerous frequency band-related extensions to the notion of soft topology adaptations which are promising and related to the millimeter-wave communication paradigm in 5G networks.

- We have considered nodes with a single transmit antenna in this dissertation. We could re-consider the problems which we have explored with when the nodes are equipped with multiple antennas.

- In Chapters 4 and 5, we have considered the capacity of the backhaul links as independent and with a fixed bandwidth. Another avenue for future work is to explore how the relay nodes can autonomously adapt the bandwidth dedicated to the backhaul links in response to data rate demand and PoA selections by the UEs.

6.4 List of Publications

We finally provide a list of publications associated with the work in the dissertation:

- Syed Amaar Ahmad and Luiz A. DaSilva, "Power control and soft topology adaptations in multihop cellular networks with dual connectivity," *submitted to IEEE Transactions on Communications.*

- Syed Amaar Ahmad, Claudio R. C. M. da Silva and Luiz A. DaSilva, "Marginal power efficiency considerations for power control adaptations in multihop cellular networks," *to appear IEEE Transactions on Vehicular Technology, 2014.*

- Syed Amaar Ahmad and Luiz A. DaSilva, "A link adaptive scheme for multihop cellular systems using congestion feedback", IEEE GLOBECOM, Atlanta, GA, Dec. 2013.

- Syed Amaar Ahmad, Claudio R. C. M. da Silva and Luiz A. DaSilva, "Relay-feedback based power control for multihop wireless networks", IEEE MILCOM, Orlando, FL,Oct.-Nov. 2012.

Appendix A

Waterfilling Allocations and Discussion

Proof of Theorem 5.3.1

Consider the peak RS-RS transmission data rate $\zeta_i^{(rr)}$ for UE i:

$$\underbrace{\max}_{P_i^{(a)}, P_i^{(d)}} W \log_2 \left(1 + \frac{P_i^{(a)}}{E_i^{(r)}}\right) + W \log_2 \left(1 + \frac{P_i^{(d)}}{E_i^{(d)}}\right)$$

$$P_i^{(a)} + P_i^{(d)} \leq P_{\max,i}$$

$$P_i^{(a)}, P_i^{(d)} \geq 0$$

Using Lagrangian multipliers and KKT conditions we obtain:

$$\underbrace{\max}_{P_i^{(a)},P_i^{(d)}} W\log_2\left(1+\frac{P_i^{(a)}}{E_i^{(r)}}\right)+W\log_2\left(1+\frac{P_i^{(d)}}{E_i^{(d)}}\right)-$$

$$\lambda_1(P_i^{(a)}+P_i^{(d)}-P_{\max,i})-\lambda_2 P_i^{(d)}-\lambda_3 P_i^{(a)}$$

$$\frac{W}{\ln(2)}.\frac{1}{P_i^{(d)}+E_i^{(d)}}-\lambda_1-\lambda_2=0$$

$$\frac{W}{\ln(2)}.\frac{1}{P_i^{(a)}+E_i^{(r)}}-\lambda_1-\lambda_3=0$$

$$\lambda_1(P_i^{(a)}+P_i^{(d)}-P_{\max,i})=0$$

$$\lambda_2 P_i^{(a)}=0$$

$$\lambda_3 P_i^{(d)}=0$$

Case 1: With $\lambda_2=\lambda_3=0,\lambda_1\neq 0$, we obtain:

$$\frac{W}{\ln(2)}.\frac{1}{P_i^{(d)}+E_i^{(d)}}-\frac{W}{\ln(2)}.\frac{1}{P_{\max,i}-P_i^{(d)}+E_i^{(r)}}=0$$

$$P_i^{(d)}=\frac{1}{2}(P_{\max,i}+E_i^{(r)}-E_i^{(d)})^+$$

$$P_i^{(a)}=P_{\max,i}-P_i^{(d)}=\frac{1}{2}(P_{\max,i}-E_i^{(r)}+E_i^{(d)})^+$$

Case 2: With $\lambda_3\neq 0,\lambda_2=0$ (i.e. $P_i^{(d)}=0$) we obtain:

$$\lambda_1=\frac{W}{\ln(2)}.\frac{1}{P_i^{(d)}+E_i^{(d)}}$$

$$P_i^{(d)}=0$$

$$P_i^{(a)}+0=P_{\max,i}$$

In either case, we thus have $P_i^{(a)}=P_{\max,i}-P_i^{(d)}$. We thus have $P_i^{(d)}=\min\left(P_{\max,i},\frac{1}{2}\left(P_{\max,i}-E_i^{(d)}+E_i^{(r)}\right)^+\right)$. The peak BS-RS or BS-BS transmission data rates $\zeta_i^{(br)}$ and $\zeta_i^{(bb)}$ have the same allocations as their maximization is identical.

Proof of Corollary 5.3.2

Recall that $\eta(\gamma) = W \log_2(1+\gamma)$. We define $P_i^{(d)^*}$ and $P_i^{(d)'}$ as the waterfilling allocations given $E_i^{(r)}$ and $E_i^{(r)'}$ respectively from the previous result. When $E_i^{(r)} < E_i^{(r')}$ then $P_i^{(d)^*} > P_i^{(d)'}$, and we have:

$$\zeta_i^{(rr)} > \tau_i^{(rr)'}$$
$$\eta\left(\frac{P_i^{(d)^*}}{E_i^{(d)}}\right) + \eta\left(\frac{P_{\max,i} - P_i^{(d)^*}}{E_i^{(r)}}\right) > \eta\left(\frac{P_i^{(d)'}}{E_i^{(d)}}\right) + \eta\left(\frac{P_{\max,i} - P_i^{(d)'}}{E_i^{(r')}}\right) \tag{A.1}$$

Thus, the result holds when $E_i^{(b)} = E_i^{(r)'}$.

Congestion Feedback Overhead

In a practical implementation of the proposed schemes, supplying each UE with the precise values of the rate differential V_r may not be necessary. Note that in all the schemes discussed in this dissertation, the congestion level at a PoA is defined in terms of three states: (i) $V_r \geq 0$, (ii) $-\tau \leq V_r < 0$ and (iii) $V_r < -\tau$. To adapt as per any of the proposed schemes, a UE only needs to know what is the current congestion level at its PoA is in terms of these three states which can in turn be denoted in 2 bits. Moreover, since any PoA would compute V_r for an interval of several LTE resource blocks (comprising several hundred bits), the 2 bits of congestion feedback would have a negligible overhead.

Bibliography

[1] 3GPP, "Feasibility study for further advancements for E-UTRA (LTE-Advanced)," *TR 36.912*, Apr. 2011.

[2] L. Garcia, K. Pedersen, and P. Mogensen, "Autonomous component carrier selection: interference management in local area environments for LTE-Advanced," *IEEE Commun. Magazine*, vol. 47, pp. 110–116, Sep. 2009.

[3] D. Amzallag, R. Bar-Yehuda, D. Raz, and G. Scalosub, "Cell selection in 4G cellular networks," *IEEE Trans. Mobile Computing*, vol. 12, pp. 1443 – 1455, Jul. 2013.

[4] S. W. Peters, A. Y. Panah, K. Truong, and R. W. Heath, "Relay architectures for 3GPP LTE-Advanced," *Eurasip Journal Wireless Commun. and Networking*, Jul. 2009.

[5] A. Ghosh and et al, "Heterogeneous cellular networks: From theory to practice," *IEEE Commun. Magazine*, vol. 50, pp. 54–64, Jun. 2012.

[6] 3GPP, "Coordinated Multi-Point operation for LTE physical layer aspects," *TR 36.819*, 2011.

[7] C. Hoymann, D. Larsson, H. Koorapaty, and J.-F. Cheng, "A lean carrier for LTE," *IEEE Commun. Magazine*, vol. 51, pp. 74–80, Feb 2013.

[8] S. A. Ahmad, C. da Silva, and L. A. DaSilva, "Relay feedback-based power control in wireless multihop networks," in *IEEE Conf. Military Commun. (MILCOM)*, Oct.-Nov. 2012.

[9] M. Chiang, "Balancing transport and physical layers in wireless multihop networks: Jointly optimal congestion control and power control," *IEEE Journal Sel. Areas Commun.*, vol. 1, pp. 104–116, Jan. 2005.

[10] Y. Xi and E. M. Yeh, "Throughput optimal distributed power control of stochastic wireless networks," *IEEE/ACM Trans. Networking*, vol. 18, pp. 1054–1066, Aug. 2010.

[11] M. J. Neely, E. Modiano, and C. E. Rohrs, "Dynamic power allocation and routing for time-varying wireless networks," *IEEE Journal Sel. Areas Commun.*, vol. 23, pp. 89–103, Jan. 2005.

[12] H.-J. Lee and J.-T. Lim, "Cross-layer congestion control for power efficiency over wireless multihop networks," *IEEE Trans. Veh. Tech.*, vol. 58, pp. 5274–5278, Nov. 2009.

[13] E. Matskani, N. D. Sidiropoulos, and L. Tassiulas, "Convex approximation algorithms for back-pressure power control," *IEEE Trans. Signal Processing*, vol. 60, pp. 1957–1970, Apr. 2012.

[14] M. Elmusrati, H. El-Sallabi, and H. Koivo, "Applications of multi-objective optimization techniques in radio resource scheduling of cellular communication systems," *IEEE Trans. Wireless Commun.*, vol. 7, pp. 343–355, Jan. 2008.

[15] C. Long, B. Li, Q. Zhang, B. Zhao, B. Yang, and X. Guan, "The end-to-end rate control in multiple-hop wireless networks: Cross-layer formulation and optimal allocation," *IEEE Journal Sel. Areas Commun.*, vol. 26, pp. 1957–1970, May 2008.

[16] X. Lin, N. B. Shroff, and R. Srikant, "A tutorial on cross-layer optimization in wireless networks," *IEEE Journal Sel. Areas Commun.*, vol. 24, pp. 1452–1634, Aug. 2006.

[17] P. Hande, S. Rangan, M. Chiang, and X. Wu, "Distributed uplink power control for optimal SIR assignment in cellular data networks," *IEEE Trans. Networking*, vol. 16, pp. 1420–1423, Dec. 2008.

[18] G. J. Foschini and Z. Miljanic, "A simple distributed autonomous power control algorithm and its convergence," *IEEE Trans. Veh. Technol.*, vol. 42, pp. 616–646, Nov. 1993.

[19] N. Bambos, S. C. Chen, and G. J. Pottie, "Channel access algorithms with active link protection for wireless communication networks with power control," *IEEE/ACM Trans. Networking*, vol. 8, pp. 583–596, Oct. 2000.

[20] C. U. Saraydar, N. B. Mandayam, and D. J. Goodman, "Efficient power control via pricing in wireless data networks," *IEEE Trans. Commun.*, vol. 50, pp. 291–303, Feb. 2002.

[21] Y. Xi and E. M. Yeh, "Node-based optimal power control, routing, and congestion control in wireless networks," *IEEE Trans. Info Theory*, vol. 54, pp. 4081–4115, Sep. 2008.

[22] K. Leung and C. W. Sung, "An opportunistic power control algorithm for cellular network," *IEEE/ACM Trans. Networking*, vol. 14, pp. 470–478, Jun. 2006.

[23] M. Xiao, N. Shroff, and E. Chong, "A utility-based power-control scheme in wireless cellular systems," *IEEE Trans. Networking*, vol. 11, pp. 210–221, Apr. 2003.

[24] M. Canales, J. Ortn, and J. R. Gallego, "Game theoretic approach for end-to-end resource allocation in multihop cognitive radio networks," *IEEE Commun. Letters*, vol. 16, pp. 654–657, May 2012.

[25] R. Devarajan, S. C. Jha, U. Phuyal, and V. K. Bhargava, "Energy-aware resource allocation for cooperative cellular network using multi-objective optimization approach," *IEEE Trans. Wireless Commun.*, vol. 11, pp. 1997–1806, May 2012.

[26] A. Manolakos, V. Karyotis, and S. Papavassiliou, "A cross-layer-based topology control framework for wireless multihop networks," *IEEE Trans. Veh. Technology*, vol. 61, pp. 2858–2864, Jul. 2012.

[27] R. S. Komali, R. W. Thomas, L. A. DaSilva, and A. B. MacKenzie, "The price of ignorance: Distributed topology control in cognitive networks," *IEEE Trans. Wireless Commun.*, vol. 9, pp. 1434–1445, Apr. 2010.

[28] Z. Khan, J. J. Lehtomaki, L. A. DaSilva, and M. Latva-aho, "Autonomous sensing order selection strategies exploiting channel access information," *IEEE Trans. Mob. Computing*, vol. 12, pp. 274–288, Feb. 2012.

[29] A. Goldsmith, *Wireless Communications*. Cambridge University Press, 2005.

[30] J. Zander, "Distributed cochannel interference control in cellular radio systems," *IEEE Trans. Veh. Technol.*, vol. 41, pp. 305–311, Aug. 1992.

[31] C. W. Sung and K. Leung, "A generalized framework for distributed power control in wireless networks," *IEEE Trans. Info. Theory*, vol. 51, pp. 2625–2635, Jul. 2005.

[32] J. Zheng and M. Ma, "A utility-based joint power and rate adaptive algorithm in wireless ad hoc networks," *IEEE Trans. Commun.*, vol. 57, Jan. 2009.

[33] M. Rasti and A. R. Sharafat, "Distributed uplink power control with soft removal for wireless networks," *IEEE Trans. Commun.*, vol. 59, pp. 833–843, Mar. 2011.

[34] M. Rasti, A. R. Sharafat, and J. Zander, "A distributed dynamic target-SIR-tracking power control algorithm for wireless cellular networks," *IEEE Trans. Veh. Technol.*, vol. 59, pp. 906–916, Feb. 2010.

[35] A. B. MacKenzie and L. A. DaSilva, *Game theory for Electrical Engineers*. Morgan and Claypool, 2006.

[36] S. Hanly, "An algorithm for combined cell-site selection and power control to maximize cellular spread spectrum capacity," *IEEE Journal Sel. Areas. Commun.*, vol. 7, Sep. 1995.

[37] L. Gao, X. Wang, G. Sun, and Y. Xu, "A game approach for cell selection and resource allocation in heterogeneous wireless networks," in *IEEE Communications Society Conference on Sensor, Mesh and Ad Hoc Communications and Networks (SECON)*, 2011.

[38] K. Zhu, E. Hossain, and D. Niyato, "Pricing, spectrum sharing, and service selection in two-tier small cell networks: A hierarchical dynamic game approach," *to appear IEEE Trans. Mob. Computing*, 2013.

[39] C. Qian, S. Zhang, and W. Zhou, "A novel cell selection strategy with load balancing for both idle and RRC-connected users in 3GPP LTE network," in *Intl. Conf. wireless commun. and sig. processing (WCSP)*, 2012.

[40] K. Pedersen, F. Frederiksen, C. Rosa, H. Nguyen, L. Garcia, and Y. Wang, "Carrier aggregation for LTE-Advanced: functionality and performance aspects," *IEEE Commun. Mag.*, vol. 49, Jun. 2011.

[41] L. G. U. Garcia, I. Z. Kovacs, K. I. Pedersen, G. W. O. Costa, and P. E. Mogensen, "Autonomous component carrier selection for 4g femtocells a fresh look at an old problem," *IEEE Journal Sel. Areas Commun.*, vol. 30, Apr. 2012.

[42] J. E. C. Hartmann and L. Berlemann, "Decentralized inter-cell interference coordination by autonomous spectral reuse decisions," in *14th European Wireless Conf.*, 2008.

[43] H. Wang, C. Rosa, and K. Pedersen, "Uplink component carrier selection for lte-advanced systems with carrier aggregation," in *IEEE Intl. Commun. Conf. (ICC)*, 2011.

[44] B. Lorenzo and S. Glisic, "Traffic adaptive relaying topology control," *IEEE Trans. Wireless Commun.*, vol. 8, pp. 5612 – 5620, Nov. 2009.

[45] R. Tahar, A. Belghith, and R. Braham, "A generic mobile node architecture for multi-interface heterogenous wireless link layer," in *3rd Intl. Conf. Net. of the Future)*, 2012.

[46] J. Lee, Y. Kim, , H. Lee, B. L. Ng, D. Mazzarese, J. Liu, W. Xiao, and Y. Zhou, "Coordinated multipoint transmission and reception in LTE-Advanced systems," *IEEE Commun. Magazine*, vol. 50, pp. 44–50, Nov. 2012.

[47] B. Schein and R. Gallager, "The Gaussian parallel relay network," in *Symp. Infor. Theory (ISIT)*, 2000.

[48] S. C. Rezaei, S. O. Ghara, and A. K. Khandani, "Relay scheduling in the half-duplex Gaussian parallel relay channel," *IEEE Trans. Info. Theory*, vol. 56, pp. 2668 – 2687, Jun. 2010.

[49] K. Bakanoglu, S. Tomasin, and E. Erkip, "Resource allocation for the parallel relay channel with multiple relays," *IEEE Trans. Wireless Commun.*, vol. 10, pp. 792 – 802, Mar. 2011.

[50] L. Yingbin, V. Veeravalli, and H. Poor, "Resource allocation for wireless fading relay channels: Max-min solution," *IEEE Trans. Info. Theory*, vol. 53, pp. 3432 – 3453, Oct. 2007.

[51] Y. Liang and V. Veeravalli, "Gaussian orthogonal relay channels: Optimal resource allocation and capacity," *IEEE Trans. Info. Theory*, vol. 51, pp. 3284 – 3289, Sep. 2005.

[52] M. Chen, S. Serbetli, and A. Yener, "Distributed power allocation strategies for parallel relay networks," *IEEE Trans. Wireless Commun.*, vol. 7, pp. 552 – 561, Feb. 2008.

[53] R. Etkin, D. Tse, and H. Wang, "Gaussian interference channel capacity to within one bit," *IEEE Trans. Info. Theory*, vol. 54, pp. 5534 – 5562, Nov. 2008.

[54] L. Sankar, Y. Liang, N. B. Mandayam, and H. Poor, "Fading multiple access relay channels: Achievable rates and opportunistic scheduling," *IEEE Trans. Info. Theory*, vol. 57, pp. 1911 – 1931, Apr. 2011.

[55] O. Sahin, O. Simeone, and E. Erkip, "Interference channel with an out-of-band relay," *IEEE Trans. Info. Theory*, vol. 57, pp. 2746 – 2764, May 2011.

[56] Y. Tian and A. Yener, "Symmetric capacity of the Gaussian interference channel with an out-of-band relay to within 1.15 bits," *IEEE Trans. Info. Theory*, vol. 58, pp. 5151 – 5171, Aug. 2012.

[57] O. Sahin, O. Simeone, and E. Erkip, "Gaussian interference channel aided by a relay with out-of-band reception and in-band transmission," *IEEE Trans. Commun.*, vol. 59, pp. 2976 – 2981, Nov. 2011.

[58] P. Razaghi, S.-N. Hong, L. Zhou, W. Yu, and G. Caire, "Two birds and one stone: Gaussian interference channel with a shared out-of-band relay of limited rate," *IEEE Trans. Info. Theory, accepted for publication*, 2013.

[59] R. Amin and et. al., "Balancing spectral efficiency, energy consumption, and fairness in future heterogeneous wireless systems with reconfigurable devices," *IEEE Journal Sel. Areas Commun.*, pp. 969–980, Apr. 2013.

[60] A. Zappone and et. al., "Energy-aware competitive power control in relay-assisted interference wireless networks," *IEEE Trans. Wireless Commun.*, vol. 4, pp. 1860–1871, Apr. 2013.

[61] M. Rasti, A. R. Sharafat, and J. Zander, "Pareto and energy-efficient distributed power control with feasibility check in wireless networks," *IEEE Trans. Info. Theory*, vol. 57, pp. 245–255, Jan. 2011.

[62] M. Bazaraa, J. Jarvis, and H. Sherali, *Linear Programming and Network Flows*. Wiley, 4 ed., 2010.

[63] A. Dana and B. Hassibi, "On the power efficiency of sensory and ad hoc wireless networks," *IEEE Trans. Info. Theory*, vol. 52, pp. 2905–2914, Jul. 2006.

[64] A. Goldsmith, "Design and performance of high-speed communication systems over time-varying radio channels," in *PhD Dissertation*, University of California at Berkeley 1994.

[65] C. Meyer, *Matrix Analysis and Applied Linear Algebra*. SIAM, 2000.

[66] M. Medard, "The effect upon channel capacity in wireless communications of perfect and imperfect knowledge of the channel," *IEEE Trans. Info. Thery*, vol. 3, pp. 933–946, May 2000.

[67] I. Maric, B. Bostjancic, and A. Goldsmith, "Resource allocation for constrained backhaul in picocell networks," in *Info. Theory and Applications Workshop (ITA), San Diego, CA*, 2011.

[68] M. Sikora, J. N. Laneman, M. Haenggi, D. Costello, and T. Fuja, "Bandwidth- and power-efficient routing in linear wireless networks," *IEEE Trans. Info. Theory*, vol. 52, pp. 2624–2633, Jun. 2006.

[69] A. Frommera and D. B. Szyld, "On asynchronous iteations," *Journal of Computational and Applied Mathematics*, vol. 123, pp. 201–216, Nov. 2000.

[70] D. B. Szyld, "The mystery of asynchronsou iterations convergence when the spectral radius is one," *Report 98-102*, Oct. 1998.

[71] J. Chang, Y. Li, S. Feng, H. Wang, C. Sun, and P. Zhang, "A fractional soft handover scheme for 3GPP LTE-Advanced system," in *Int. Conf. Commun. (ICC)*, 2009.

[72] P. Bhat, S. Nagata, L. Campoy, I. Berberana, T. Derham, G. Liu, X. Shen, P. Zong, and J. Yang, "LTE-Advanced: An operator perspective," *IEEE Commun. Magazine*, Feb. 2012.

[73] R. Menon, R. M. Buehrer, and J. H. Reed, "On the impact of dynamic spectrum sharing techniques on legacy radio systems," *IEEE Trans. Wireless Commun.*, vol. 11, pp. 4198 – 4207, Nov. 2008.

[74] F. Boccard, R. W. Heath, A. Lozano, T. L. Marzetta, and P. Popovski, "Five disruptive technology directions for 5G," *IEEE Commun. Magazine*, pp. 74–80, Feb. 2014.